The Dissertation Committee for Aditya Hindupur certifies that this is the approved version of the following dissertation:

DESIGN AND CONSTRUCTION OF AN ANTI-HIV PROTEASE TRANSDUCER

Committee:

Robert O. Fox, Ph.D., Supervisor

Wlodzimierz Bujalowski, Ph.D.

Miles W. Cloyd, Ph.D.

Susan J. Marriott, Ph.D.

Henry F. Epstein, M.D.

Andres F. Oberhauser, Ph.D

Dean, Graduate School

DESIGN AND CONSTRUCTION OF AN ANTI-HIV PROTEASE TRANSDUCER

By

Aditya Hindupur, M.Sc.

Dissertation

Presented to the Faculty of the Graduate School of Biomedical Sciences

The University of Texas Medical Branch

in Partial Fulfillment

of the Requirements

for the Degree of

Doctor of Philosophy

The University of Texas Medical Branch

December 2011

To my mother and sister.

ACKNOWLEDGEMENTS

I would like to convey my sincere gratitude and appreciation to my mentor Dr. Robert O. Fox for guiding me throughout my Ph.D. studies. I am grateful for his advice and ability to inspire me to pursue challenging ideas that have laid the foundation for my doctoral work. It has been a great pleasure working under his mentorship and I am indebted to him for the opportunity to pursue this work.

I would also like to thank my committee members, Dr. Wlodzimierz Bujalowski, Dr. Susan J. Marriot, Dr. Henry F. Epstein, Dr. Andres Oberhauser and Dr. Miles.W. Cloyd. I would like to specially thank Dr. Miles Cloyd for his advice and support in working with HIV infected cells.

I would also like to express my appreciation to my colleges and friends Dr. Kris Tesh, Deqian Liu, Jason K Allison, Dr. Rohit K. Jangra, Keerti Gottipati, Dr. Larry Bellot, Dr. Jeeba Kuriakose, Dr. Jenny Gu, Dr. Aditya D. Joshi, Abhishek Mukherjee, Dr. Vinay K. Mamidala, Dr. Wendy Baker and Dr. Munia Mukherjee. I would especially like to thank Dr. Raza S. Khan for his scientific advice, help and guidance throughout and Dr. Kevin R. Mackenzie for his invaluable advice in data interpretation and discussions.

I would like to express my deepest appreciation and gratitude to my mother Lakshmi Rao for her constant support and encouragement, my sister Smriti Rao, and my grandmother Shanta Rao. This work was possible is part due to the teachings of my father Hindupur Chandrasekhar Rao and my grandfather Lt. Col. K. V. S. Rao; it is their memory that has kept me going.

TABLE OF CONTENTS

LIST OF TABLES

LIST OF FIGURES

LIST OF ABBREVIATIONS

CARD	Caspase Recruitment Domains
CTD	Cytoplasmic Transduction Domain
CTP	Cytoplasmic Transduction Peptide.
DED	Death Effector Domain
ESI	Electrospray Ionization Mass Spectrometry.
FADD	Fas Associated Death Domain
HAART	Highly active anti retroviral therapy.
HDAC	Class I Histone Deacteylase
PBS	Phosphate-bufferedsaline
PCR	Polymerase chain reaction
SDS	Sodium dodecyl sulfate
SDS-PAGE	Sodiumdodecyl sulfate polyacrylamide gel electrophoresis.
PTD	Protein Transduction Domain
SAHA	SuberoylanilideHydroxamic Acid
VPA	Valproic Acid

CHAPTER 1: INTRODUCTION

Current therapies against HIV, mainly the highly active anti-retroviral therapy (HAART), concentrate on reducing the viral load and recovering CD4 levels, however they are faced with a rebound of HIV levels on cessation of therapy(*1*). Also of concern is the number of reports on resistance to such therapies. There has been a realization that control of HIV requires a multi-pronged approach targeting viremia and a strong antiviral response (*2*), and there are new treatment regimens being tested. There has however been a limited success with the elimination of HIV reservoirs (*3, 4*). In this dissertation we propose the design and development of Anti- HIV transducer proteins. The transducers are activated by the HIV protease, and when activated by the HIV protease causes the death of cells expressing the viral protease. This mechanism can be used to treat all cells within the host, with only those cells having HIV protease being killed. We believe this to be an efficient manner for viral eradication. Upon incorporating recognition signals to other HIV proteins we can make our Anti-HIV transducers more specific in recognizing HIV infected cells.

SYNTHETIC SIGNALING PATHWAYS:

The underlying goal of Synthetic Biology is to build systems inspired by biological principles combining autonomous, modular and reusable components, examples of which include input components sensing the environment, internal components processing the information and output components broadcasting processed information (*5*).

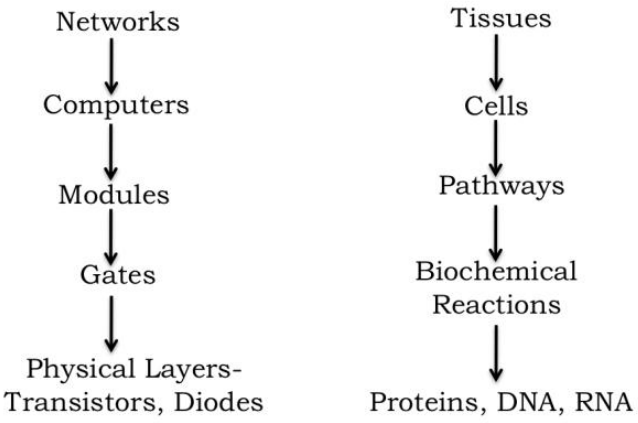

Figure 1.1: The hierarchical layers of biological systems.

These components can be used to construct biological networks that help express biological behaviors. Artificial networks based on gene circuit design have been developed that show feedback mechanisms, stability, toggle switching and intercellular communications (*6*). Based on a similar modular and circuit-based design, we can construct complex signaling pathways.

As the topic of this dissertation is the design of proteins that involve signaling pathways, the focus will revolve around synthetic protein systems. The majority of the proteins have a modular design comprised of multiple domains mediating specific protein-protein interactions. These interaction domains show great flexibility, with different members showing distinct binding affinities (*6*). Examples of such domains range from SH3 and SH2 to the WW and PDZ domains. These domains in signaling proteins show a switch like behavior, modulating downstream events (*7*).

It has been shown that complex output signals (AND, OR, NAND-NOT) could be generated by recombination of simple output and regulatory domains with the specific output. The actin regulatory switch N-WASP containing two inhibitory domains, a highly basic domain and a GTPase binding domain (GBD), has been used to test the modular nature of signaling pathways. In the presence of the activators phosphoinositide PIP2 and Cdc42, the N-WASP auto inhibitory interaction is disrupted allowing the output domain VCA to interact and activate Arp2/3 leading to actin polymerization. As activation of VCA requires the cooperativity of the two inputs PIP2 and Cdc42, it acts as an AND gate. Replacement of the basic domain and the GBD domain with a PDZ binding domain and a PDZ ligand show expected auto inhibitory interactions. Tethering two modular domains to the N-WASP output domain can require more complex input, such that the intramolecular interactions repress function. The two modular domains used were SH3 and PDZ or PDZ and the GBD domain. By generating combinations of the linkers, domain types, domain-ligand interactions and domain architecture, a number of varied outputs can be generated (*8*).

In a similar manner by systematically engineering the Dbl RhoGEF (Guanine Exchange Factor), a modular protein that contains a regulatory and catalytic domain, one is able to redirect actin polymeriziation by non-native signals. One such design involves the use of the Protein Kinase A to control the activity of the synthetic GEF(*9*).

Further work in redirecting input signal to the apoptosis extrinsic pathway has been tested. The Receptor tyrosine kinases were linked to the death effector domain of FADD, effectively converting a cell growth signal to a death signal (*10*), Similarly the LMP1 oncoprotein was linked to caspase-8 using a heterodimerizing agent leading to selective apoptosis in LMP1 expressing cells (*11*).

Other work in using the modular architecture of multi-domain proteins was the design of photoactivated Rac1. Rac1 is a GTPase that regulates actin cytoskelatal dynamics in metazoan cells. Steric blocking of Rac1 activity by fusing it to the Light Oxygen Voltage (LOV) domain allows one to regulate Rac1 activity with the help of 458/473nm light. This mechanism was shown to generate very precise local and temporal control of Rac1 in cells, making possible the detailed study of cellular movement (*12*).

This dissertation involves the design of an Anti-HIV protease transducer. The aim is to specifically target HIV infected cells with the aim of preventing infection from latently infected cells. This allows one to achieve eradication of the disease.

HIV INFECTION AND APOPTOSIS

HIV is a retrovirus closely related to other lentiviruses. The retroviruses and the herpes virus are characterized by their ability to maintain long term infection in contrast to viruses causing influenza and the common cold, with the cytopathic viruses being cleared by the immune system. Patients in the absence of a super-infection maintain for some time a degree of resistance to the same viral strain.

The persistent viruses show three characteristics: 1) long term persistence of viral genome in the host; 2) an absence of systematic cytopathy; and 3) evasion of the host immune response. The virus can also maintain persistence by not expressing its genome or by residing in immune-privileged cells (*2*).

HIV infects the immune system and is characterized by the gradual loss of $CD4^+$ T cells and progressive immune deficiency leading to opportunistic infections and ultimately death. A number of mechanisms have been proposed to explain this loss of $CD4^+$ T cells in infected individuals ranging from impaired production of T cells in the

thymus, movement of virus specific T cells to the lymphoid tissue, and increased rates of HIV induced apoptosis.

The HIV virus has developed mechanisms to evade the host immune response by regulating apoptosis through a variety of pro-apoptotic and anti-apoptotic proteins. HIV mediated lymphocyte destruction includes direct killing of infected cells, death of bystander cells by pro-apoptotic proteins. High turnover rates of T cells can be attributed to persistent production of the virus leading to increased T-cell proliferation controlled by apoptosis.

HIV mediated T-cell apoptosis is by the direct killing of infected cells on viral gene expression, or is the death of uninfected bystander cells by pro-apoptotic viral proteins or altered expression of cellular apoptotic regulatory molecules in lymphocytes and antigen presenting cells due to virus mediated immune activation.

The viral proteins are also known to be apoptotic in nature where Tat an HIV accessory protein up-regulates TNF related apoptosis inducing ligand (TRAIL); gp120, Tat and HIV protease up-regulate caspase-8; and gp120 and Nef increase caspase-3 activity (*13*). However, HIV infected cells are resistant to apoptosis, and uninfected cells 'bystanders' that are dying, the resistance being linked to Tat. Secreted Tat (sTat) sensitizes bystander cells to Fas induced apoptosis and within infected cells up-regulates the anti-apoptotic proteins and T-cell growth factors (*14*). A defense mechanism used by the host against viral infections is the induction of apoptosis in infected cells; with the Cytotoxic T cells (CTL) recognizing and inducing apoptosis in virally infected cells. This induction of apoptosis is by various mechanisms, some involve the production of the Fas ligand by the CTLs and cause an induction of the Fas mediated apoptotic pathway in Fas-bearing cells while others deliver protease containing granules to infected cells. Granzyme B, one of the protease carried in the granules, is capable of activating the

caspases by cleavage after aspartate residues (*14*). Conversely a number of viral proteins, by virtue of their shared structural similarities with human proteins, can regulate apoptosis.

Inhibition of cellular apoptosis is beneficial for HIV allowing high levels of progeny virus to be produced. *In vivo* studies have shown apoptosis to be inhibited in productively infected cells which results in resistance to HIV induced killing (*15*). The HIV proteins Nef, gp120 and Vpu down-regulate CD4 receptor expression preventing gp120-CD4 mediated apoptosis.

Nef is an abundantly expressed viral protein with a wide range of cellular distribution from the cytosol to the nucleus. One of the better-studied aspects of Nef is its ability to down-regulate the expression of CD4 early post infection (*16*). One plausible benefit of CD4 down-regulation by endocytotic degradation is preventing superinfection of actively infected cells. Nef down-regulates MHC-I molecules and up-regulates CD95L in infected cells, potentially protecting the infected cells from CTLs or NK cells (*13, 16*). Down-regulation of the MHC-1 by Nef, mediated by endosomal degradation, prevents the presentation of foreign peptide antigens circumventing the cytotoxic T-lymphocyte response against infected cells (*17*). Nef inhibits apoptosis signal regulating kinase-1 (ASK-1), thereby protecting infected cells form Fas (CD95) and TNF-alpha mediated apoptosis (*18*); further inhibition of the Fas apoptotic pathway by inhibition of caspase-8 and caspase-3 have also been reported (*19*). Nef, by interacting with the tumor suppressor protein p53, potentially decreases the half-life of p53 and thereby affects p53-mediated apoptosis (*16*). Interactions of Nef with PI3 kinase and PAK2 result in phosphorylation of Bad, a pro-apoptotic protein, resulting in inactivation of Bad. Inactivation in turn inhibits the mitochondrial apoptotic pathway (*20*).

The protein Vpr has been shown to up-regulate survivin, a member of the IAP (Inhibitor of apoptosis Proteins) family (*21*). Up-regulation is through the survivin promoter transactivation leading to cell cycle arrest in the G_2/M transition. Depending on time after infection, it was found that survivin protected early post infection Jurkat cells from apoptosis from exogenous stimuli. The protective effect disappears 72 hours after infection (*22*).

Tat, an arginine rich protein that acts as a transactivator or viral gene expression, shows both pro-apoptotic and anti-apoptotic characteristics. Stable, endogenously expressed Tat inhibits TRAIL mediated apoptosis in Jurkat cells. It also shows down-regulation of the upstream activator caspase-10 mRNA and up-regulation of c-FLIP, a protein that plays a role in the anti-apoptotic NF-kB and MAPK/ERK pathways (*23*). Endogenous expression of Tat increases the expression of the proto-oncogenic protein Bcl-2, and may contribute to suppression of apoptosis. This protective effect is lost when a C22G mutant of Tat is observed (*24*).

In addition to T-cells, Monocytes and Macrophages are also infected by HIV-1 and are thought to be reservoirs for HIV persistence. These cells, when compared to T-cells, are relatively refractory to HIV induced apoptosis. It has been shown that HIV -1 infection in U937 cells abrogated caspase-3 activation induced by DNA-damaging agents in turn suppressing apoptosis (*25*).

HAART AND HIV PERSISTENCE

HIV infection can be divided into two phases: acute and chronic. Within 2-4 weeks of initial infection, during the acute phase there is a massive increase in plasma virus levels; up to a million copies of viral RNA are detected within this period. There is widespread dissemination of the virus, rapid establishment of viral reservoirs, destruction

of gut lymphoid tissue, destruction of CD4+ T-cells, with the immune response lagging in response leading to a partial control of replication (*26*).

VIRAL RESERVOIRS:

A viral reservoir has been defined as a cell type or anatomical site where replication competent infected cells persist longer than the main pool of actively replicating viruses (*1*)

After the introduction of HAART (Highly retroactive anti-retroviral therapy), clearance of virus levels and time an individual must be on therapy for eradication to be achieved were mathematically modeled (*27*). However these predictions were made based on the assumption- of no viral reservoirs. Following this, it was shown resting CD4+ cells harbor latent HIV-1 with low frequency ranging from 0.2 -16.4 cells per 10^6 cells; and these did not reduce with increasing times of HAART. These resting cells with latent HIV did not show any mutations towards drugs used in HAART (*28, 29*).

Based on the integration of the HIV genome into the latent reservoir cells, latency may be either A) post integration latency where productive cells enter into the resting stage - after escaping from immune response or cytotoxic effects of viral production or B) pre-integration latency exhibited by resting cells directly infected with HIV. They are characterized by the absence of integration of the HIV-1 DNA (*30*). The half-life of the unintegrated genome is around 1 day and these cells do not contribute significantly to reservoir population.

In post-integration latency, the viral life cycle is impaired in quiescent CD4+ T-cells due to 1) low level of nucleotides for reverse transcriptase, 2) hyper-mutation of G->A leading to a defective viral genome, and3) impaired nuclear import of pre-integration complex (PIC). The impairments of PIC are overcome when the cells become activated.

The general view being the virus infects CD4+ cells while transiting to the resting state.(*31*)

In addition, the site of viral integration also plays a role in post integration latency. In CD4+ T-cells, HIV actively integrates into introns of active genes. Once the viral genome is integrated into the genomic DNA, it faces the same restrictions and epigenetic control as the host DNA. The viral genome must be able to overcome the physical barrier of the nucleosome structure to activate gene transcription(*31*). There are two types of HIV reservoirs:lymphoid tissue and CD4+ cells. The lymphoid tissue provides a large population of target cells, with the added aspect of close proximity for efficient cell-to-cell propagation (*26*).The alternate reservoirs of HIV are: Naive CD4+ cells, CD8+ cells, Monocytes, B-cells, Dendritic cells, NK cells.

Other sanctuary sites where viral replication can take place in patients on HAART are normally where access of HAART is limited or the cells at the site are immuno-privileged. HIV can penetrate the CNS and infect perivascular macrophages, meningeal macrophages, macrophages of the choroid-plexus and microglia. The genital tract and renal epithelium have shown HIV, but their role in HIV persistence is yet to be determined (*32*). Based on current therapy and the half-life of memory cells that show slowed decay (half-lives of 44 months), calculations predict it would take 60 years to deplete the reservoir (*32, 33*).

APPROACHES TO ERADICATION OF HIV:

Due to the presence of resting T-cells with HIV and low residual viral replication that are responsible for the rebound in viral levels after cessation of HAART, alternative approaches have been suggested to achieve eradication. Some of these approaches are:

1. Increasing the potency of HAART.

2. Structured Treatment Interruptions.

3. Activating the T-Cells:

The rationale is simple nonspecific activation of quiescent T-cells would lead to activation and release of the virus, and the subsequent productive infection of cells being prevented by the presence of antiretroviral drugs. Factors like OKT3 and IL-2 have been used to achieve T-cell activation, leading to high T-cell activation with corresponding toxicity. However the number of latent cells did not change. Due to the complications, large-scale activation of T-cells does not appear to be feasible (*1*). Class I Histonedeactetylases (HDACs) are critical to maintaining HIV-1 latency in chronically infected cell lines, inhibition of which leads to viral expression in resting CD4+ cells(*34*). Uses of synthetic HDAC inhibitors like Valproic acid (VPA) or trichostatin conjugation with HAART gave mixed results (*1, 35*), with no reactivation of latent HIV in infected primary CD4 T-cells(*36*). It has recently been reported that it is possible to reactivate HIV-1 transcription without T-cell activation using an alternatively spliced form of the transcription factor ΔVII-Ets-1 (*37*). Clinical trials using Class1 HDAC inhibitor suberoylanilidehydroxamic acid (SAHA) are in development, the concept being that exposure with SAHA will prevent the establishment of latent HIV infected cells.

The Aim of this dissertation is to apply the ideas of protein engineering and synthetic biology to design protein transducers that would be activated by HIV protease in HIV infected cells but not uninfected cells. The long-term goal of this project is to be able to achieve eradication of the HIV infection by selectively killing HIV infected cells. To address this goal we have aimed to design, construct and test an HIV protease transducer.

CHAPTER 2: DESIGN OF AN HIV PROTEASE ACTIVATED PROTEIN TRANSDUCER.

The principle aim of this dissertation is the design and testing of a Protease transducer. Here I shall detail the design of the second generation Protease transducer. The design details for the first generation are described in the appendix.

One primary observation for multi-domain proteins is their modular nature (*38*), a property of great use when trying to design new signaling pathways using preexisting domains. This approach has been well documented in other synthetic systems whereby recombining domains from different sources, one can design new signaling pathways or redirect preexisting ones.(*8-10, 12, 39-41*)

DESIGN OF THE TRANSDUCER:

The design goals for the Protease transducers are:

1. Individual transducers must be monomeric in nature.
2. Transducers must be inactive in uninfected cells.
3. Active transducers must be created through proteolytic cleavage by HIV protease.
4. Transducer proteins must be capable of being taken up by a wide variety of cells from the extracellular milieu.
5. Inactive transducers must not interact with each other and initiate a false positive signal.
6. Active monomers, after HIV protease mediated cleavage, must rapidly recombine to yield an active hetero-dimer capable of initiating apoptosis.

As our protease transducer is based on a modular design approach, each - module will be discussed individually.

After deciding on the design criteria, we perused the literature and selected individual domains, which might work in the final design. Based on the design goals listed above we proposed a HIV-Protease "activatable" transducer (Figure 2.1) that would be an inactive monomer by virtue of multiple intra-molecular interactions. These interactions were so designed such that on cleavage by the HIV protease, the intra-molecular interactions would become intermolecular, allowing dissociation and reassembly. The two activated monomers heterodimerize yielding an active dimer (Figure 2.2). This dimer recruits procaspase-8 leading to active caspase-8 causing cell death. Each domain in the transducers was selected to allow easy swapping with other domains when refining the design.

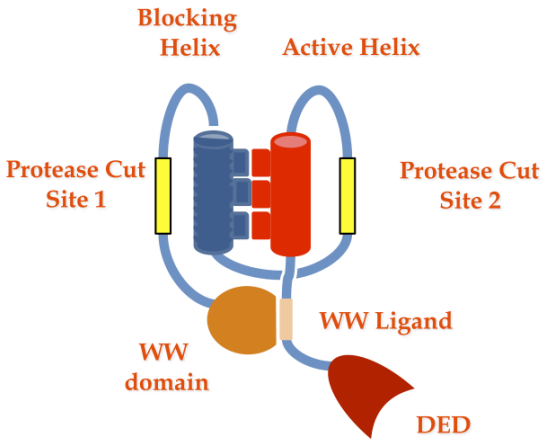

Figure 2.1: A schematic representation of the individual transducer design. The blue and red domains - are the dimerization complex.

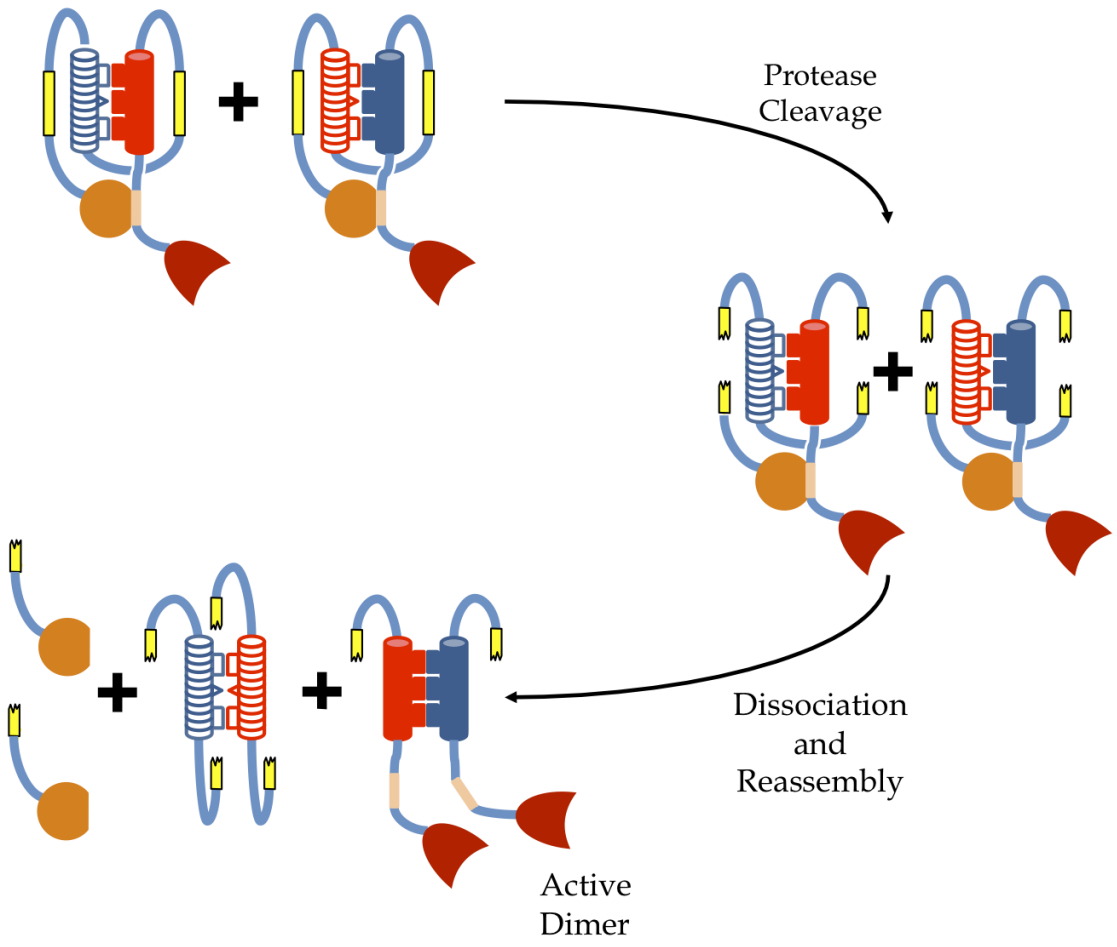

Figure 2.2: A schematic representation of the individual transducers being activated by HIV protease. Cleavage by HIV protease leads to the formation of helices which heterodimerize yielding an active dimer and later apoptosis.

A retro synthetic approach was used to design the transducers. As our principle aim is to achieve killing of infected HIV cells, killing of cells in general was tackled first.

APOPTOSIS AND THE EXTRINSIC PATHWAY:

Apoptosis is a specific form of programmed cell death, occurring in evolutionary well-conserved pathways (*42*). The principal recruiters of apoptosis activate the

executioner caspases that play a central role in the pathway. The executioner caspases are activated by two distinct pathways, namely the extrinsic and intrinsic pathway. The extrinsic pathway is activated by the ligand-bound activation of the death receptor as in TNF, Fas or TRAIL, which are death domain (DD) containing proteins. Ligand binding probably results in the formation of receptor trimers which recruit the adaptor molecule Fas Associated Death Domain (FADD, containing the DD domain and a separate Death Effector Domain (DED). The DED of FADD interacts with the DED of inactive procaspase-8 and leads to formation of the Death Inducing Signaling Complex (DISC) represented in figure 2.3.This results in in-trans cleavage of the pro-caspase 8 to active caspase-8, which in turn activates the effector caspase-3 leading to the downstream cleavage of 100 or more proteins. The cascade of cleavages propagates apoptosis (*43*).

Activation of the procaspase-8 has been characterized by fusing recombinant procaspase-8 with FK506 binding protein instead of the DED domains. In the presence of dimer FK506, cells undergo apoptosis (*44*).

As we aim to induce apoptosis in HIV infected cells through the extrinsic pathway, we used dimerization-induced activation of procaspase-8 (*45, 46*). Activation of procaspase-8 leads to the downstream activation of the effector caspases followed by programmed cell death.

DED DOMAINS:

The Death Effector Domain (DED) belongs to a family of Caspase Recruitment Domains (CARD). In the extrinsic apoptosis pathway the adaptor protein FADD is recruited to the cytoplasmic Death domain (DD) of the Death Receptors (DR) upon activation. The FADD is a tandem repeat of homologous CARD, (DED) and (DD) domains. The C-terminal DD interacts homotypically with the DR/DD while the N-

terminal Death Effector Domain interacts homotypically with procaspase-8 and/or -10(*47, 48*). The FADD DED domain interacts with one of the DED domains on procaspase-8(*49*).

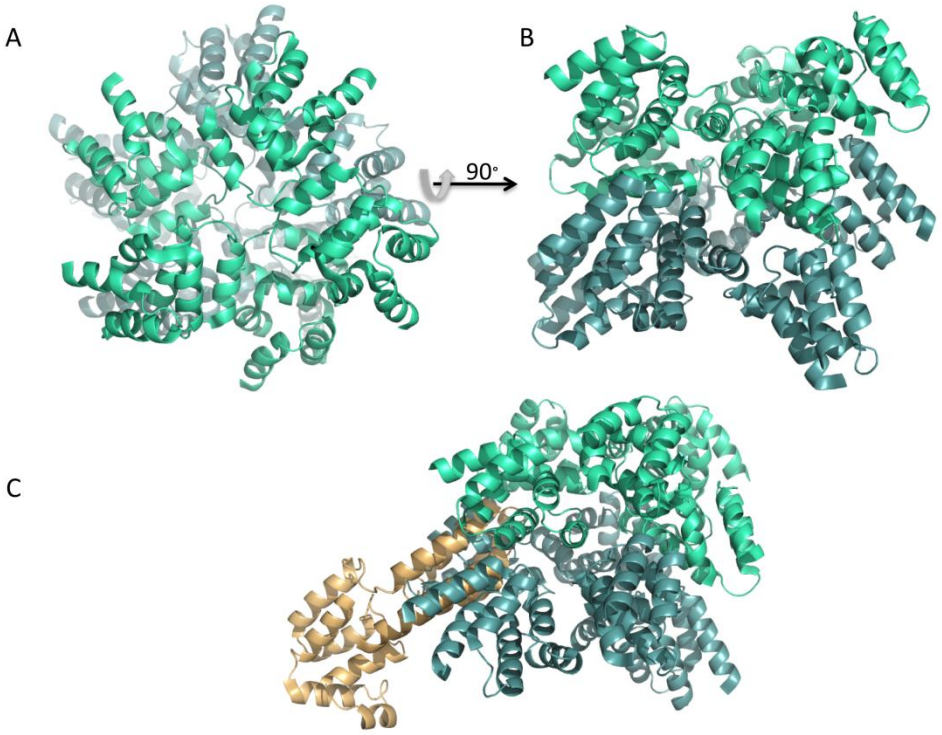

Figure 2.3: The FasL-Receptor C-terminal in complex with the FADD-DD domain.(A) Complex viewed down bundle; (B) viewed rotated 90 degrees; (C) complex with FADD-FL (gold) added. The FADD-DED Domain is not clashing with the FASLR-FADD-DD complex and is free to interact with the procaspase-8 DED domains. On recruitment of procaspase-8 to the FADD-DED domain, the DISC is formed leading to procaspase-8 activation.

As it has already been established that dimerization of procaspase-8 is sufficient to induce apoptosis in cells, it was decided to use the FADD DED domain tethered to a dimerization domain to spatially bring together the procaspase-8 molecules. This would

lead to in-trans activation of procaspase-8 yielding active caspase-8 molecules, initiating apoptosis (*50, 51*).

Activation of the procaspase-8 molecules is through the adaptor protein FADD DED domain. The DED domain is a F25YC27S mutant, shown in figure 2.4. It has been shown previously that the F25Y mutant does not aggregate in solution and is capable of inducing apoptosis (*49*). In the structure Cysteine was replaced by a serine on account of design requirements of having only a single cysteine in the final sequence.

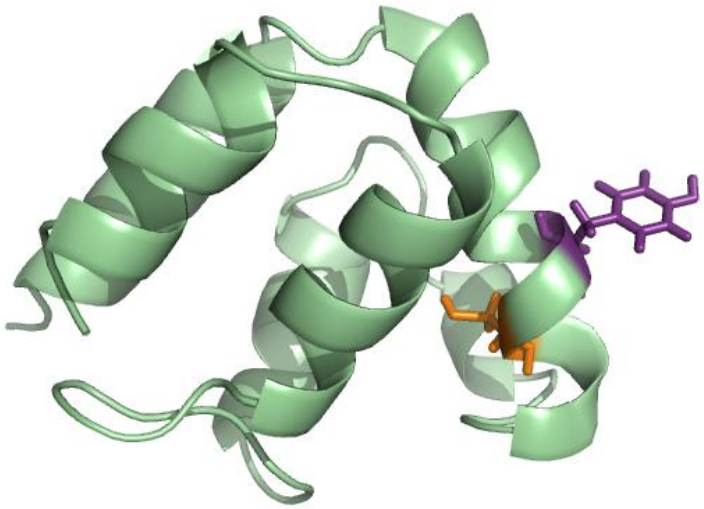

Figure 2.3: Solution structure of the FADD Death Effector Domain. The F25Y mutation is highlighted in purple. A single Cysteine residue located towards the interior of the protein is highlighted in orange. The Cysteine was mutated to a serine in the Protease transducers.

Tethering of the DED domain to the dimerization domain is by a 14 amino acid linker. The length of the linker was determined based on the length of the linker region connecting the FADD DD and DED domains as well as the residues connecting the two

domains in the *molluscum contagiosum* viral FLICE-inhibitory protein (V-FLIP) MC159 (*52*).

THE DIMERIZATION DOMAIN: COILED COILS

The coiled coil is one of the most commonly found oligomerization domains. Based on genomic data, it is predicted that around 10% of eukaryotic proteins are composed of predicted coiled coils (*53, 54*). It consists of two or more alpha helices in a super-coiled bundle. The helices are encoded by a sequence of 7 amino acid residue repeats $[abcdefg]_n$ called a heptad repeat. The coiled coil is of considerable interest due to the wide range of structure and oligomerization states they exhibit and as a model for protein design (*55*). They have been used in a wide spectrum of applications ranging from cellular engineering to hydrogels and metal nanostructures (*40, 56-63*).

The heptad repeat has hydrophobic residues encoded by **a** and **d** whose side chains of residues pack against each other in a "knobs-into-holes" manner(*64*) forming a hydrophobic core. This packing is maintained throughout the length of the helix yielding a left-handed super-coil. The residues at positions e and g are alongside the hydrophobic core and are typically occupied by charged residues that participate in i to i'+5 electrostatic interactions. The interactions that stabilize the coiled coils are shown in figure 2.4. It is these electrostatic interactions, which are important for association – homo or hetero-association (*54, 65-67*).

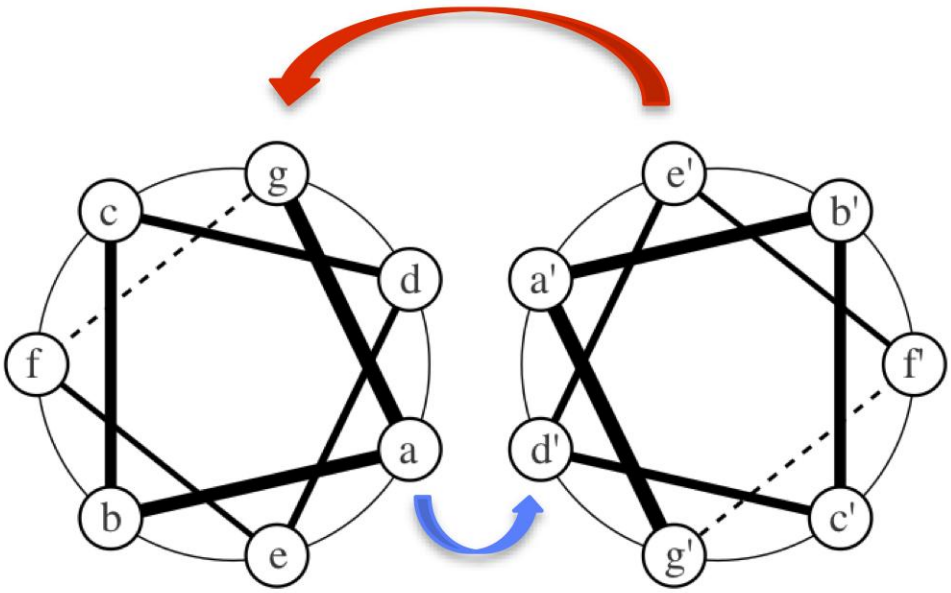

Figure 2.4: The heptad repeat [abcdefg]$_n$ within the coiled coils. The positions e and g' are responsible for electrostatic interactions (red arrow); whereas the core hydrophobic interactions are through the positions and a and d' (blue arrow).

ROLE OF IONIC INTERACTIONS IN COILED COILS:

In coiled coils, the positions **e** and **g** are most often charged residues which play a role in inter-helical interactions. It has been shown in de novo designed coiled-coils inter-helical ionic interactions are not required for coiled-coil formation, with inter-helical repulsions destabilizing the assembly of homo-stranded coiled coils and electrostatic attractions stabilizing hetero-strand interactions (*68, 69*). Inter-helical repulsions in designed coiled coils between glutamic acid residues show effects in i to i'+5 spacing. In a designed coiled-coil with no glutamates, increasing number of glutamate residues from 2-8 at positions e and g reduced the helicity and stability of the peptides (*70, 71*).

The destabilizing effects by negatively charged glutamate are also dependent on their locations. When located at the N-terminal of the coiled coil with no glutamate at positions **e** or **g** in the core, the peptides are stabilized by charge-helix dipole interactions

at pH 7.0, with the stability modulated by pH or salt concentration. Changing the location of the glutamate side chain to the core of the coiled coil or the C-terminal end destabilized the coiled coil, the C-terminal glutamate substitution being more destabilizing(*72*).

Inter-helical electrostatic interactions also play a role in determining the orientation of coiled-coils, parallel (P) or anti-parallel (AP). Inter-helical electrostatic attractions between positions e-g' or g-e' and g-g' or e-e' determine the stability of the parallel or anti-parallel coiled coils. The degree of stability of the coiled coils is AP-Attractive > P-Attractive > AP-Repulsive > P-Repulsive (*73-75*).

Coiled coil	Length	Oligomerization	Kd(app)	Reference
AB4C	86	Dimer		(*76*)
WinZipA1B1	37	Dimer	24nM	(*77*)
IAAL E3/K3	21	Dimer	70nM	(*54*)
VAAL E4/K4	28	Dimer	4nM	(*54*)
ecE/ecK	28	Tetramer		(*78*)
GNC4-pL1	32	Tetramer		(*79*)
EE12345L/RR12345L _ A	47	Dimer	$1.1X10^{-11}M$	(*80*)
RR12EE345L/EE12RR345L	47	Dimer	$1.3X10^{-11}M$	(*80*)

Table 2.1: A list of coiled-coils considered -with their lengths and affinities.

A number of synthetic coiled coils were designed and a few were considered for this work as listed in the Table 2.1. Based on the affinity of the coiled coils, the specificity for forming heterodimers, and the length, we selected to use the IAALE3K3 coiled coil system (Table 2.1, Figure 2.5, 2.6) (*54, 81*).

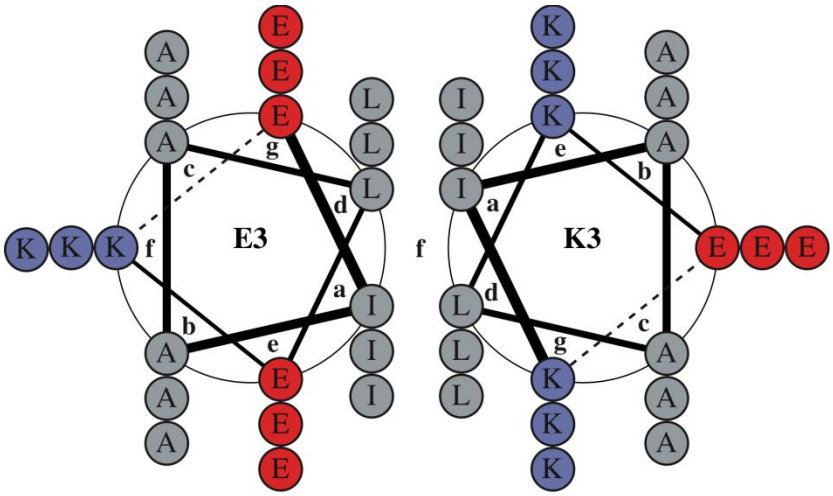

Figure 2.5: Helical wheel representation of IAAL- E3/K3 coiled coil. The electrostatic interactions between positions g and e' dictate specificity of the coiled coils. The presence of isoleucine at position a instead of leucine increases the hydrophobicity of the core.

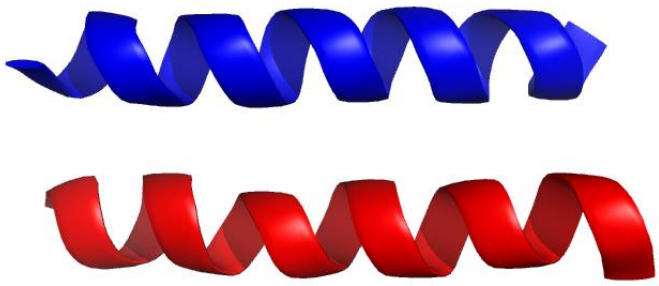

Figure 2.6: The ribbon diagram of the solution structure of the IAAL- E3/K3. IAAL-E3 (Red) and IAAL- K3 (Blue) coiled coil.

The E3/K3 coiled coil is a short 21 residue long coiled coil. The individual monomers on their own are not helical, but gain full helicity when mixed together. This key feature allows one to design transducers that hetero-dimerize.

The blocking helix and the effect of core Leu to Asn on the stability of the coiled coil.

One of the design parameters for the transducer protein is keeping the protein inactive in the absence of HIV protease. To achieve this goal the active helix is blocked with another helix forming hetero-dimerizing partner. The blocking helix has a core hydrophobic leucine residue mutated to asparagine to destabilize the inter-helical hydrophobic interactions (*82-84*). It is the hydrophobic interactions which impart the specificity and orientation of the coiled coils. The presence of a single buried polar residue changes the orientation of the helix-helix interactions of the coiled coil. Based on previously published data it was believed the individual blocking helices, having a buried polar residue, will preferentially interact with each other to satisfy the electrostatic bonding potential of the single asparagine in the generally hydrophobic core of the coiled coil (*83*). Also the inactive sink dimers are likely to be anti-parallel heterodimer coiled coils (*84*).

An additional role for the blocking helix is to shift the equilibrium of the population towards the active dimer and to prevent the formation of inactive heterodimers as shown in Figure 2.9 to one in Figure 2.10

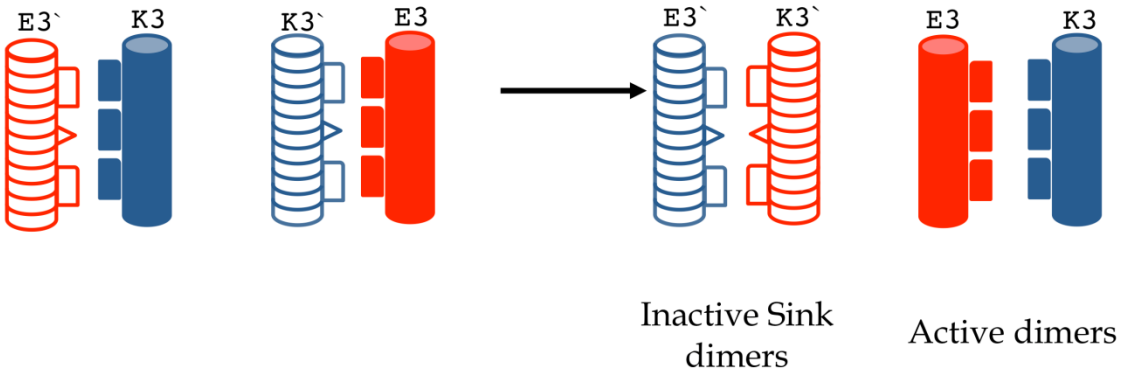

Figure 2.7: A cartoon representation of the interactions between the active helix (Solid) and blocking helix (Striped). The blocking helix has a single core asparagine residue (triangle) interacting with an opposite hydrophobic leucine (block).

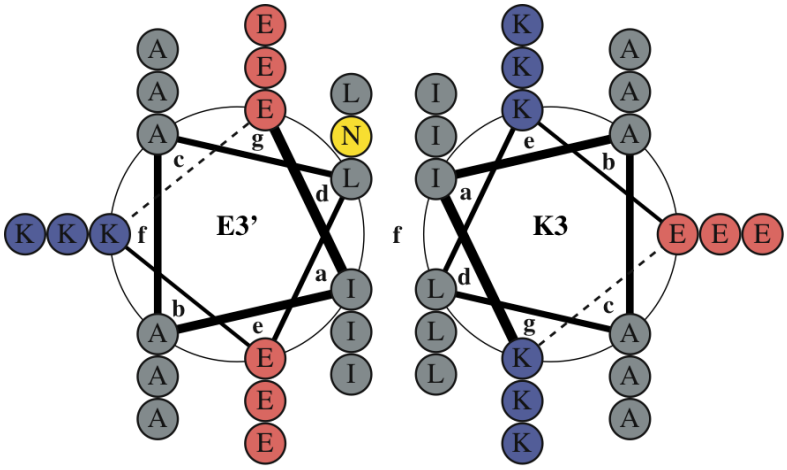

Figure 2.8: Helical wheel representation of the blocking helix E3' interacting with the active helix K3. The core asparagine residue is highlighted in yellow.

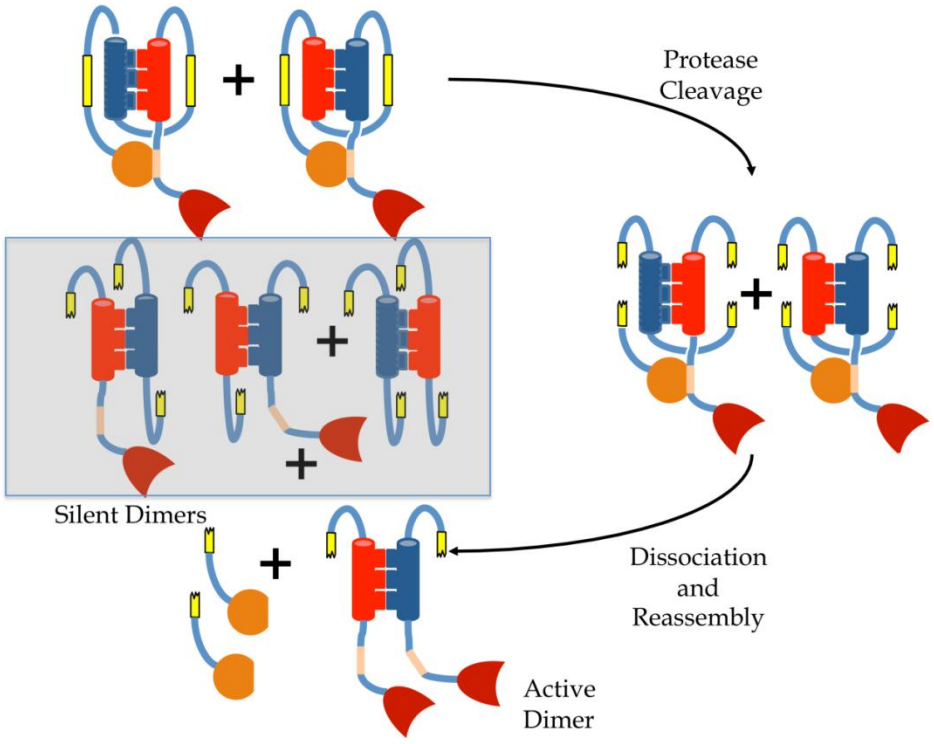

Figure 2.9: The blocking helix forms silent dimers that are inactive due one of the helices lacking a DED domain. This shifts the equilibrium away from the active dimer. Redesigning the blocking helix would allow us to yield predominantly active dimers.

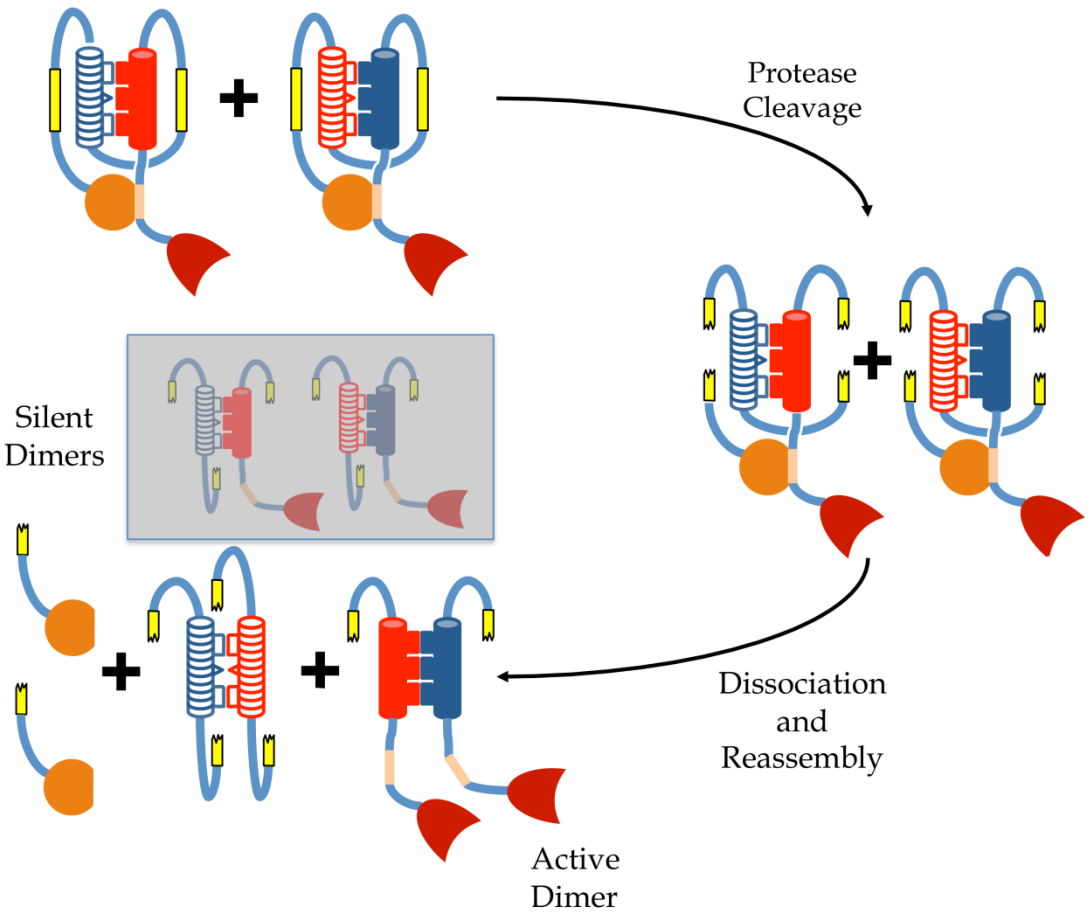

Figure 2.10: Incorporating a single aspargine residue within the core of the blocking helix (Stripped) shifts the equilibrium. The equilibrium is shifted towards the active dimers at the same time reducing the population of the inactive sink dimers that are formed.

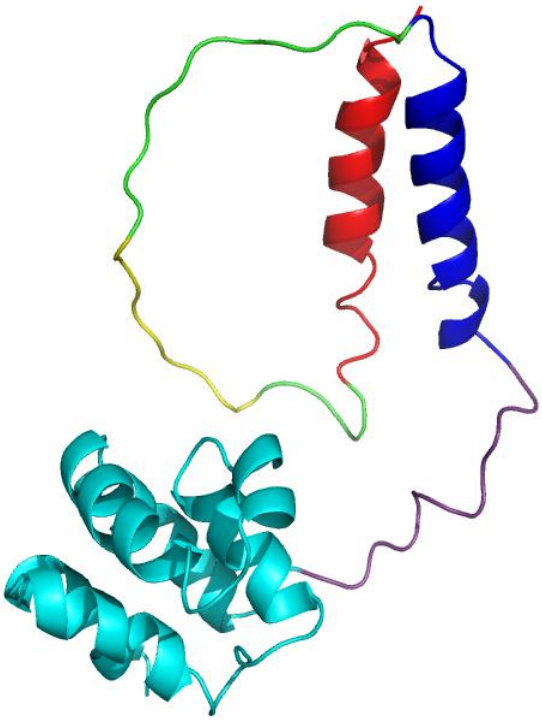

Figure 2.11: A representation of the active helix (Blue) tethered to the FADD DED domain. The blocking helix is connected to the N-terminal of the active helix by a linker that favors intramolecular interactions between the active helix and the blocking helix. The DED domain is illustrated underneath the coiled coil.

To keep the transducer inactive by intramolecular interactions, the 14 amino acid linker region connecting the DED domain to the dimerization domain was designed as a WW ligand (described below); Intra-molecular interactions between the N-terminal WW domain and the C-terminal linker keeps the transducer in an inactive state.

WW DOMAINS:

The WW domain is an antiparallel three-stranded small binding domain with two-conserved Tryptophans (WW). It binds to poly-proline rich ligands, with binding

overlapping with the SH3 domain. It also binds to phosphoserine and threonine/proline rich sites.

The domain is common being found in around 50 human proteins and plays a role as a scaffold for the assembly of multi-protein networks. Ten human WW domains have been found to be associated with 148 different partners (*85*).

The WW domain has two different ligand binding grooves and can be divided into 4 different groups based on their binding Motifs:

Group I - PY motif.

Group II - PPLP motif

Group III - PR motif

Group IV - p (S/T) P motif

Group II and III are versatile and additionally bind to polyproline regions containing glycine, methionine or arginine.

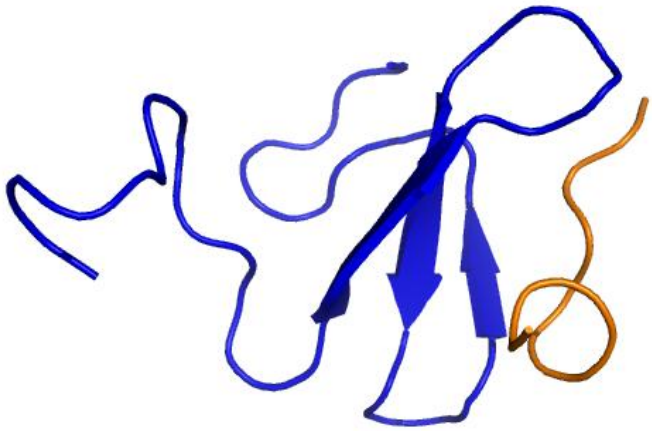

Figure 2.12: The solution structure WW domain: [2EZ5] of dNedd4 (blue) bound to Commissureless (Comm) ligand peptide TGLPSYDEALH (gold).

In the design of the protease transducer, Drosphilla Nedd4 (dNedd4) cells were used. The solution structure of the protein was used for modeling purposes (Fig 2.12).

One of the main advantagedNedd4 conferred was it was a non-human WW domain. The ligand is an 11-residue peptide from the Comm protein. This complex is critical for central nervous system and muscle development(*86*).The WW3 domain has a Kd of ~3μM to the Comm ligand(*86*). Based on the design of the transducers proteins, the association of the WW domain for its ligand will be much tighter by virtue of the interaction being intermolecular instead of intermolecular. Activation of the transducers by HIV protease shifts the domain-ligand interactions from intramolecular to intermolecular.

The individual proteins have a single cysteine at the N-terminal end of the active helix to fluorescently label the proteins for easy tracking within cells.

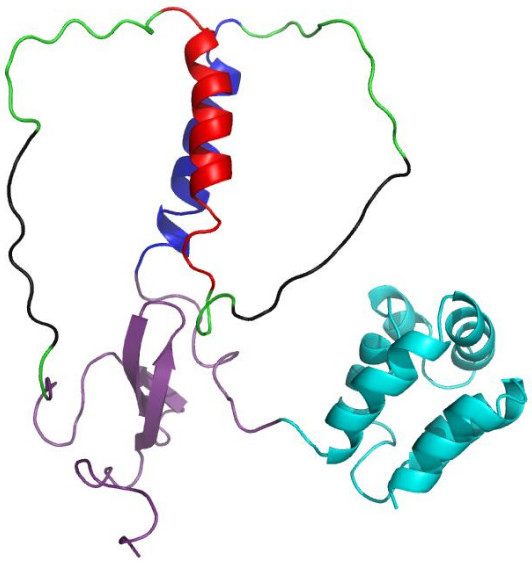

Figure 2.13: Addition of the N-terminal WW domain added an additional constraint in keeping the transducer inactive. The WW domain (purple) has intramolecular interactions with its ligand, designed as the linker connecting the active helix to the DED domain.

PROTEASE CLEAVAGE SITE:

The main aim of the Protease transducer is its activation by HIV protease. HIV protease is an aspartyl protease that is structurally similar to others in the pepsin family. It is a symmetrical dimer that is stabilized by a 4-stranded β-sheet formed by N and C-terminal B-strands. The active site is at the interface of the two subunits and the catalytic triad formed Asp25-Thr26-Gly27 is responsible for the cleavage reactions of the protease (*87, 88*). The protease is required for viral infectivity(*89*) and is a significant target for drug design. Currently there are a number of structures now in the PDB of the protease with inhibitors bound. The viral protease causes apoptosis by cleaving Bcl-2, an anti-apoptotic factor in infected cells (*90*). Additionally it has been shown this protease cleaves procaspase-8 to yield a novel casp8p41 fragment that causes apoptosis *in vivo* (*91*).

Previously it has been shown that placing the HIV p17-p24 gag cleavage site within the caspases-3 cleavage site, one was able to achieve activation of Procaspase-3 in cells transduced with HIV protease and in cells infected with HIV(*92*). It may be possible to design a protein cleaved by intracellular HIV protease in HIV infected cells.

For the purpose of our design the protease cleavage site is include is GSGIF/LETSL, a peptide sequence with 15 fold higher efficiency for cleavage at pH 6.7 when compared to the RT/IN peptide (*93*).The various other cleavage sites that can also be incorporated are given in Table 2.2.

	Peptide sequence	pH	
		pH 5.6	pH 6.7
	P3 P2 P1 | P1` P2` P3`	K_m(μM)	K_m(μM)
1	GSGIF|LETSL	5± 1	60±20
2	GSGVF|VETSL	6.2±0.8	51±7
3	SSGSGV|HVSTLVPEF	580±20	500±100
4	GSGVF|VEMPL	25±4	160±10
5	GSGNY|LVTSL	50±9	120±20
6	IRKIL|FLDG	1300±100	830±20
8	GSGLF|TEYGL	300±80	920±40

Table 2.2: A partial list of peptides efficiently cleaved by HIV protease. The peptide sequences were discovered using phage display. Modified from (*93*)

Activation of the inactive transducers is by proteolytic cleavage of the linkers connecting the blocking helix to the active helix, releasing the active helix to dimerize and induce apoptosis.

One of the design criteria that were established was the intracellular delivery of our designer proteins.

CELLULAR DELIVERY OF PROTEINS: USE OF PROTEIN TRANSDUCTION DOMAINS (PTD)

Since the discovery that the HIV accessory protein sTat (soluble tat) was responsible for the killing of uninfected cells (bystander cells) by neighboring infected cells(*94*), a lot of work was done to establish the region of Tat responsible for uptake by these bystander cells. An arginine-rich region of the sequence was found to be responsible. It was also shown that when this peptide sequence was attached to a cargo protein like GFP or β-lactamase, there was tissue wide delivery and uptake of the proteins. Also, intraperitoneal injection of β−galactosidase tagged with the Tat peptide

crosses the blood brain barrier (*95*). Later work showed clear uptake of GFP into muscle cells within 30mins compared to the 14 hours for endogenous expression (*96*). Other works include the induction of induced pluripotent cells (iPS) using Tat-tagged transcription factors (*97*). Currently a number of different payloads are being transduced into cells ranging from RNA, DNA (*98*), plasmids(*99*), proteins, and siRNA(*100*),some of which are now in clinical trials. Many of protein transduction peptides are arginine or lysine containing sequences ranging in length from 8-30 residues. Examples of a few of such peptides are given in Table 2.3. In addition to positively charged residues in the peptide sequence, recently proline containing transduction peptides have been reported (*101*).

Name	Sequence	Length
Tatp	YGRKKRRQRRR	11
Penetratin	RQIKIWFQNRRMKWKK	16
Arg8	RRRRRRRR	8
HIV Rev	TRQARRNRRRRWRERQR	17
CTP_{512}	RRARRRRRR	9
MAP	KLALKLALKALKAALKLA	18
Transportan	GWTLNSAGYLLGKINLKALAALAKKIL	27
Transportan-10	AGYLLGKINLKALAALAKKIL	21
KALA	WEAKLAKALAKALAKHLAKALAKALKACEA	30
ppTG1	GLFKALLKLLKSLWKLLLKA	20
MPG	GALFLGFLGAAGSTMGAWSQPKSKRKV	27

Table 2.3: A partial list of cellular targeting peptides.Tatp: HIV tat derived peptide, CTP_{512}: Cytoplasmic targeting peptide. Modified from (*102*).

MECHANISM OF UPTAKE:

There has been considerable controversy concerning the mechanism of uptake of the cell penetrating peptides. It was originally thought that uptake of the proteins was by endocytic mechanisms. Current work done with TAT and R4 show calthrin/cavleonin independent and calthrin mediated or caveolin mediated endocytic mechanisms are not responsible for the uptake of the peptides and their cargoes (*103*). These studies were done using calthrin and caveolin knockouts for dependent studies and at $4^{o}C$ for calthrin and caveolin independent uptake studies. The studies clearly show that uptake of the peptide and their cargos are independent of endocytosis or pinocytosis. However short poly-arginine sequences do appear to be in endocytic vesicles with a minimum number of six arginines required for non-endocytic uptake.

It has been shown that the presence of heparansulfate proteoglycans on the surface of cells is responsible for the uptake of the protein. Deletion of key steps in the synthesis reduces uptake of the TAT peptides. Cells deficient in heparan sulfate or glycosaminoglycan show increased uptake of PTDs(*104*) when the proteins are transduced in the presence of dextransulfate.

PROTEIN TRANSDUCTION DOMAIN (PTD)

A specific cytoplasmic targeting peptide (CTP_{512}) (*105*) was selected due to the following criteria:

1. Increased distribution in the cytosol.
2. Increased efficiency of uptake into cells.
3. Non-dependence on the endocytic pathway for uptake.
4. High delivery across cell types unlike other PTDs.

Hereafter, CTP will be referred to as CTD (Cytoplasmic targeting Domain).

MODEL BUILDING:

The amino acid sequence of the modular protease transducer was chosen after identifying the relevant domains. To understand the individual modules of the transducer, a representative 3-D model was built and evaluated for improvements.

The X-ray or NMR structures for each module were identified in the PDB. With the help of the crystallography modeling software XFit(*106*), the varying pieces were positioned near each other. Depending on the spacing of the various fragments, extended loops were built to connect the individual domains. Then the models were minimized using CNS(*107*). Based on the final model (Figure 2.14), HIV protease was docked to the cleavage sites to determine substrate accessibility. Once complete, the sequence details were laid out in amino acid code to be constructed (Figure 2.16).

The proteins were then expressed and tested, a description of which is given in Chapter 4.

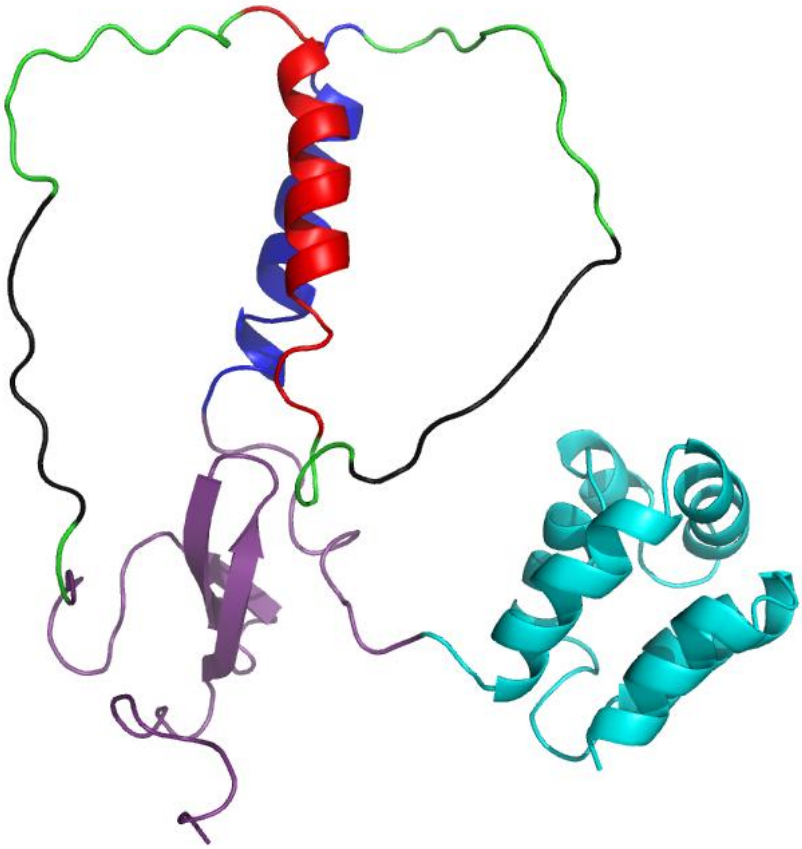

Figure 2.14: Model of the protease transducer PTK3_2The various domains are WW and WW ligand (violet), Linker (green), HIV Protease cut sites (grey), E3` blocking helix (red), K3 active helix (blue), DED domain (cyan). The model was built using Xfit and minimized using CNS.

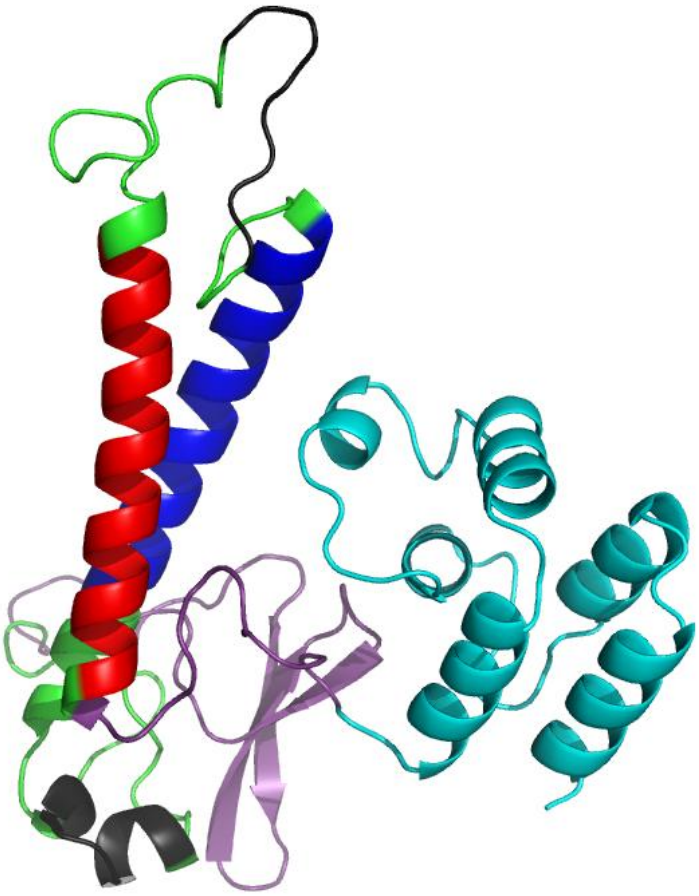

Figure 2.15: Model of the protease transducer PTE3_2. The various domains are WW and WW ligand (violet), Linker (green), HIV Protease cut sites (grey), K3` blocking helix (red), E3 active helix (blue), and DED domain (cyan). The model was built using Rosetta (*108*). The model generated differs from that built by Xfit in having the blocking and active helixes in an anti-parallel orientation. This anti-parallel orientation dictated by the presence of a single Asn residue in the hydrophobic core of the coiled coil (*84*).

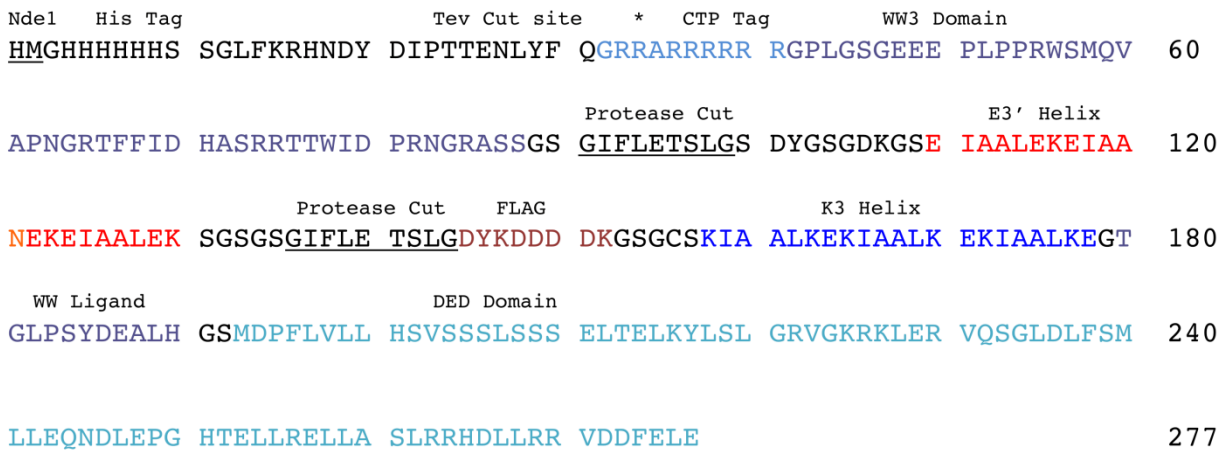

Figure 2.16: Sequence of PTE3_2 as designed after modeling the protein. The sequence was then synthesized with E. coli codon usage for protein expression.

CHAPTER 3: DESIGN, CONSTRUCTION AND TESTING OF THE ACTIVE DIMER

INTRODUCTION

The goal of the dissertation is to design and test an HIV-activated transducer protein. The transducer protein was designed to achieve apoptosis in HIV infected cells and leave uninfected cells unharmed. The viral protease cleaves the inactive transducer protein to yield an active molecule that hetero-dimerizes after cleavage within cells leading to the recruitment and activation of procaspase-8, eventually causing apoptosis.

This chapter is devoted to testing how well the transducer proteins meet the design criteria. The chapter aims to address a few design parameters that are part of the final protease transducer design. These parameters are:

1) Cell Killing: Is it possible to kill cells using the DED domain to recruit procaspase-8?
2) Cellular Targeting: Is it possible to get proteins into the cells as envisioned in our protease transducer design?
3) Induction of Apoptosis: At what concentrations of the active dimer do we induce apoptosis in cells?
4) Causes for apoptosis: Does the cytoplasmic targeting peptide alone cause apoptosis in cells?
5) Solubility of the proteins.

To address these questions, we first designed P5501, an active homodimer coiled coil system in which each monomer is tethered at the C-terminal end of the coil to the FADD-DED domain. The linker was a Gly-Ser repeat 14 residues long. The reasoning

for the length of the linker connecting the coiled coil to the DED domain has been described in Chapter 2.

In this first design iteration, we selected the TAT tag for protein transduction into cells as reported by Vocero-Akbani in their Trojan horse mechanism for targeting infected HIV cells (*109*).

The protein, P5501, was designed with a homodimerizing coiled coil WinZipA1(*77*) in mind. The helical representation for P5501 is given in Figure 3.1, and the final DNA and amino acid sequence of the protein is given in Figure 3. 2.

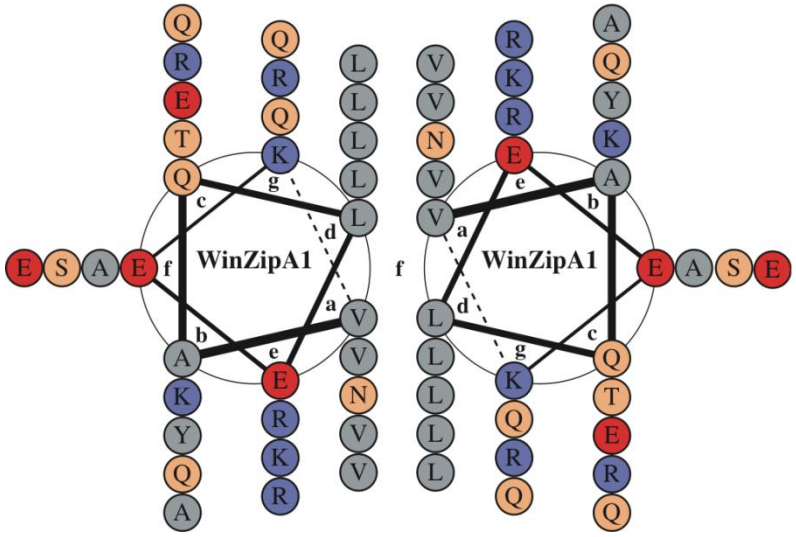

Figure 3.1: Helical diagram of the homodimer coiled coil WinZipA1 used in P5501. The 3 N-terminal capping residues and 2 C-terminal residues are not shown in the helical projection.

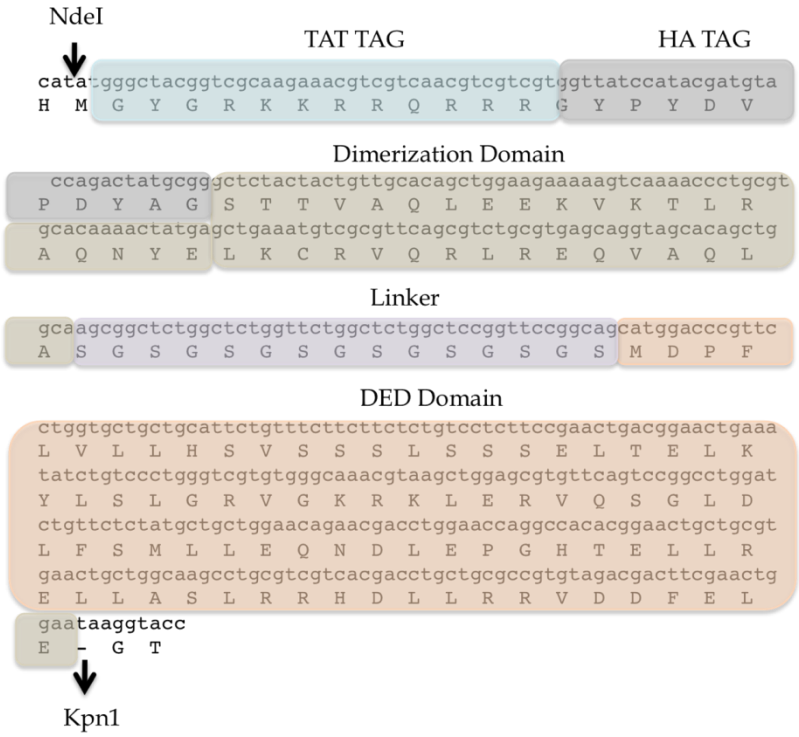

Figure 3.2: DNA and translated protein sequence for the homodimeric P5501 protein, the first design for the Active dimer.

ADDRESSING THE SOLUBILITY OF PROTEINS:

P5501 was abandoned for two reasons: low solubility of P5501 and identification of a new peptide transduction domain (*105*) with improved cellular uptake and cytoplasmic distribution as compared to the Tat tag.

The new design included a heterodimerizing coiled coil IAAL-E3/K3 which had been shown to have a high degree of heterospecificity and modest length (21 residues). The coiled coils used were primarily selected due to their helical characteristics as

mentioned in Chapter 2. They do not form homodimers and are random coils when monomeric with coiled coil structure attained only on heterodimerization. Additionally, peptides with this sequence have Kds of around 70nM(*110*).

As both P5501 and the newly designed proteins (CTD-E3/K3-DED) had issues with solubility in native buffer conditions, we had to determine which part of the active dimer was responsible for causing the solubility problems. The individual parts alone were soluble at NMR concentrations or were previously crystallized, so we began sequentially either deleting or replacing individual fragments of the active dimer (Figure 3.3).

We started by deleting the C-terminal DED domain as in the construct CTD-STPDED (Figure 3.4). This did not improve the solubility of the protein.

Next, we reasoned that the linker region separating the dimerization domain and the DED domain may be responsible due to the repetitious nature of the Gly-Ser linker (Table 3.1). The linker was replaced creating two versions, namely E3-L1-DED and E3-L2-DED (Table 3.1, Figure 3.4). Replacing the linkers did not improve the solubility of the constructs made.

The deletion of the dimerization domain between the linker and CTD-tag improved the solubility of the protein: CTD-DED (Figure 3.4). A new active dimer was constructed based on the active molecules BPC-E3/K3 (Figure 3.4) formed within the cells from cleavage of the protease transducers by HIV protease. These proteins were soluble. Based on the sequence of BPC-E3/K3, the polyarginine CTD tag was replaced with a more acidic FLAG tag to improve the solubility of the proteins. In addition, a new linker was introduced, the WW ligand between the dimerization domain and the DED domain. This linker, “Linker 3”, was derived from the protease transducer.

An active dimer is needed to transduce into cells. Replacement of the N-terminal FLAG tag with a CTD tag was considered, keeping all other parts of the protein constant with BPC-E3/K3 for cellular uptake. The presence of the N-terminal FLAG was thought to be detrimental to cellular uptake due to the intramolecular electrostatic interactions between the highly positive CTD tag and negatively charged FLAG tag, a property that has been previously demonstrated (*111*). Replacing the N-terminal FLAG tag with the CTD tag negatively changed the solubility properties of the protein: NF-K3-DED (Figure 3.4). Moving the FLAG tag to the C-terminal end of the DED domain improved the solubility of the protein CTD-E3/K3-DEDF (Figure 3.4).

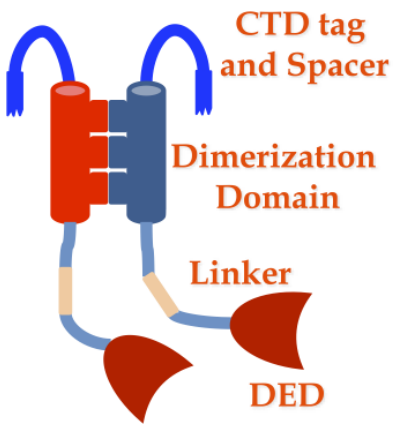

Figure 3.3: A cartoon representation of the active dimer with a core dimerization domain.

NAME	N-TERMINAL TAG	COILED COIL	LINKER	DED DOMAIN	SOLUBILITY
P5501	TAT Tag, HA tag	+	(GS)7	+	
E3-DED	CTP, HA tag	+	(GS)7	+	INSOLUBLE
CTD-DED	CTP, HA tag	N/A	(GS)7	+	SOLUBLE
CTD-STOPDED	CTP, HA tag	+	(GS)7	N/A	INSOLUBLE
CTD-TETRA-DED	CTP, HA tag	+	(GS)7	+	INSOLUBLE
E3-L1-DED	CTP, HA tag	+	GGGSGGGTGGGSGG	+	INSOLUBLE
E3-L2-DED	CTP, HA tag	+	GASGGGSTRGHY	+	INSOLUBLE
BPC	Flag tag	+	GTGLPSYDEALHGS	+	SOLUBLE
NF-K3-DED	CTP tag	+	GTGLPSYDEALHGS	+	INSOLUBLE
CTD-E3/K3-DEDF	CTP tag	+	GTGLPSYDEALHGS	+, Flag	SOLUBLE

Table 3.1: A list of active dimers constructed to solve the solubility problems associated with the original E3/K3-DED proteins.

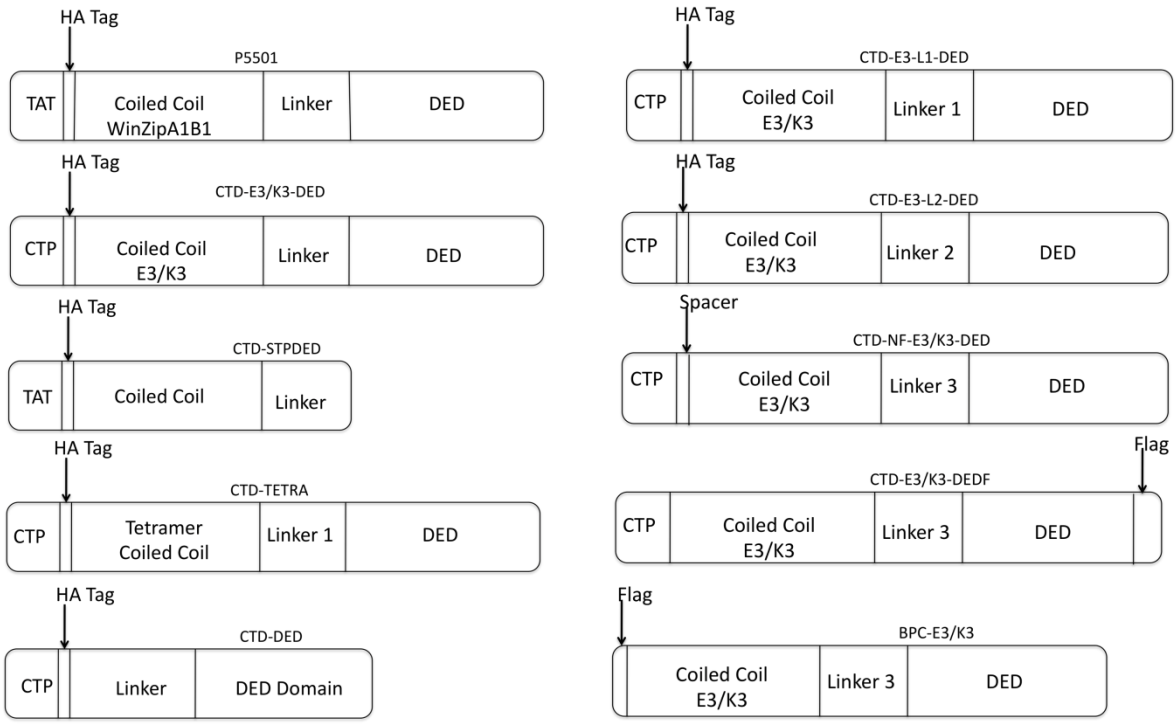

Figure 3.4: Block representation of the various constructs mentioned in Table 3.1.

Replacing the dimerization domain with a tetramerization domain (*112*) was also tested. . An active tetramerization system was designed to induce a switch like on/off state within the cells (CDT-Tetra in Figure 3.5).

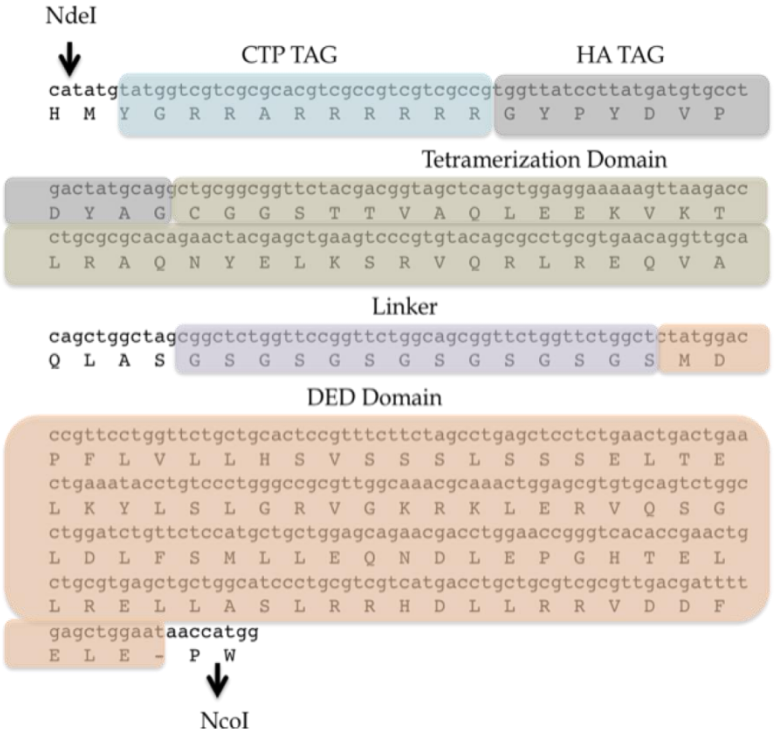

Figure 3.5: CTD-Tetra DNA sequence and translation of the CTD-Tetra protein.

On comparing the solubility properties of the various constructs, the presence of the CTP tag, a very positively charged tag, reduces the overall solubility of the proteins. By comparing the charge average with and without the CTP or FLAG tag, the predicted solubility of the proteins based on CV-CV` where negative values infer greater solubility (*113, 114*), helps better predict the solubility behavior in native buffer conditions, conditional to whether one is dealing with a globular folded protein or predominantly unstructured protein.

In parallel to testing various constructs to improve the solubility of the active dimer, various buffer conditions for refolding our proteins were evaluated (Table

3.2)when constrained to compatibility with tissue culture, a significant fraction of the conditions tested for keeping our proteins soluble were discarded. It was on further analysis of the conditions that arginine as an additive was identified to improve the solubility of our proteins (Figure 3.6). The use of arginine as a solubility-enhancing additive is well reported. Using arginine as the solubility additive, we tested out the 2nd generation of active dimers (CTD-E3/K3-DED). In addition to arginine, proline in PBS was sufficient to keep our proteins (CTD-E3/K3-DED) in solution for cell studies. As proline as an additive was identified quite late in the work, much of what is discussed here is work done with Arginine HCl as an additive. We are currently close to testing the proteins CTD-E3-DED/K3-DED in a proline containing buffer on uninfected H9 cells.

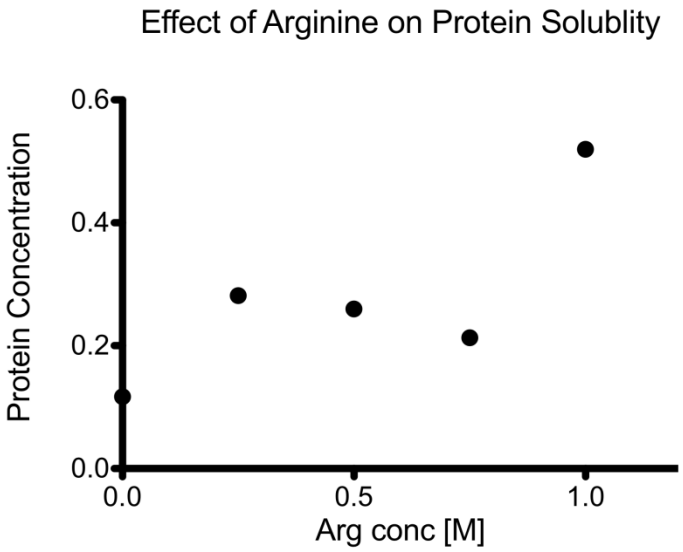

Figure 3.6: Increasing concentrations of arginine help improve the solubility of the protein P5501.

	Buffer	Salt	Salt	Cation	Chaoptropic Agent	Reducing Agent	Additive	Additive1	Temp
1	MES 4.0	214mM	11mM	2mM 2mM		5mM		0.06%	RT
2	MES 4.0	214mM	11mM			10mM	10mM		RT
3	MES 4.0	214mM	11mM			10mM	10mM	1%	RT
4	MES 4.0	214mM	11mM	2mM 2mM		10mM		0.06%	RT
5	MES 4.0	214mM	11mM			5mM		0.06%	RT
6	MES 4.0	214mM	11mM			10mM		0.06%	RT
7	MES 4.0	214mM	11mM			5mM		2%	RT
8	MES 4.0	214mM	11mM			10mM		2%	RT
9	MES 4.0	214mM	11mM			5mM	10mM	0.06%	RT
10	MES 4.0	214mM	11mM			5mM	10mM		RT
11	MES 4.0	214mM	11mM	2mM 2mM		5mM		0.06%	4C
12	MES 4.0	214mM	11mM	2mM 2mM		5mM	440mM Sucrose	0.06%	RT
13	MES 4.0	214mM	11mM	2mM 2mM		5mM	440mM Sucrose	0.06%	RT
14	MES 4.0	214mM	11mM	2mM 2mM		5mM	440mM Sucrose	0.06%	4C
15	Tris 8.2	18mM	8mM		Guanidine 0.4M	5mM			4C
16	Tris 8.2	18mM	8mM		Guanidine 0.4M	X1	0.4M Arginine		4C
17	Tris 8.2	18mM	8mM		Guanidine 0.4M	X1	0.8 Arginine		4C
18	Tris 8.2	18mM	8mM		Guanidine 0.9M	X1			4C
19	Tris 8.2	18mM	8mM		Guanidine 0.9M	X1	0.4 Arginine		4C
20	Tris 8.2	18mM	8mM		Guanidine 0.9M	5mM	0.8 Arginine		4C
21	Tris 8.2	18mM	8mM		Guanidine 1.4M	X1			4C
22	Tris 8.2	18mM	8mM		Guanidine 1.4M	5mM	0.4 Arginine		4C
23	Tris 8.2	100mM			1.2M Urea	5mM			RT
24	Tris 8.0	150mM				5mM	1M Arginine	10mM	RT
25	potassium phosphate 8.0	300mM NaCl				10mM	1M		RT

Table 3.2: Refolding conditions that have been attempted with the E3DED to determine conditions where the protein was found to remain in solution as determined by UV spectroscopy. The conditions supplemented with Guanidine or Arginine Hydrochloride kept the proteins in solution.

TESTING THE PROTEINS:

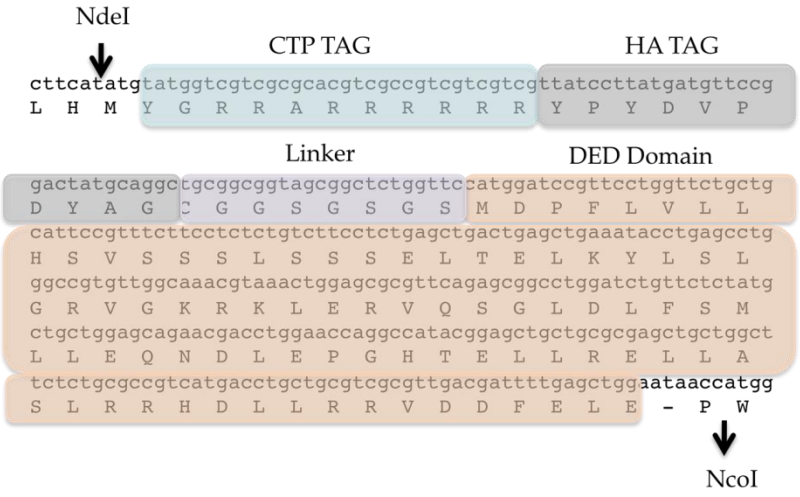

Figure 3.7: CTD-DED DNA sequence and translation of the positive control protein designed and constructed from CTD-Tetra.

As the CTD-DED protein (Figure 3.7) was more soluble than other proteins we constructed, it was used to determine whether there was cellular uptake of the protein and at what concentration the DED domain would cause apoptosis in cells. The protein was fluorescently labeled and incubated overnight with Jurkat cells. Uptake of the protein was determined by Flow Cytometry. The cell population showed a progressive uptake of the protein with increasing protein concentration (Figure 3.8). By comparing the distribution of cells between trypsin treated and untreated cells, most of the protein was associated with the cells.

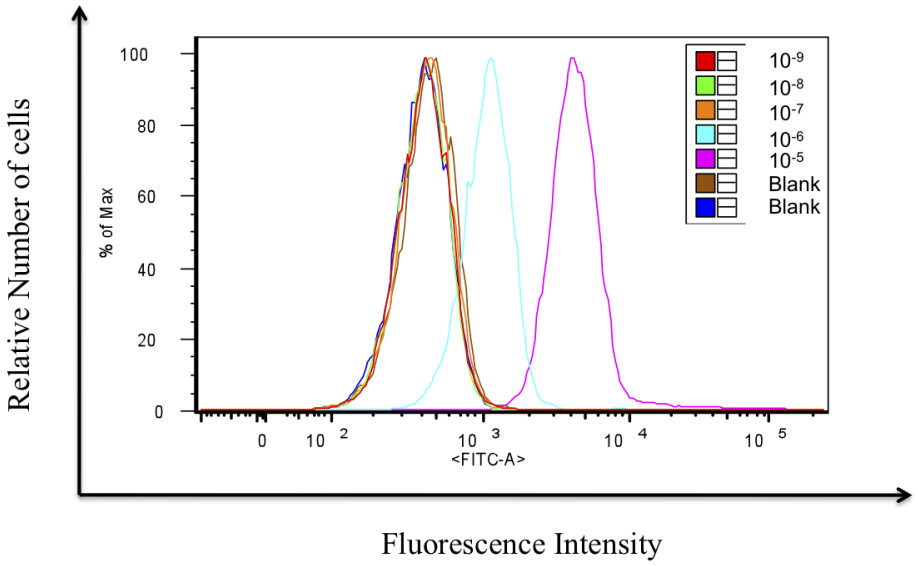

Figure 3.8: Uptake of monomeric CTD-DED into Jurkat cells. Jurkat cells were treated with increasing concentrations of CTD-DED. The cells were incubated for 15 hrs and treated with 7-AAD and analyzed using the BD FacsCanto flow cytometer. Total number of events collected was 10,000. The population was gated on Fluorescein emission at 535 nm. Data were analyzed using Flowjo.

We tested the proteins CTD-E3-DED/CTD-K3-DED individually and mixed together on Jurkat cells overnight and analyzed the sample for apoptosis. As a control for the addition of L-Arginine HCl in the buffer, equivalent-volume buffer blanks without the protein were also tested against Jurkat. After overnight incubation, the cells were analyzed by flow cytometry. Overnight incubation showed that 80% of all cells were either Annexin V+/7-AAD -ve or Annexin V+/7-AAD +ve, however, there was significant apoptosis observed in the corresponding buffer blanks (Figure 3.9). The difference in the apoptosis rates observed between the buffer and the premixed sample of CTD-E3-DED/CTD-K3-DED leads us to believe that our positive controls are active within the cells. To address the issue of buffer artifacts, the time Jurkat cells were exposed to the protein and buffer was reduced from 15 hrs to 1 hr. Additionally we

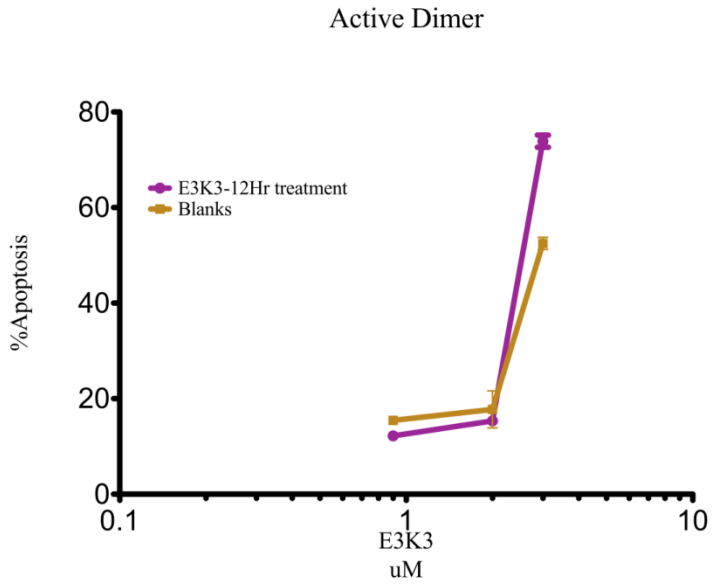

Figure 3.9: Overnight incubation of Jurkat cells with the Active dimers showed significant apoptosis (Annexin V+/7AAD-ve; Annexin V+/7AAD+). Buffer alone shows significant amount of apoptosis due to the high ionic strength contributed by the use of L-Arginine HCl. SEM derived from two experiments.

incorporated a trypsin digestion step following the 1 hr incubation. The trypsin digestion step following protein incubation was to rid all cell surface bound transducer proteins. The individual monomers alone and premixed were tested. The CTD-E3-DED monomer (Figure 3.10) does not induce apoptosis even at higher concentrations when compared to CTD-K3-DED (Figure 3.11). This difference in induction of apoptosis can be attributed to a small fraction of CTD-K3-DED forming trimers as seen by sedimentation velocity (data not shown).When the two monomers were premixed and incubated with cells for an hour followed by additional 12 hours incubation, apoptosis was induced at a much lower concentration in the dimers when compared to the individual monomers, with a 10-28% apoptosis seen at 3uM when compared to the monomers on their own (Figure 3.10, 3.11). Due to the problems associated with the ionic strength of arginine and its ability to induce apoptosis (Figure 3.12), we tried to resolve the protein solubility issue by modifying different parts of the active monomer. Various constructs were tested to improve the solubility of the proteins as previously mentioned (Table 3.2.)

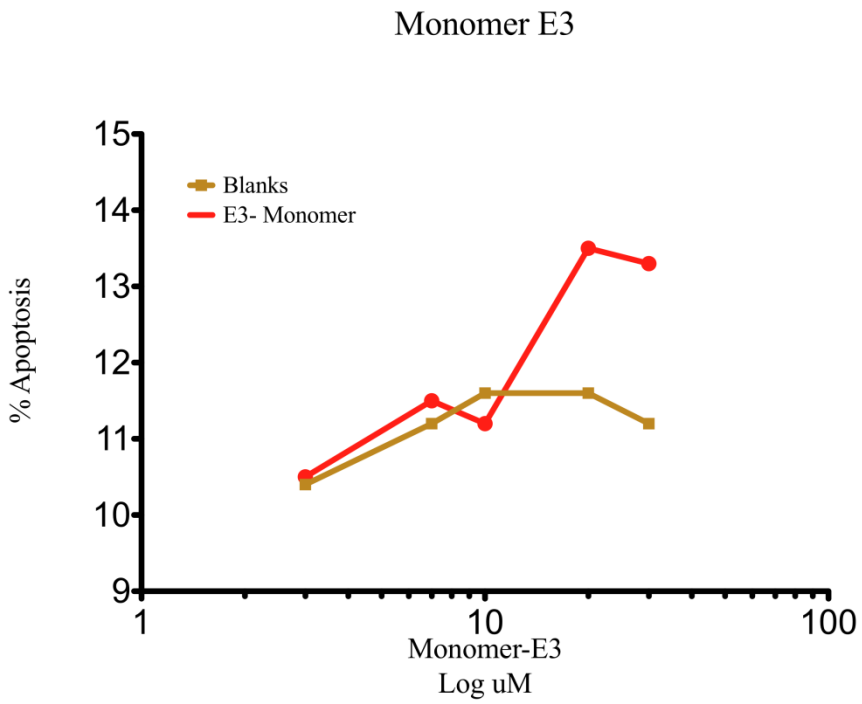

Figure 3.10: Overnight incubation of Jurkat cells with E3-DED showed apoptosis (Annexin V+/7AAD-ve; Annexin V+/7AAD+). Buffer alone shows significant amount of apoptosis due to the high ionic strength contributed by the use of Arginine HCl.

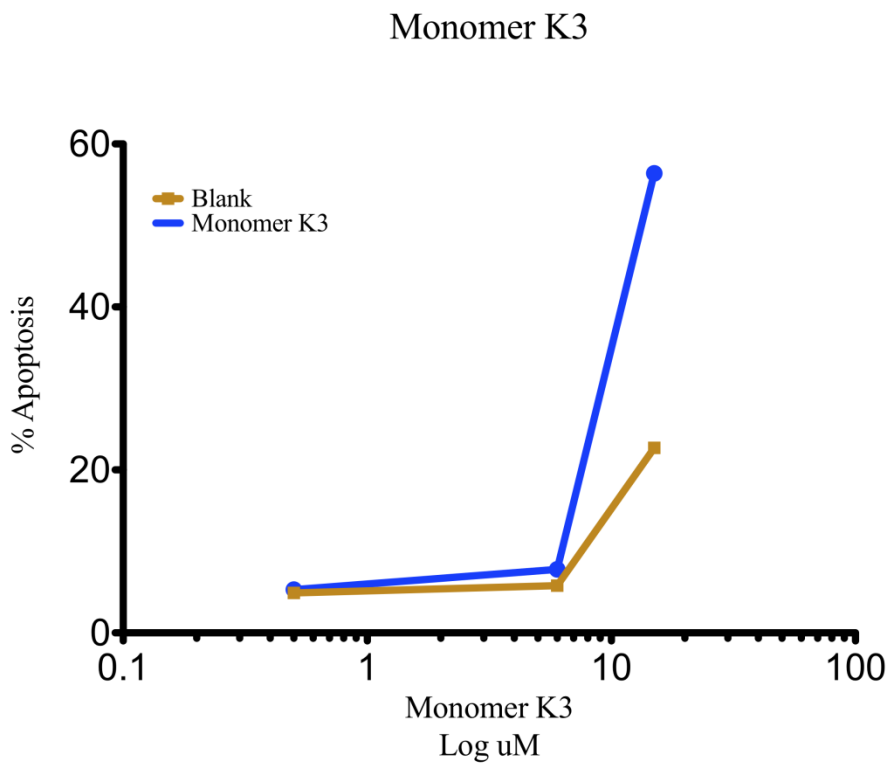

Figure 3.11: Overnight incubation of Jurkat cells with K3-DED showed apoptosis (Annexin V+/7AAD-ve; Annexin V+/7AAD+). Buffer alone shows significant amount of apoptosis due to the high ionic strength contributed by the use of Arginine HCl

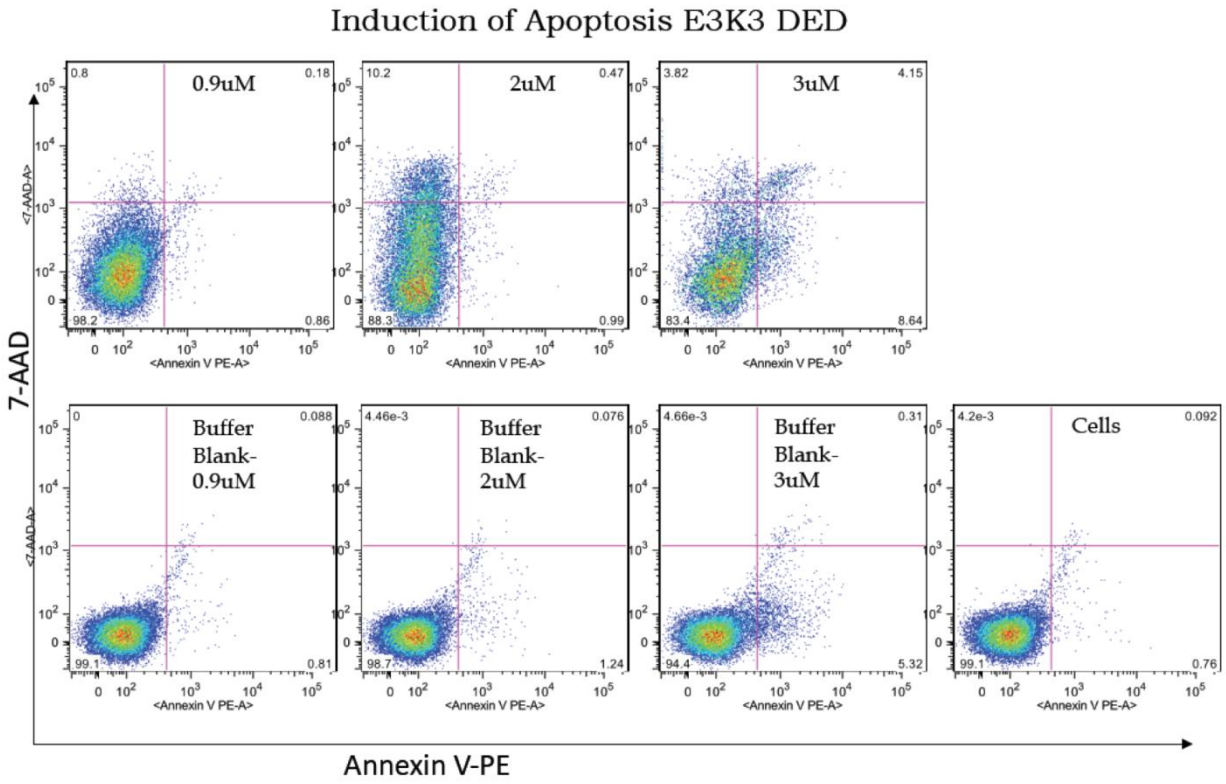

Figure 3.12: Jurkat cells treated with protein E3/K3-DED for 1 hr followed by 15-hour incubation. As the proteins are soluble only in the presence of arginine, volume equivalence of buffer without proteins was also tested. Annexin V is an early indicator of apoptosis, 7-AAD binds DNA and indicates late apoptosis.

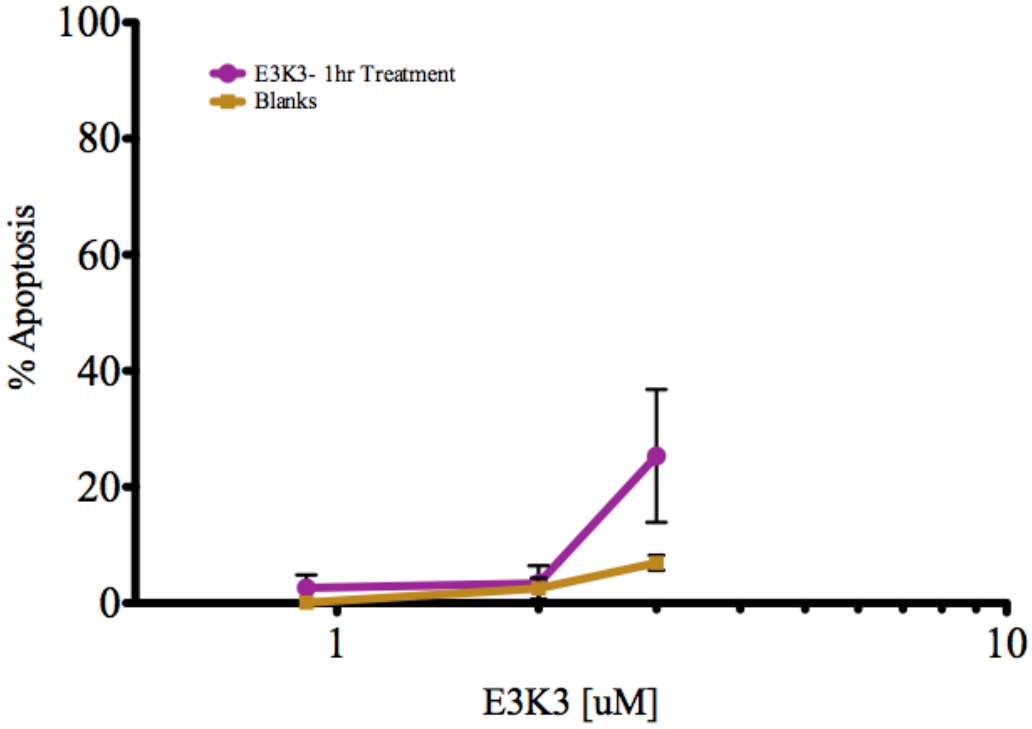

Figure 3.13: Induction of apoptosis by proteins E3/K3-DED on Jurkat cells treated for 1 hr followed by 15 hrs incubation. The cells were analyzed for apoptosis using Annexin V and 7AAD as apoptotic markers. SD derived from three independent experiments.

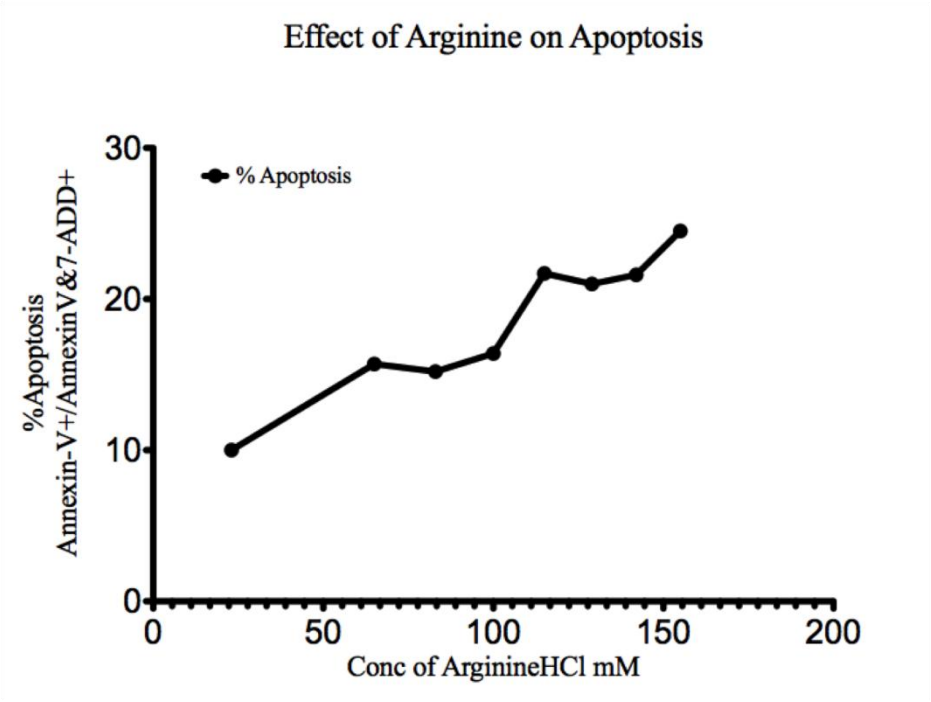

Figure 3.14: Effect of Arginine HCl on Jurkat cells: Increasing concentrations of L-Arginine had a direct effect on increasing levels of apoptosis. The cells were treated overnight followed by analysis by flow cytometry. The percentage early apoptotic and late apoptotic are plotted against ArginineHCl concentration. 10,000 events were measured and the percent Annexin V+ or Annexin V+/7AAD+ve are plotted.

FLUORESCENCE IMAGING OF CELLS

As we were interested in testing the effect of active dimers (CTD-E3/K3-DED) in cells, we were also interested in the uptake of the proteins into cells. Previously it had been reported that cells show uniform uptake of transduced protein. However based on the type of tag used, the transduced protein was either predominantly in vesicles or was unevenly distributed between the cytosol and the nucleus, with distribution being predominant in the nucleus. Jurkat cells were treated for 2 hours with 2.5uM of fluorescein labeled CTD-E3-DED to determine cellular distribution. After two hours the

cells were either treated or not treated with 0.25% Trypsin and immobilized on a poly lysine coated slide and imaged under a fluorescence microscope. Based on the images shown in Figure 3.15, cells treated with the labeled CTD-E3-DED show a uniform distribution in the cells. This uniform distribution is not lost even after digestion with trypsin. In addition, trypsin treatment changes the cell surface properties of Jurkat. Untreated cells do not adhere to each other, whereas trypsin treatment shows a high degree of clumping, and affect the size and shape of the cells.

To better understand the distribution of the transduced protein in cells, a more powerful technique like confocal imaging with nucleus specific dyes may help better understand and characterize cellular distribution.

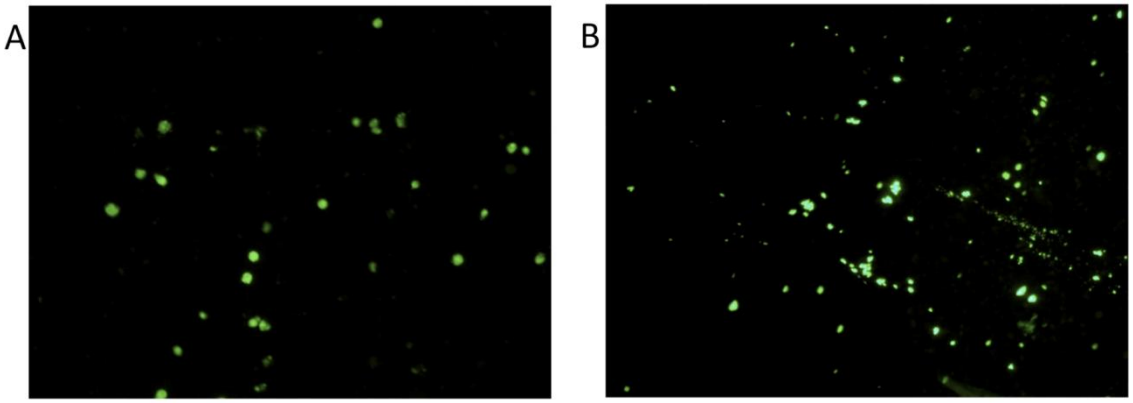

Figure 3.15: Fluorescence imaging of Jurkat cells treated with 2.5uM of fluorescein labeled CTD-E3-DED for two hours. The cells were coated onto a polylysine-coated slide and imaged under a fluorescence microscope. Figure A) Cells treated with CTD-E3-DED without trypsin digestion. Figure B) Cells treated with CTD-E3-DED followed by trypsin digestion for 5 minutes at 37°C.

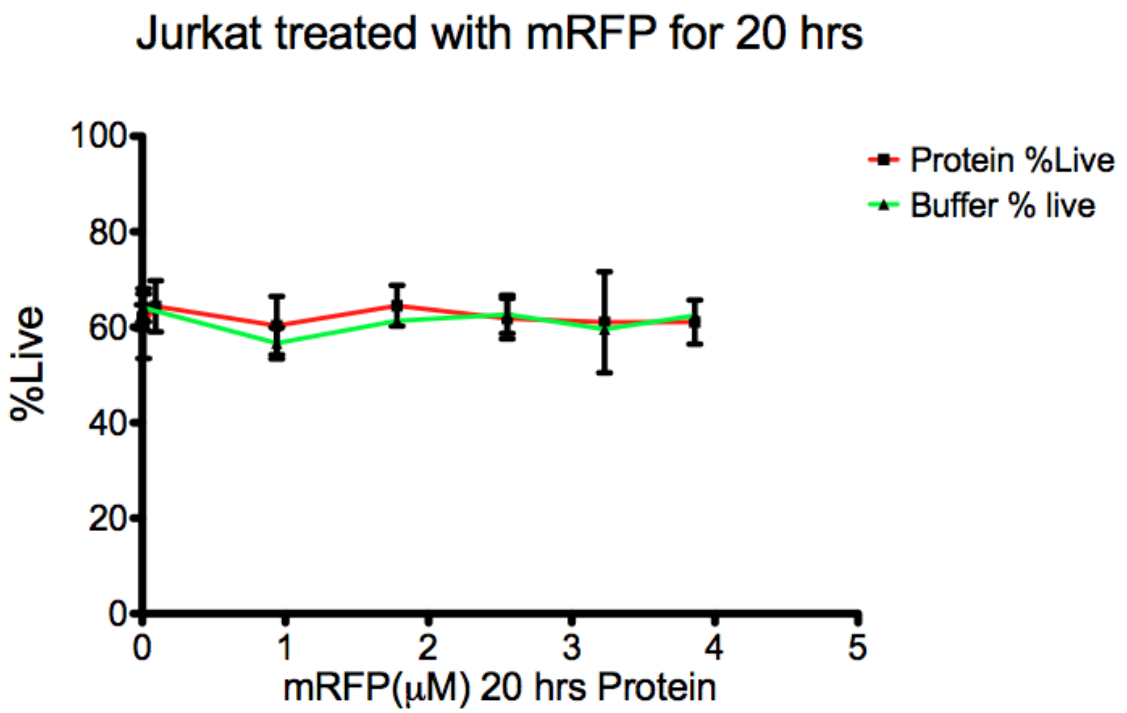

Figure 3.16: CTP tag does not cause apoptosis in Jurkat cells. Jurkat cells were treated with CTD-mRFP and analyzed by Trypan Blue exclusion assay using a TC 10 counter after 20hrs. CTD-mRFP does not cause increased apoptosis in cells, validating our use of the CTP in various protein constructs. Three samples were measured and plotted with SD.

CYTOTOXICITY OF CTP TAG

It has been shown that commonly used cellular targeting peptides show cytotoxicity (*115, 116*). To address the question of cytotoxicity mediated by the cytoplasmic targeting peptide used throughout this dissertation, a CTP tagged monomeric Red fluorescent protein (*117*) was constructed, a protein that has been used substantially in cell biology applications with no apparent cytotoxicity. Additionally, it has been shown that highly charged GFPs are taken up by mammalian cells without cytotoxic effects (*118, 119*). Based on these published results, it was confirmed that CTD-mRFP

protein is not cytotoxic against Jurkat cells and hence the addition of the CTP tag did not induce apoptosis in Jurkat cells (Figure 3.15).

In one of the pairs of active dimers constructed (E3DEDF, K3DEDF), it was found the proteins, though soluble, caused significant apoptosis when incubated with Jurkat cells overnight either as monomers or as mixed heterodimers. Based on this observation, moving the FLAG tag to the C-terminal end of the DED domain did not serve the design criteria: monomeric protein (E3/K3-DED) being inactive within the cell and only the heterodimer actively inducing apoptosis.

AFFINITY OF THE ACTIVE DIMERS

In addition to determining whether the individual active monomers are capable of inducing apoptosis on their own and when mixed together, dimerization constants of the active monomers after HIV proteolysis of the protease transducers were determined. After proteolytic cleavage, two active monomers are formed that interact to yield the active dimer (Figure 3.16).

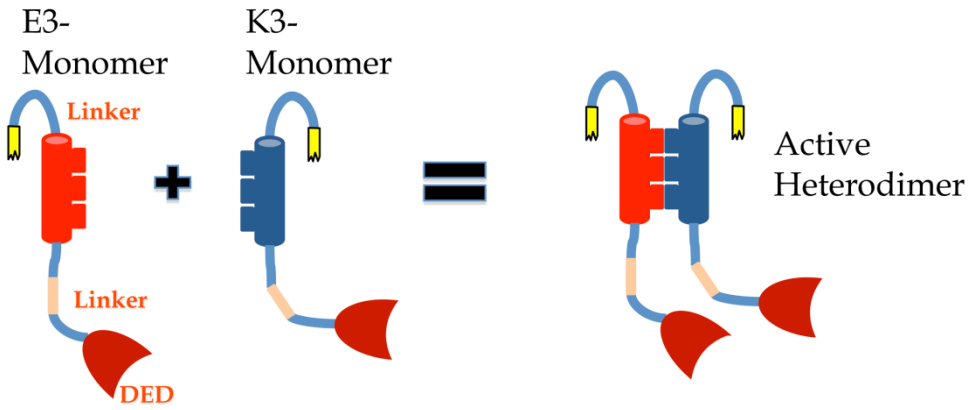

Figure 3.17: A cartoon representation of the interaction of BPC-E3-monomer with the BPC-K3-monomer to yield the active heterodimer. Due to the addition of the N-and C-terminal domains to the core coiled coils, the dimerization constant was determined to understand the affect volume exclusion has on affinity.

Due to volume exclusion effects introduced by the addition of N and C-terminal residues to the 21 residue coiled coil, a determination of whether there would be a significant difference between the dimerization affinities of the coiled coil peptides vs. the active heterodimers was made. By comparing the effective concentration of the protein within the cell to the dimerization constant of the two monomers, allows us to better iterate over the protease transducer design by modulating the affinities of the dimerization domains used.

To address this issue, FRET (Förster resonance energy transfer) was used to determine the Kd between the two monomers. Based on the quenching of fluorescence intensity of BPE3-Alexa Fluor 488 on the addition of the BPK3 monomer labeled with the fluorophore Alexa Fluor 633 (Figure 3.17), the Kd_{app} of the two monomers was 105nM (Figure 3.18). When compared to the previously published value

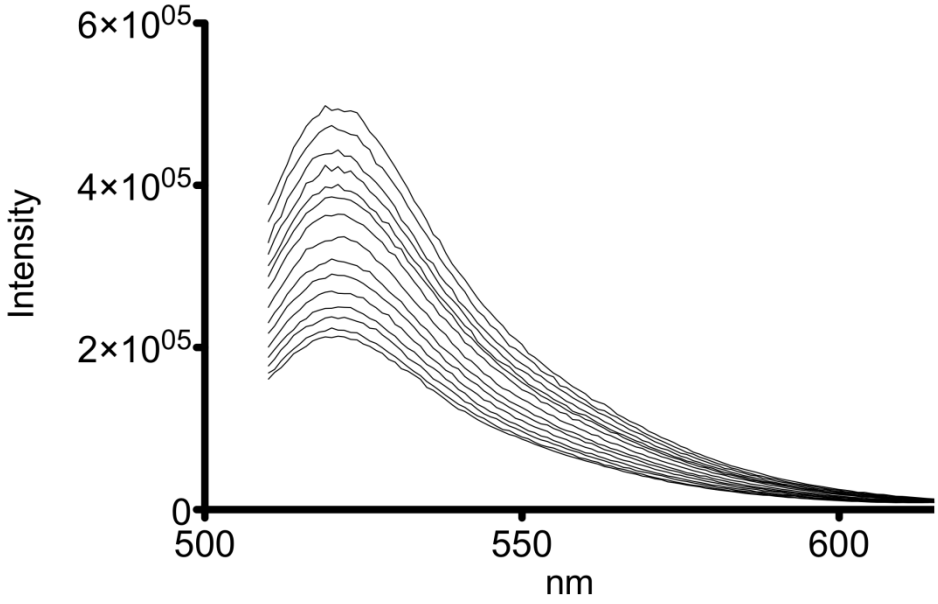

Figure 3.18: Decrease in intensity of BPE3-AF488 with increasing concentrations of BPK3-AF633. The integrated intensities from 510-550nm were plotted and used to determine the affinity between the two monomers (BPE3 and BPK3)

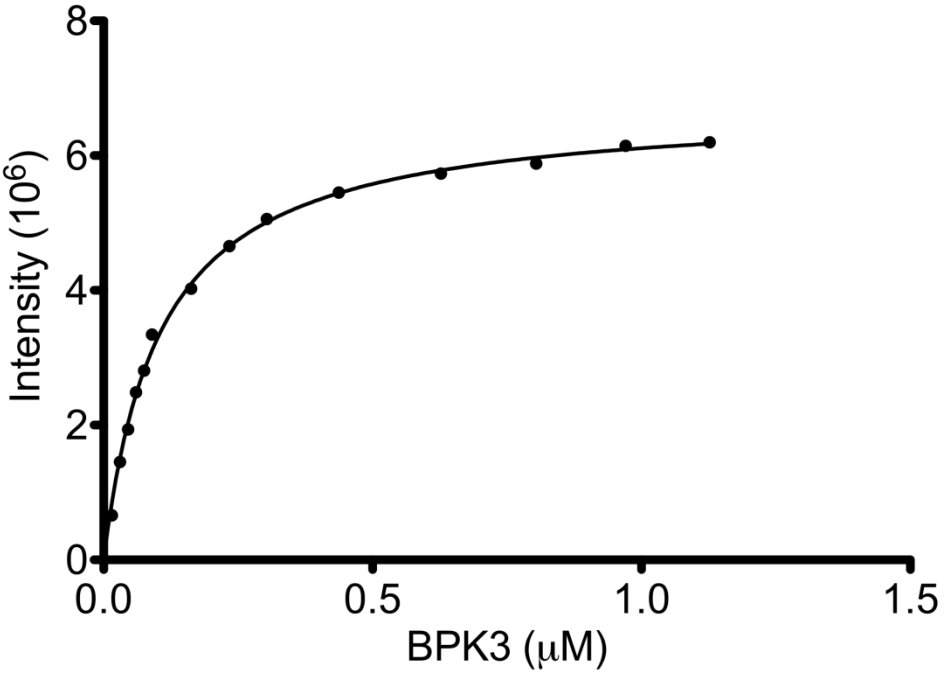

Figure 3.19: The change in integrated intensities from Figure 3.18 was plotted against concentration of BPK3. The data were fit using Prism.

of 70nM, the addition of N and C-terminal residues does not significantly impact the affinity of the coiled coils.

CONCLUSION:

The primary aim for the work presented in this chapter was to determine whether we could design proteins that would be taken up by the cells from the medium. This was clearly seen in the case of the CTD-DED, CTD-E3-DED and CTD-K3-DED proteins. Additionally, it was determined whether it would be possible to induce apoptosis in cells using the DED domain as a recruitment domain for procaspase-8 associated with a heterodimerizing domain. Though we do see an increase in apoptosis in cells when

incubated with the heterodimer, due to the problems associated with solubility we have not been able to completely resolve the true effect of the active dimer in inducing apoptosis. Currently new buffer conditions that include the addition of 1M Proline to improve the solubility of the proteins have been identified. Further studies will aim to determine the active dimers ability to induce apoptosis without the buffer artifacts due to Arginine HCl. Addition of a random coil followed by a spherical DED domain to the E3K3 peptides was thought to change the affinities of the E3K3 coiled coils to each other due to volume exclusion effects. We observe that the affinities of the coiled coils are within a factor of two to the published values. This allows us to continue using the published values for various coiled coils in future iterations of the design of the protease transducers.

The active heterodimer (CTD-E3/K3-DED) shows a 12% induction of apoptosis. It may be possible to increase the ability of the active heterodimers to induce apoptosis by modifying key elements of design. By modifying the linker lengths connecting the active helix to the DED domain, one will be able to modulate procaspase-8 recruitment. Increasing the length of the linker from the current 14 residues to ones that are longer may prevent any steric clashes with the active monomer and procaspase-8. Alternatively reduction in length of the linker, thereby effectively reducing the volume sampled by the bound procaspase-8, increases its effective concentration for procaspase-8 trans-cleavage.

Construction of the plasmids:

Most of the proteins constructed in this dissertation were done by assembly PCR as given in Figure 3.16.

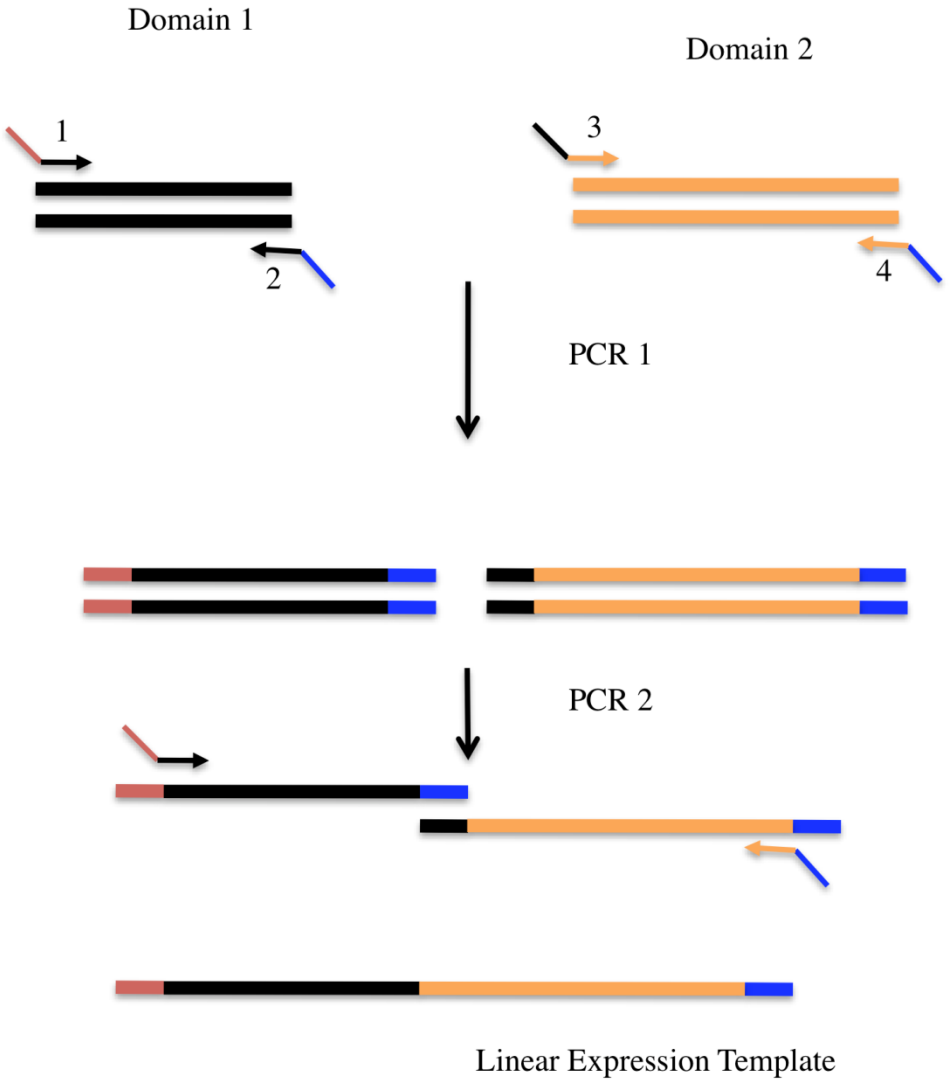

Figure 3.20: A cartoon representation of assembly PCR used to construct the various proteins tested.

Construction of CTD-DED: The gene for CTD-DED was constructed from the CTD-Tetra (DNA- 2.0) by assembly PCR using the primers -

1. >CTP-HA-Forward:

5'-CATATGTATGGTCGTCGCGCACGTCGCCGTCGT

2. >CTP-HA-DED-Reverse:

5'-CCAGAGCCGCTACCGCCGCAGCCTGCATAGTC

3. >CTP-HA-Overlap-F:

5'CTGCGGCGGTAGCGGCTCTGGTTCC

The gene that was constructed was ligated to the pCR2.1 TA cloning vector and transformed into DH5alpha cells. Individual colonies were selected and the sequence of the insert confirmed. The sequence confirmed gene was then cut with *Nde1* and *Nco1* and the gene ligated to YP001 previously linearised with the same restriction sites. The ligated product was transformed into BL21DE3 cells.

The primers used to construct E3-L1-DED:
>Nde1-E3-F:
GTCGCTGACATATGTATGGTCGTCGTGCTCGT
>Linker-E3-Rev
CAGTACCGCCTCCAGATCCGCCACCCTTCTCCAGCGCAGCGATCTCTTT
>Linker-DED-For
GGAGGCGGTACTGGAGGGGGATCAGGAGGAATGGACCCTTTTCTGGTACT
>DED-Rev-AS
GACGCCATGGTTACTCCAGCTCAAAATCATC

The primers used to construct E3-L2-DED:
>Nde1-E3-F:
GTCGCTGACATATGTATGGTCGTCGTGCTCGT
>E3-Coil-L2-AS
AGTAGAACCGCCTCCAGAAGCACCCTTCTCCAGCGCA
>L2-DED-For
GGAGGCGGTTCTACTGGAGGTCATTATATGGACCCTTTTCTGGTACTGCT

>DED-Rev-AS
GACGCCATGGTTACTCCAGCTCAAAATCATC

Construction of BPE3/BPK3: The genes for BPE3 and BPK3 were constructed from the parent genes PTE3_2 and PTK3_2. The primers used were

1)>Nde1-Prot1-F:

CATATGCTGGAAACCAGCCTG

2)>Nco1-PTE3_2-R:

5'CCTGCTGAAGCTCGACCTCATTGGTACCGGGGGATCGTATTGG

The PCR product was ligated to the pCR2.1 TA cloning shuttle vector and transformed into DH5alpha cells, individual colonies were selected, checked for the presence of the insert, sequenced and the insert cut out from the plasmid with Nde1 and Nco1. The insert was then ligated to the expression vector YP001 previously cut with Nde1 and Nco1. The ligated plasmid was transformed into BL21DE3 cells (NEB).

Construction of CTD-E3/K3-DEDF: The genes were constructed from the parent genes PTE3_2 and PTK3_2. The primers used were

1) > NoFLAG-PT*3_2-F

CCGTCGCGGTGAAACCAGCCTGGGTAGCGGCTGCAGC

2) CTD-NoFLAG-PT*3_2-F

CATATGCGTCGTGCGCGTCGTCGTCGCCGTCGCGGTGAAA

3)>DED-FLAG-R

CCATGGTTACTTATCATCGTCGTCCTTGTAGTCCTCCAGCTCGAAGTCGTCCA

CACG.

The product treated similar to BPE3/BPK3. The insert ligated to YP001 cut with *Nde1* and *Xho1*.

CTD-mRFP was constructed by PCR from plasmid 13032:pcDNA3-mRFP (courtesy Roger Tsien, UCSD). The primers used were

1. mRFP-1: TCGTCGCCGTCGCATGGCCTCCTCCGAG
2. mRFP-2 :CATATGCGTCGTGCGCGTCGTCGTCGCCGTCGC;
3. mRFP-R-AS:CCATGGTTATTAGGCGCCGGTGGAGTG.

The final product was ligated to YP001 at an *Nde1-Xho1* site.

Expression of the Proteins:

The expression plasmids were transformed into BL21DE3 cells. The cells were plated on LB plates supplemented with 100ug/ml ampicillin. Individual colonies were selected and grown in 50ml of LB overnight. The 50ml seed was used to inoculate 2L of LB supplemented with 100ug/ml ampicillin. At OD600 = 0.8 the cells were induced with 1mM IPTG. The cells were incubated at room temperature overnight.

CTD-mRFP was grown in 2L of 2YT medium at 37°C. At OD 600 of 0.4, the cells were induced with 1mM IPTG. Induced cells were grown at 37°C for 5 hrs.

Purification of proteins:

After induction, the cells were spun down and resuspended in Buf1A [300mM NaCl, 50mM Tris, pH 8.0, 5mM BME]. The cell suspension was sonicated and then spun down at 17K rpm in an SS-34 rotor.

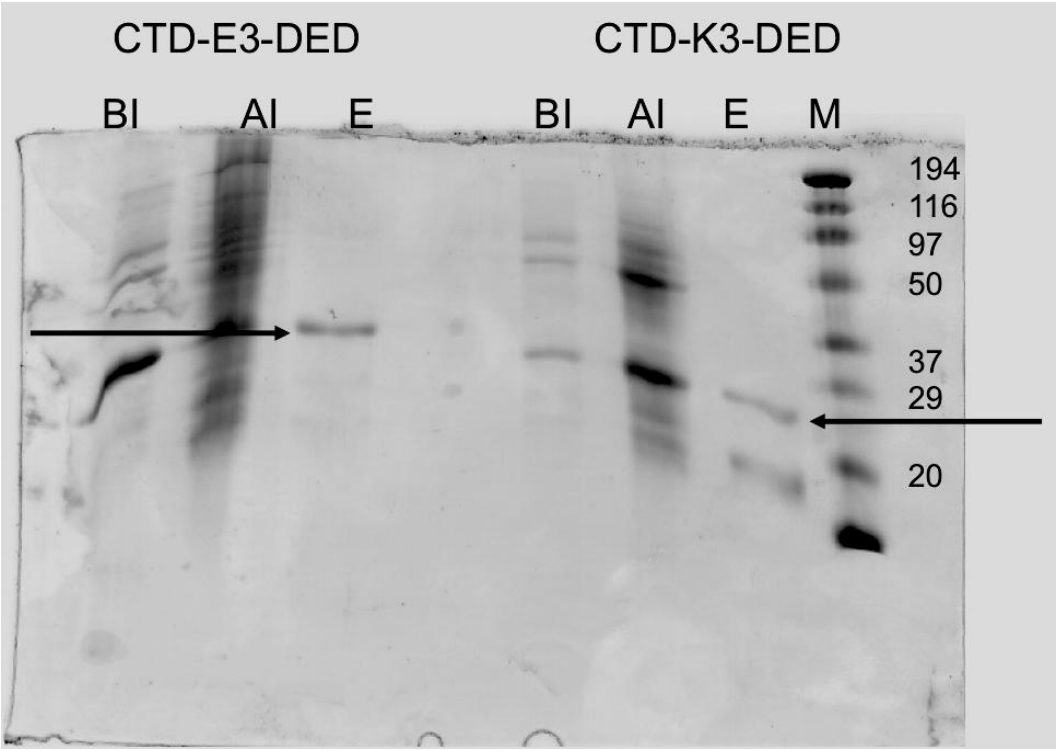

Figure 3.21: Expression and purification of CTD-E3/K3-DED. The proteins were expressed and purified in 6M GnHCL. BI: Before induction, AI After induction, E elute in 6M GnHCL.

For proteins CTD-E3-DED, CTD-K3-DED, CTD-DED, CTD-L1-DED, CTD-L2-DED, BPE3, and BPK3, the cell pellet was then resuspended in 6M GNHCL, 50mM Tris, 5mM BME, pH 8.0[EquiBuf]. The suspension after thorough mixing was spun down as earlier. The supernatant was loaded onto a Ni-NTA fast flow column (Qiagen) pre-equilibrated with 6M GNHCL, 50mM Tris, 5mM BME. After load, the column was washed with EquiBuf. After OD280 reached baseline, the protein was eluted with EquiBuf containing 1M imidazole.

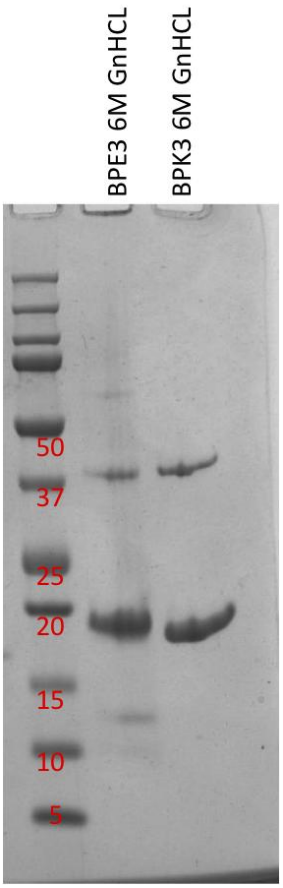

Figure 3.22: NI-NTA purification of BPE3/BPK3. The proteins were purified in 6M GnHCL.

The proteins CTD-DED, BPE3, and BPK3were eluted in 6M GnHCl and then rapidly diluted to 0.1mg/ml. The diluted protein was dialyzed extensively against 300mM NaCl, 50mM Tris, pH 8.0 10mM BME at room temperature. After dialysis, the protein solution was spun down to pellet out any precipitate. TEV protease at a concentration of 1mg/ml was added to the refolded protein to cut the His tag; cleavage at room temperature was performed overnight without shaking. Then, the cut protein was loaded onto a fresh Ni-NTA column equilibrated with EquiBuf; the protein flow through was reloaded onto the column several times to ensure complete binding of the uncut protein and Tev. The flow through was collected and concentrated for further studies. BPE3 and

BPK3 in 300mM NaCl, 50mM pottasium phosphate, 5mM BME pH 8.0 was further purified on a Superdex-75 sizing column.

For proteins CTD-E3-DEDF/CTD-K3-DEDF, the cell pellet was resuspended in 8M Urea, 300mM NaCl, 50mM Tris, 5mM imidazole, 5mM BME, pH 8.0[EquiBuf2A]. The suspension, after though mixing overnight, was spun down as earlier. The supernatant was loaded onto a Ni-NTA fast flow column (Qiagen) pre-equilibrated with EquiBuf2A. After load, the column was washed with EquiBuf2A. After OD280 reached baseline, the protein was eluted with EquiBuf2A containing 0.5M imidazole.

The proteins eluted in 8M urea were dialyzed extensively against 1.7M urea, 300mM NaCl, 50mM potassium phosphate, 5mM BME, pH 8.0 at room temperature. After dialysis, the protein solution was spun down to pellet out any precipitate. 10mM EDTA was added to the protein solution, TEV protease at a concentration of 1mg/ml was added to the refolded protein to cut the His tag; cleavage was performed at room temperature overnight. The cut protein was dialyzed against 300mM NaCl, 50mM potassium phosphate, 5mM BME, pH 8.0 to remove EDTA. Loaded onto a fresh Ni-NTA column equilibrated with EquiBuf2A, the protein flow-through was collected and concentrated to 2mgs/ml in 50mM potassium phosphate, 150mM NaCl, pH 8.0; it was later desalted and blocked for cells studies.

Purification of CTD-mRFP was done by solubilizing the cells pellet collected after induction in Buf1A. The suspension was sonicated and the debris pelleted by centrifugation at 14K rpm in an SS-34 rotor. The supernatant was loaded onto a Ni-NTA column pre-equilibrated with Buf1A. The column was washed thoroughly till baseline was reached. The protein was then eluted with Buf1A containing 1M imidazole.

The purified protein was cut with Tev protease at room temperature while being dialyzed against Buf1A to get rid of excess imidazole. The cut protein was loaded onto a Ni-NTA column pre-equilibrated with Buf1A and the flow-through collected. The flow through was concentrated and loaded onto a Superdex-75 column pre-equilibrated with Buf1A. The fractions that were colored were pooled and stored at -80C.

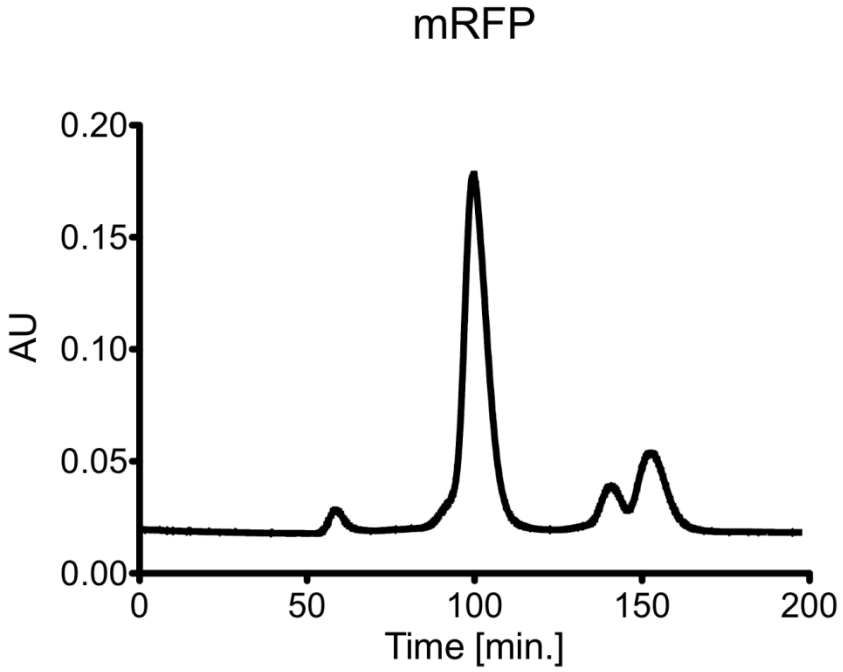

Figure 3.23: Superdex-75 elution profile of CTD-mRFP protein. The major peak eluting at 100 mins, was collected. The Flowrate for the sizing run was 2ml/min.

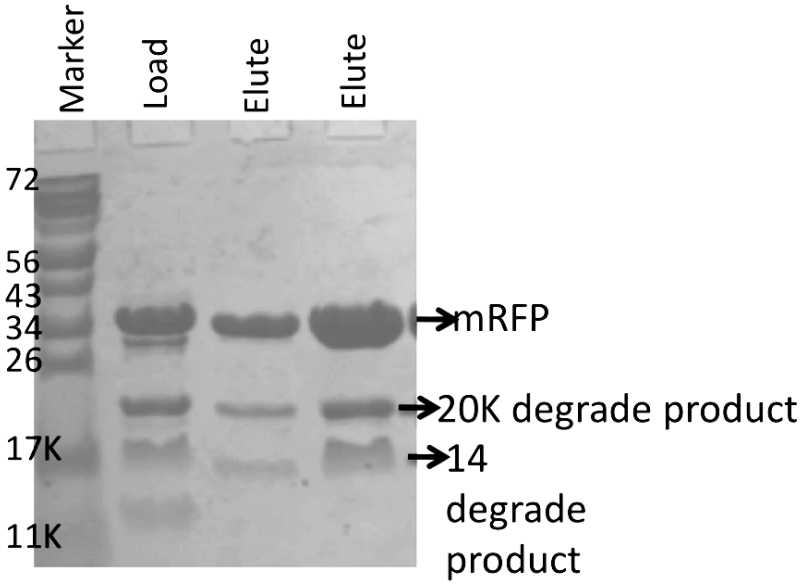

Figure 3.24: CTD-mRFP purified on a Superdex-75 Sizing column. Heating the protein in SDS sample buffer causes the degradation of the protein.

Fluorescent Labeling of Proteins:

Fluorescent labeling of the proteins was done in the denatured state. The proteins, after being purified on the Superdex 75 column, were treated with 1mM DTT (fresh) and incubated at room temperature for 4-6hrs. After incubation, the proteins were desalted on a PD-10 desalting column (GE). The PD-10 columns were equilibrated with a minimum of 25ml of 4M guanidine hydrochloride, 100mM sodium phosphate, 1mM TCEP, and 1mM EDTA, pH 7.0 (labeling buffer). 2.5ml of DTT reduced protein was loaded onto the column, allowed to completely soak into the medium, and then eluted with 3.2ml of labeling buffer.

The desalted proteins were immediately mixed with 7 fold molar excess of the maleimide dye. The reaction was allowed to incubate overnight at room temperature in

the dark. After overnight incubation, the proteins were treated with 50mM BME. The proteins were then desalted using a Zeba 10ml-desalting column (Pierce Biotech).

$$[P] = \frac{A_{280} - (A_{643} * CF)}{\varepsilon}$$

$$D = \frac{A_{643}}{\varepsilon_{dye} * [P]}$$

Correction factor (CF) for Alexa Fluor 633 –Maleimide determined to be 0.28 in 50mM ssodium phosphate, 300mM NaCl pH 8.0.

Binding Studies:

Fluorescently labeled Alexa Fluor 488-BPE3 was kept at a fixed concentration in potassium phosphate 50mM, 150mM NaCl, and pH 8.0. Fixed concentrations of Alexa Fluor 633 labeled BPK3 was added and fluorescence intensity measured from 640-700nm. Excitation was at 620nm. Excitation and emission slit sizes were kept at 1mm on an ISS fluorescence spectrophotometer. The data was exported to excel and plotted using PRISM.

Cell Culture and Flow Cytometry:

Jukrat cells TIB152 (ATCC) and H9-Cells HTB-176 (ATCC) were propagated in RPMI1640 medium with L-glutamine, 25mM HEPES (GIBCO) supplemented with 10% FBS, 1% Penicillin-Streptomycin antibiotic solution (GIBCO) at 37°C, 5% CO_2. Cells that were highly viable as determined by trypan blue staining were selected.

Cells were spun down at 1000g for 5 minutes at 20°C and the pellet was resuspended in fresh media. $2X10^5$ cells per tube were dispensed into BD FACS tubes. The cells were treated with the increasing concentrations of the proteins tested. The cells

were treated for 1 hour at 37°C and spun down at 1000g to remove the supernatant, followed by treatment with 200uL 1X Trypsin (0.25% Trypsin-EDTA, GIBCO) at 37°C for 5 minutes. The Trypsin treated cells were spun down, the supernatant discarded and the pellet taken into fresh media with 10% FBS. The resuspended cells were incubated for 12 hours at 37°C.

Mean intensity measurements were done on cells that were spun down, and treated with 1X Trypsin for 5 minutes at 37°C, followed by quenching with media supplemented with 10% FBS. The cells were then spun down and taken up into 400uL of PBS for analysis. The cells were analyzed on a FACS Canto II with excitation using the 488 laser and 635 laser and emission observed using the FITC 530/30 band pass and Alexa Fluor 633 670/40 band pass filters.

To determine the effect of the proteins on inducing apoptosis, the cells were labeled with Annexin V (BD) and 7-AAD (eBiosciences). The data was analyzed using FACS Diva or FlowJo.

CHAPTER 4: CONSTRUCTION AND TESTING OF THE HIV PROTEASE ACTIVATED TRANSDUCER.

INTRODUCTION

The ability to selectively target HIV infected cells to undergo apoptosis without affecting uninfected cells is our goal. This has been addressed with the design of a HIV protease activated transducer that is inactive in the absence of HIV protease. In cells containing HIV protease, the inactive transducer is cleaved into monomeric active fragment that hetero-dimerizes with a similarly activated partner. Formation of the active heterodimer is designed to lead to apoptosis.

This chapter is devoted to analyzing the protease transducers to determine whether they meet the specifications laid out in Chapter 2.

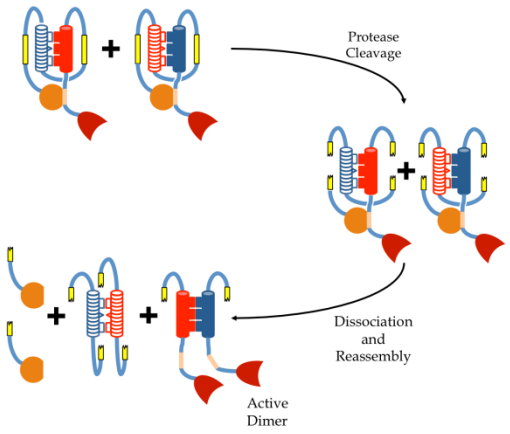

Figure 4.1: A schematic representation of the individual transducers being activated by HIV protease cleavage leading the formation of active helices that heterodimerize yielding an active dimer.

IS THE TRANSDUCER MONOMERIC

One of the design criteria for the protease transducers was their being monomeric. To address this question, we carried out sizing chromatography on the individual protease transducers using a Superdex 75 analytical column. From the run shown in Figure 4.2 we can clearly see that the predominant species is monomeric, based on elution of the protein between the markers 44 and 17kDa since the size expected is 27kDa that were previous used to calibrate the column. Due to the low absorbance of the proteins being detected the elution the higher molecular weight species that are being detected may be attributed to the formation of a dimers that would elute at 54kDa. It is possible that as we are refolding our protein from the denatured state oligomers that are formed is not in equilibrium and can be purified away. Alternatively if the oligomers were in equilibrium that would point to a design issue that would have to be addressed. As By incorporating additional purifications steps like ion-exchange chromatography it may be possible to achieve a very high degree of purity. Additionally, sedimentation velocity experiments on the protease transducers indicate that the proteins are predominantly monomeric (data not shown).

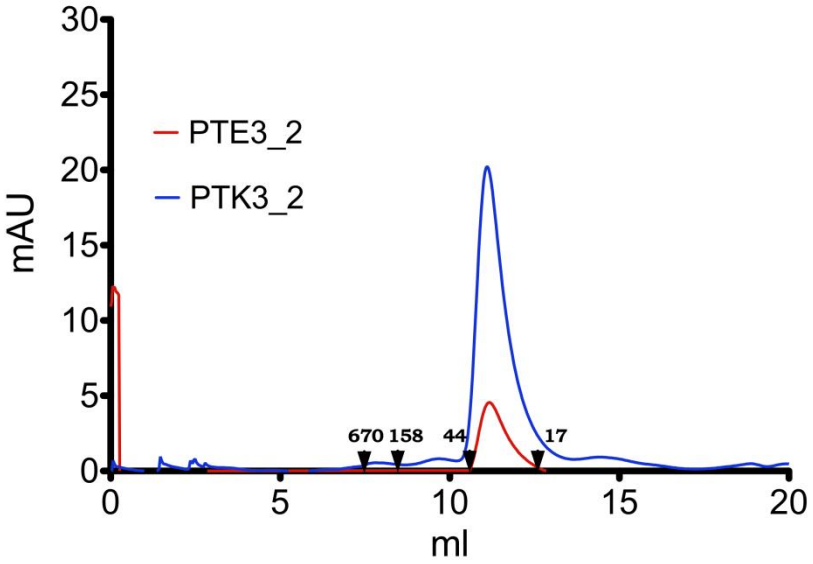

Figure 4.2: The monomeric protease transducers analyzed on a Superdex-75 analytical column. The molecular weight markers are represented on the X-axis for reference. The expected molecular weights for the Protease transducers are 26.9 kDA. The Molecular weight markers are 670kDa (Thyroglobulin), 158kDa (γ-globulin), 44(Ovalbumin) and 17(Myoglobin).

CELLULAR UPTAKE OF THE PROTEASE TRANSDUCER PROTEINS

To address this question of cell uptake, we used various concentrations of fluorescently labeled protease transducers and incubated them with Jurkat cells overnight in the presence of serum (see materials and methods for details at end of this chapter). Before analysis, the cells were trypsinised to rid of any surface of bound protein that may yield a false positive signal; then they were analyzed by flow cytometry for fluorescence intensity. Figure 4.3 clearly illustrates concentration dependent uptake of the proteins PTE3_2 and PTK3_2 in the presence of serum, a complex solution containing a number of proteins that may interact with the transducer.

We were interested in knowing if the absence of serum enhanced the uptake of the protease transducers. The protease transducer PTE3_2 was tested against Jurkat cells in the absence of serum. Serum deprived cells were treated for an hour for uptake as serum deprivation is detrimental to the cells. The absence of serum had no effect on the uptake, uptake being comparable to that of cells treated in the serum containing media (Figure 4.4), the presence or absence of serum during treatment being balanced by the stress induced in the cells when using serum free media. Protease transducers behave in a manner similar to that observed for other transduced proteins, our transducers being the first that use the CTP tag previously reported (*105*). Based on these results, the optimum conditions for proteins transductions would be high protein concentrations in the range of 1-5μM for 1 hour in the presence of serum.

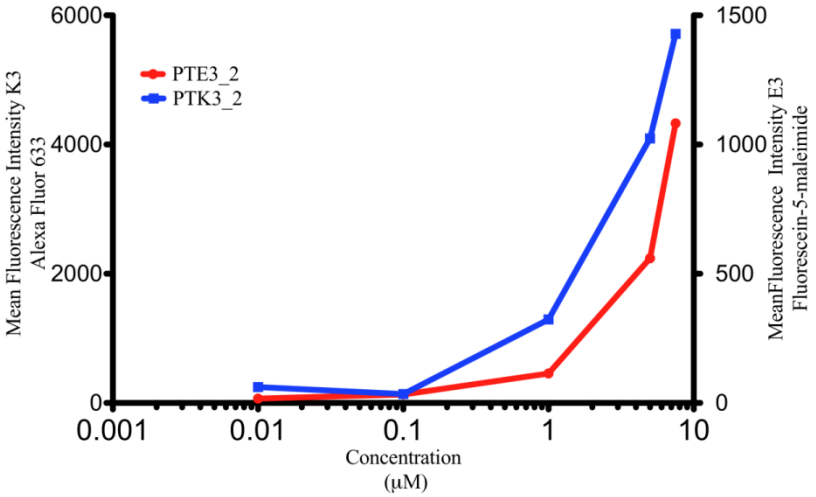

Figure 4.3: Increases in mean intensities of the protease transducers with increasing concentration of the protein tested in Jurkat cells in the presence of serum. Cells were treated overnight and fluorescence intensity measured by flow cytometry.

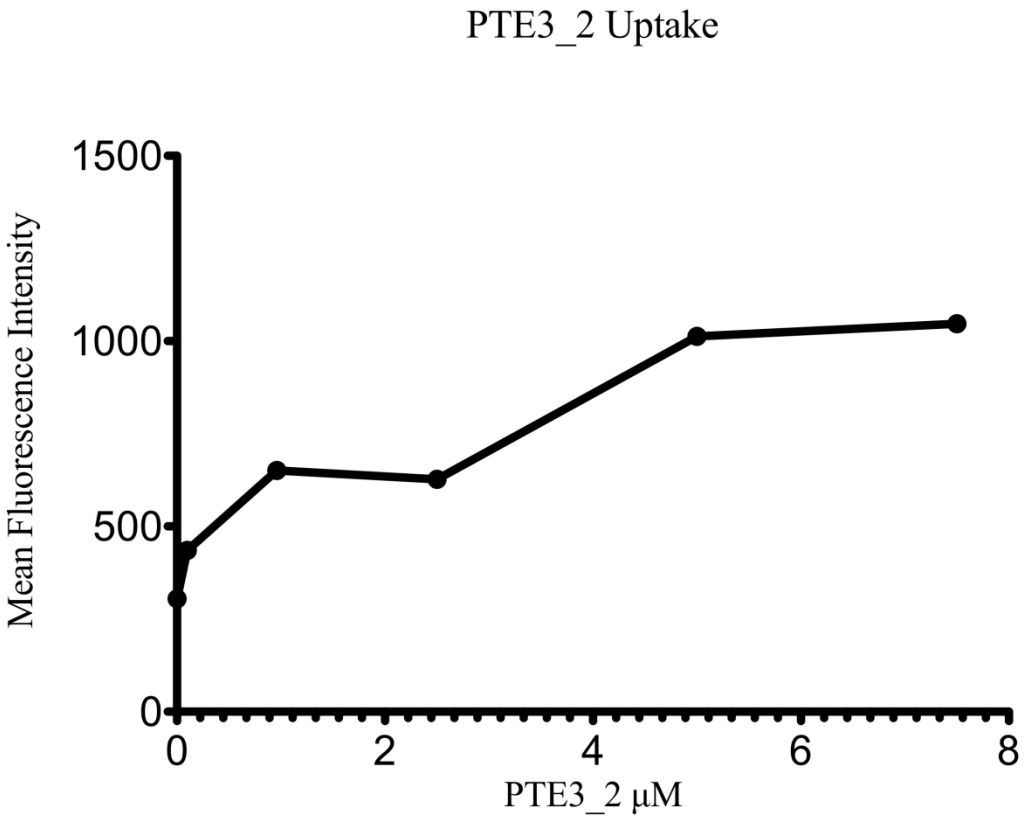

Figure 4. 4: Increase in mean fluorescence intensity of cells treated with PTE3_2 for a period of 1 hr followed by trypsin treatment. The cells were incubated with PTE3_2 in the absence of serum to determine if serum inhibited uptake. For Jurkat cells and PTE3_2, serum does not appear to inhibit uptake of the protein.

Our goal is to test the protease transducers in HIV infected H9 cells, it being previously reported that protein transduction is dependent on cell type. Transducers were tested independently in uninfected H9 cells. Additionally, length of time to cell saturation was determined. H9 cells were treated with protease transducer PTK3_2 labeled with Alexa Fluor 633 for 1 and 2 hours in the presence of serum. The cells were then analyzed by flow cytometry and the data was plotted as a function of increasing fluorescence intensity. Figures 4.5 and 4.6 show uniform distribution of the protein across the population. Based on the change in intensity from a 1 hour to 2 hours treatment, one

observes that cells treated with lower concentrations of the protein show increased uptake as a function of time. At higher concentrations of 3.5uM and after 1-hour uptake, saturation was observed based on low change in intensity observed when compared to 2 hours.

It was concluded that uptake of proteins is directly related to concentration of the proteins used for treatment and the total time of incubation.

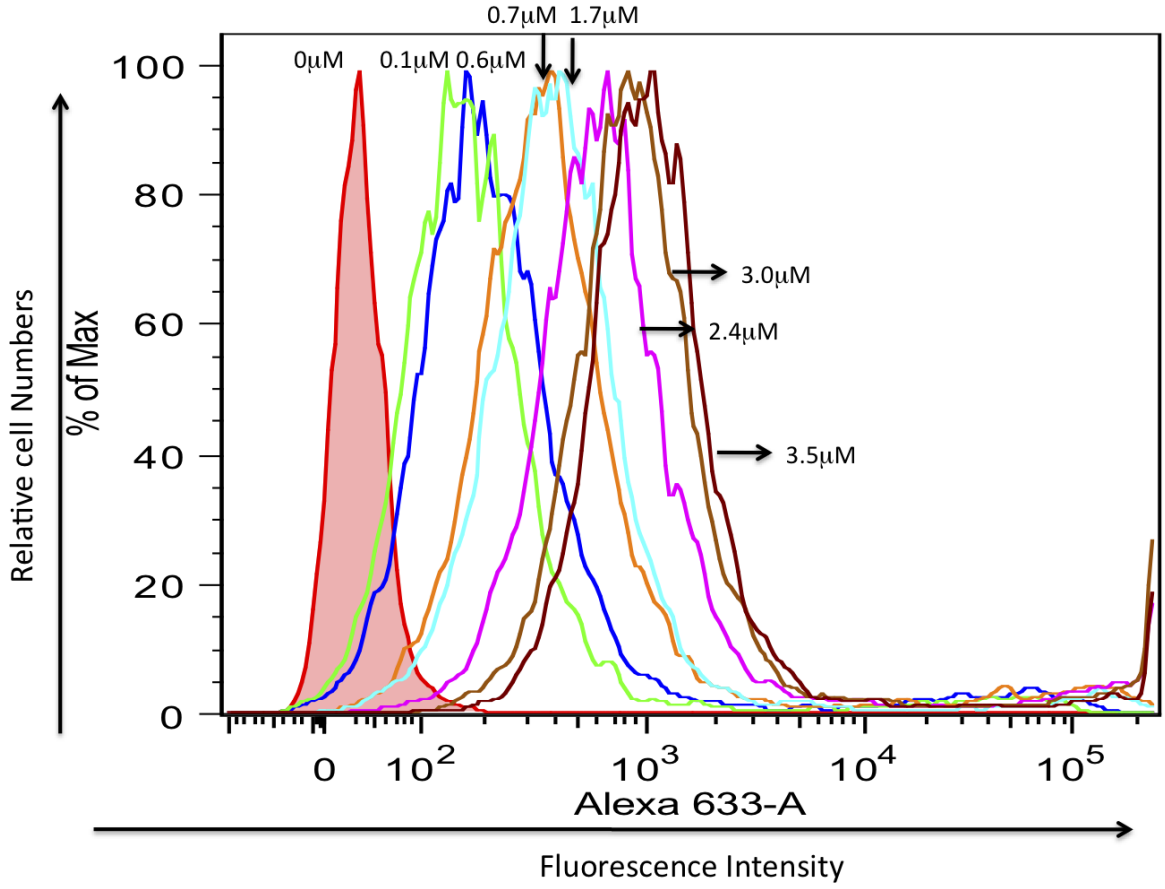

Figure 4.5: Uptake of PTK3_2 labeled with AF633 after treatment for 1hour. The cells were analyzed on a BDFortessa with excitation using the 633 laser. The data were analyzed using FloJo.

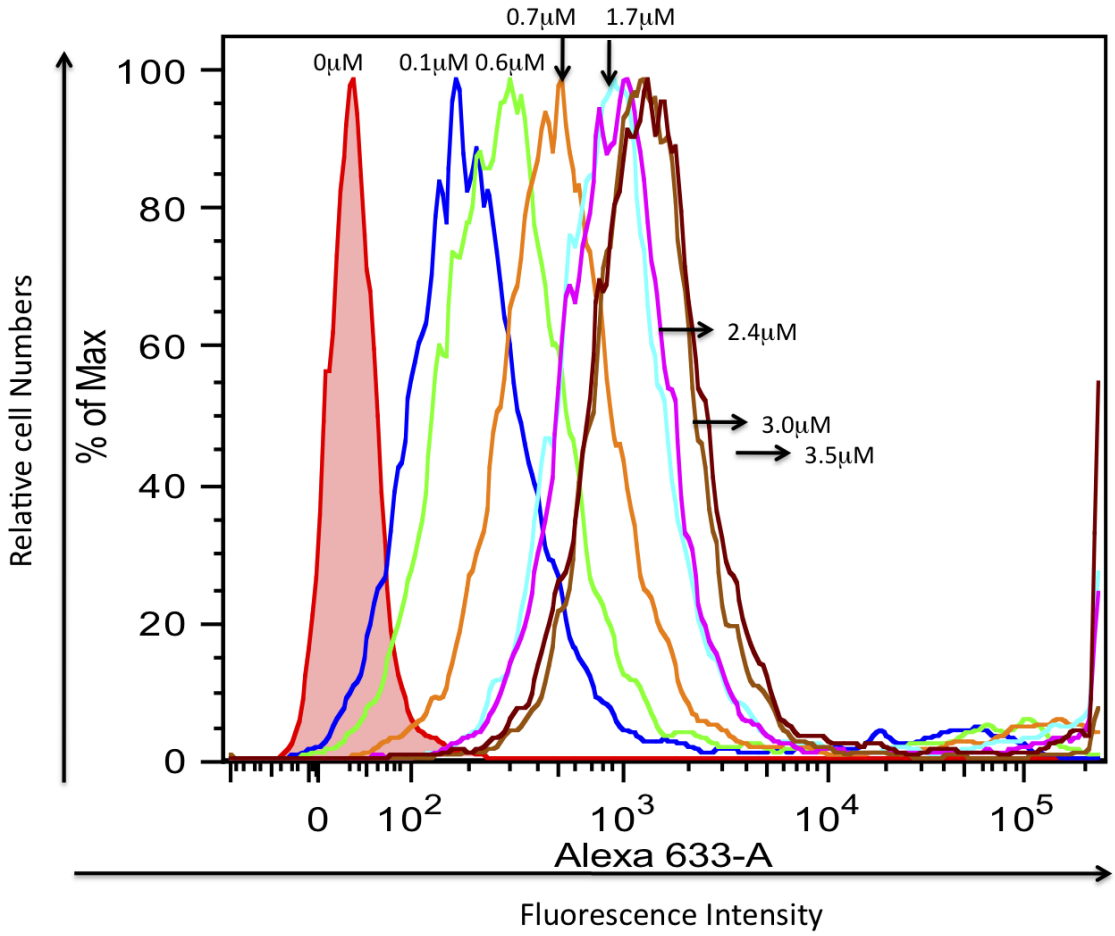

Figure 4.6: Uptake of PTK3_2 labeled with AF633 after treatment for 2 hours. The cells were analyzed on a BDFortessa with excitation using the 633 laser. The data was analyzed using FloJo.

INDUCTION OF APOPTOSIS IN CONTROL UNINFECTED JURKAT CELLS BY THE PROTEASE TRANSDUCERS

The protease transducers were designed to be inactive in the absence of HIV protease, HIV protease activating the transducers leading to apoptosis. As the long-term goal is to develop transducers as a protein drug against HIV, we had to test whether the transducers caused apoptosis in uninfected cells. Uninfected Jurkat cells were treated with increasing concentrations of our proteins overnight and cellular apoptosis was analyzed using Annexin V and 7AAD staining. In Figure 4.7, at higher concentrations of

the protease transducers in the media (1-10μM) one can see that there is an increased amount of apoptosis. The observed apoptosis is higher in cells treated with an equal mix of both transducers (PTK3_2 and PTE3_2) when compared to those treated with the individual transducers alone at the same concentration. The concentration of the DED domain is indicated, so the mix of the two transducers is of half the concentration of each of the individual components. Based on these results and previous data on the CTD-mRFP (see Chapter 3), the individual transducers may be cleaved and thus activated by cellular proteases. The potential activation of the protease transducers by cellular protease is addressed in a latter section of this chapter. Future work includes testing cellular degradation of the protease transducers by western blotting to check for their integrity in uninfected cells.

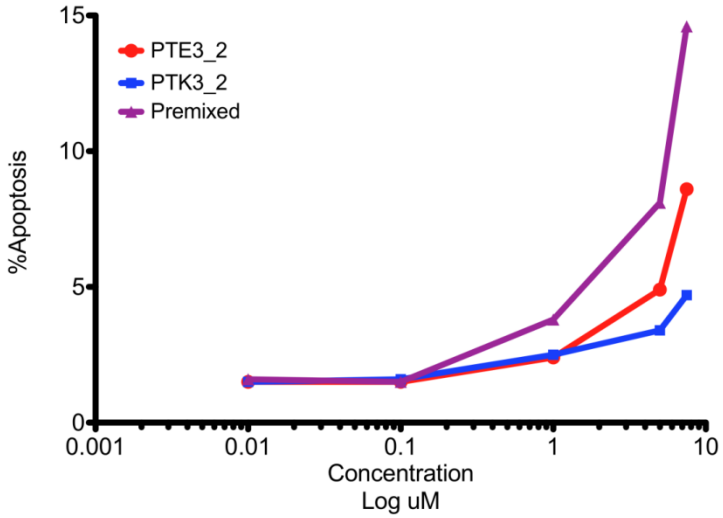

Figure 4.7: Increases in apoptosis in Jurkat cells treated overnight with increasing concentrations of the protease transducers in PBS. Corresponding buffer blanks do not show any change in base apoptosis rate. This increase in apoptosis may be cell specific.

CLEAVAGE OF TRANSDUCER BY HIV PROTEASE *IN VITRO*

An important design criterion that needed to be addressed was rates of cleavage of the protease sites within the protease transducer to yield the active monomer (Figure 4.8). As we designed the protease transducers to have two separate HIV protease cleavage sites, accessibility and ease of cleavage at those sites is of importance. The sites incorporated into the transducers were based on peptides previously reported (Chapter 2). Protease transducers were tested against purified Wt- HIV protease as described in the materials and methods. The cleavage reactions were carried out at low pH and high salt concentrations as HIV protease shows significant pH and salt dependence on stability(*120*). As the protease transducers are folded proteins with internal cleavage sites, the efficiency of cleavage of the protease transducer was determined and compared to published rates of cleavage of the *gag-pol* polyprotein by HIV protease. The wild type and mutants of a p17-p24 cleavage site within a truncated *gag-pol* polyprotein have been previously reported(*121*). In that study, the polyprotein was expressed in vitro using a cell free system and digested with HIV protease. The wt p17-p24 gal-pol substrate had a $T_{1/2}$ of 10 minutes, with the slowest rates observed for the YPMM and YPKP cleavage site mutants as substrates ($T_{1/2}$>110 minutes). HIV protease cleavage of our purified protease transducers was compared with these values. Quantitation by densitometry of the gel in Figure 4.9 shows 12% of the total transducer substrate is cleaved by HIV protease after 1000 minutes (Figure 4.10, Figure 4.11). Modifying the reactions conditions should improve the proteolytic cleavage rates of the transducer proteins. In future iterations of the protease transducer design, it may be necessary to improve the accessibility of the cleavage site by making changes in the spacers surrounding them.

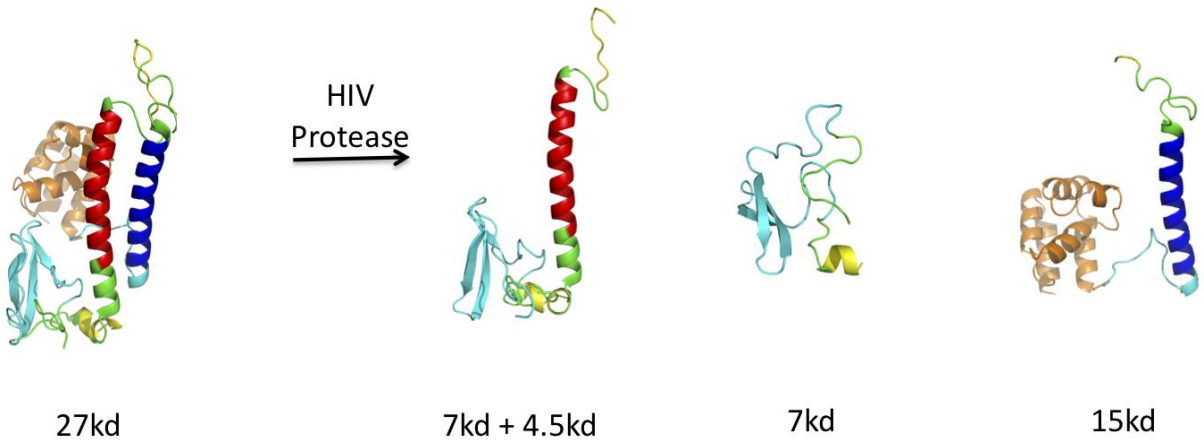

Figure 4.8: Cleavage products expected from the protease transducers on complete cleavage by HIV protease should yield 4 fragments a 7kd, 4.5kd and 15kd. The 15kd fragment being the active monomer.

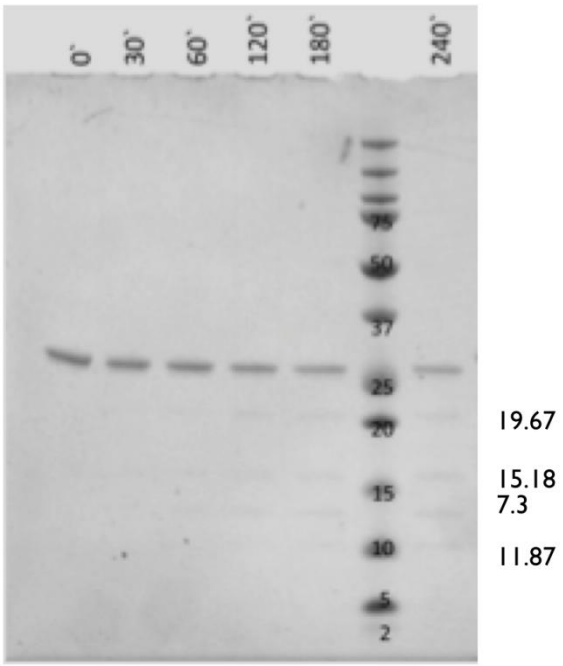

Figure 4.9: PTE3_2 was cut with HIV Protease at pH 6.0, The band labeled 7.3 runs higher than expected due the presence of the polyarginine tag at the N-terminal giving it a net pI of 12. This behavior is similar to that observed for Rev another highly positively charged protein.

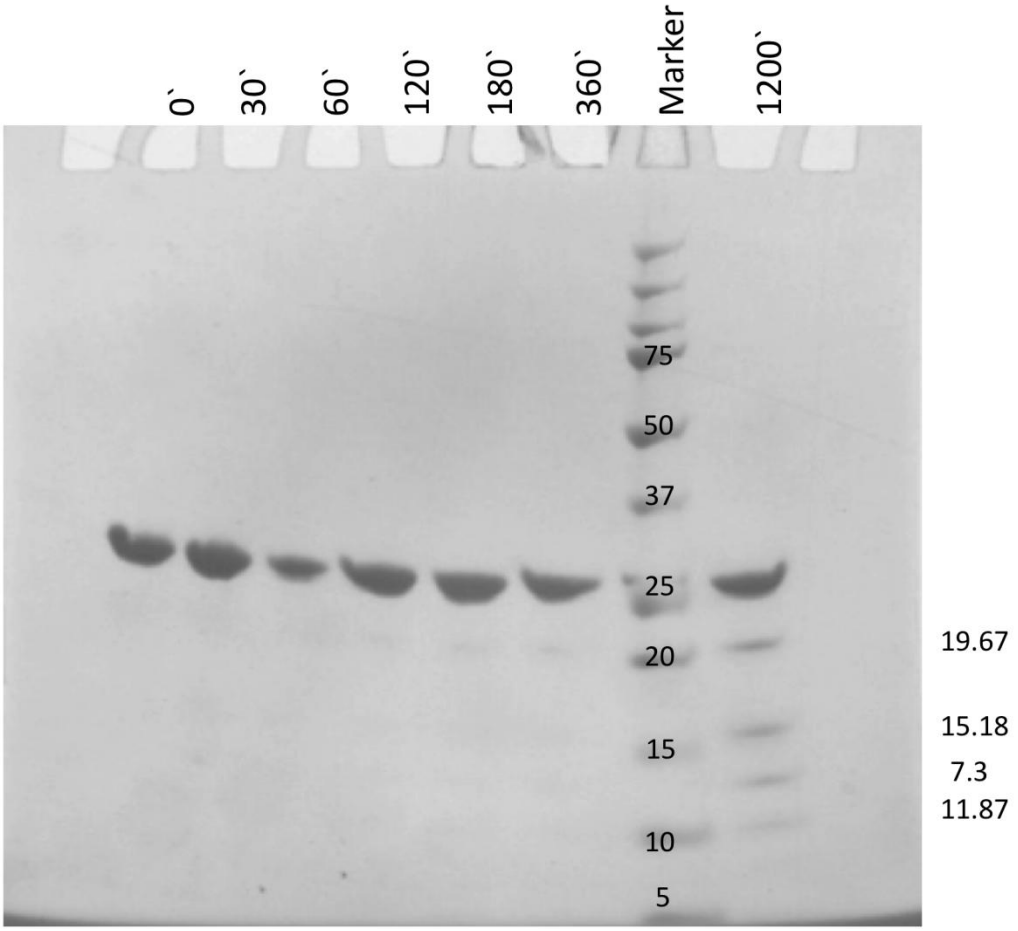

Figure 4.10: PTE3_2 was cut with HIV Protease in: 10mM Na.acetate pH 5.0, 1mM DTT, 1M NaCl, at room temperature. Samples at various time periods were collected and quenched with SDS-loading buffer.

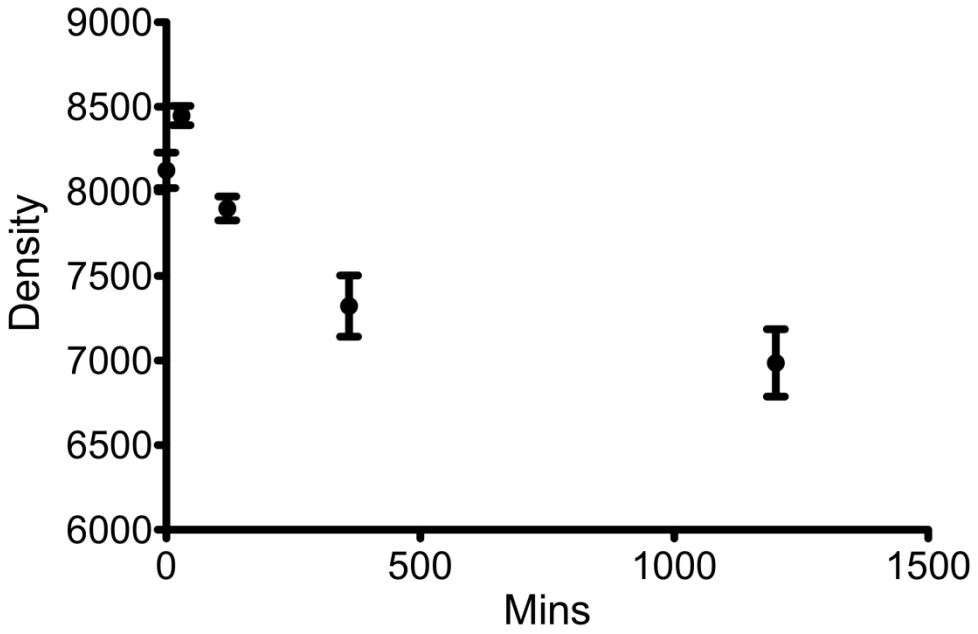

Figure 4.11: Change in intensity of uncut protein PTE3_2 at pH 5.0 in Na. acetate buffer as a function of increasing time. Errors calculated by taking three density measurements for the same band.

CELLULAR PROTEASES AND OUR PROTEASE TRANSDUCERS

Induction of apoptosis at higher concentrations by the protease transducers in uninfected Jurkat cells was shown earlier. Since our proteins are *de novo* designed, this raises the possibility of cleavage by cellular proteases and additionally the protein degradation machinery may reduce the half-life of the designed protease transducers in the cell. A partial list of potential cellular proteases (Table 4.1) was identified to test for cleavage sites within our protease transducers. For many of the human cellular proteases, there is no available information on the protease cleavage motifs. Where available, these motifs were used to identify potential cleavage sites that can either yield a false positive or negative result for our transducers. Table 4.1 shows that many of the proteases identified are located in specialized vesicles, to protect cellular proteins from indiscriminate cleavage. In addition many of the proteases are inactive zymogens that are

specifically activated. These two important facts reduce the possibility of inadvertent cleavage and activation of our protease transducers by cellular proteases.

In addition to cellular proteases, the transducers could also be degraded by the proteosome following ubiquitination. The potential unbiquitination sites are identified on the sequence and are represented in Figure 4.12. With proteosomal degradation there should be no negative consequences since one would expect no false positives due to isolation and complete degradation of the transducers.

In addition to the proteosome, some the caspase protease cleavage motifs that were identified are plotted onto the sequence as in Figure 4.13. On cleavage by the cellular caspases, the protease transducers are not activated because cleavage is at the FLAG tag. This leaves the blocking helix interacting with the active helix, preventing formation of the active monomer, and hence avoiding cell death in uninfected cells.

We also tried to identify cleavage motifs for other cellular proteases based on the cleavage of unique peptide sequences obtained from the CutDB and Merops databases (http://cutdb.burnham.org; http://merops.sanger.ac.uk/). Many of the proteases do not have motifs associated with them. To build the motif, one must be in possession of peptide sequences that have been experimentally tested. Currently some of these peptide sequences are available online. Building motifs from these sequences is beyond the scope of this dissertation. A couple of the motifs that were identified are presented in the Appendix.

A list of Intracellular proteases

S.No	Name	Type	Location	Present in Specialised Vesicles
1	Prolyl oligopepdidase	Serine		
2	Cathepsin A	Serine		Lysosomes
3	Cathepsin B	Cysteine		Lysosomes
4	Cathepsin C	Cysteine	Immune cells/Inflamatory cells	Lysosomes
5	Cathepsin D	Aspartyl		Lysosomes
6	Cathepsin E	Aspartyl	Dendritic Cells/ APCs	
7	Cathepsin F	Cysteine		Lysosomes
8	Cathepsin G	Serine	Neutrophils	Granule associated
9	Cathepsin H	Cysteine		Lysosomes
10	Cathepsin K	Cysteine		Lysosomes
11	Cathepsin L	Cysteine		Secretory
12	Cathepsin S	Cysteine		Lysosomes
13	Cathepsin V	Cysteine		Lysosomes
14	Cathepsin X	Cysteine	Dendritic Cells/ APCs	
15	Furin	Serine		Golgi
16	Caspase1	Cysteine		
17	Caspase2	Aspartyl		
18	Caspase3	Cysteine		
19	Caspase4			
20	Caspase5	Cysteine		
21	Caspase6	Cys-Asp		
22	Caspase7	Cys-Asp		
23	Caspase8	Cys-Asp		
24	Caspase9	Cys-Asp		
25	Caspase10			
26	Granzyme B	Serine	Cytotoxic T cells/NK Cells	

Table 4.1: A list of intracellular proteases that may potentially cleave the protease transducers leading to false negative or positive results.

>PTK3_2
GRRARRRRRR GPLGSGEEEP LPPRWSMQVA PNGRTFFIDH ASRRTTWIDP RNGRASSGSG 60
IFLETSLGSD YGSGDKGSEI AALEKEIAAN EKEIAALEKS GSGSGIFLET SLGDYKDDDD 120
KGSGCSKIAA LKEKIAALKE KIAALKEGTG LPSYDEALHG SMDPFLVLLH SVSSSLSSSE 180
LTELKYLSLG RVGKRKLERV QSGLDLFSML LEQNDLEPGH TELLRELLAS LRRHDLLRRV 240
DDFELE

PTE3_2
GRRARRRRRR GPLGSGEEEP LPPRWSMQVA PNGRTFFIDH ASRRTTWIDP RNGRASSGSG 60
IFLETSLGSD YGSGDKGSKI AALKEKIAAN KEKIAALKES GSGSGIFLET SLGDYKDDDD 120
KGSGCSEIAA LEKEIAALEK EIAALEKGTG LPSYDEALHG SMDPFLVLLH SVSSSLSSSE 180
LTELKYLSLG RVGKRKLERV QSGLDLFSML LEQNDLEPGH TELLRELLAS LRRHDLLRRV 240
DDFELE

High Probability
Medium Probability

Figure 4.12: Analysis of the Protease transducers for ubiquitination sites. The residues highlighted in red indicate a high probability of ubiquitanation. Ubiquitamntion of the transducers would lead them to be shunted to the proteasomal degradation pathway leading to loss of transducers from the cell (sequences analyzed at http://ubpred.org/, raw data used to map the sites onto the sequence).

```
GRRARRRRRR GPLGSGEEEP LPPRWSMQVA PNGRTFFIDH ASRRTTWIDP RNGRASSGSG  60
EEEEEEEEEE BEEEEEEEEE BBEEBBBEBB EEBBBBBBBB BEEEBEBEBB EEEEEEEEEB

IFLETSLGSD YGSGDKGSEI AALEKEIAAN EKEIAALEKS GSGSGIFLET SLGDYKDDDD  120
BBBEBBEBBB BBEEEEBEBB BEBBEEBEEB EEEBEEBEEE EEEBBBBBBB BBEEBEEEEE

KGSGCSKIAA LKEKIAALKE KIAALKEGTG LPSYDEALHG SMDPFLVLLH SVSSSLSSSE  180
EEEEBEEBEE BEEEBEEBEE EBEEBEEEEE BBEBEEBBEE BBBBBBBBBB BBBEEBEEEE

LTELKYLSLG RVGKRKLERV QSGLDLFSML LEQNDLEPGH TELLRELLAS LRRHDLLRRV  240
BEEBEBBBEE EBEEEEBEEB EEEBEBBBBB BEBEEBEEEB BEBBEEBBEB BEEEEBBEEB

DDFELE
EEBEE                                                              246
```

Figure 4.13: Sequence analysis of the protease transducer PTK3_2 for cleavage by cellular Caspases. The residues highlighted in red indicate a high probability for cleavage. However location of the cleavage site would not affect the activity of the protein.

CELLULAR CONCENTRATION OF THE PROTEASE TRANSDUCER

The designed protease transducers, after HIV protease cleavage, yield the active pieces to the dimer that induces apoptosis in HIV infected cells. Formation of this active dimer is dependent on the intracellular concentrations of the precursors PTK3_2 and PTE3_2. Their uptake is dependent on the total extracellular concentrations used to treat the cells. We determined the intracellular concentration of PTK3_2 in H9 cells by fluorescence spectroscopy using Alexa Fluor 633-labeled PTK3_2 at a fixed concentration of 1.5uM in the media, incubated for different time periods from between 30 and 180 minutes as detailed in the materials and methods. The cells were treated with trypsin to get rid of surface bound protein, washed with PBS and lysed in 5% SDS. This was diluted into PBS to reduce the SDS concentration to 0.13%, which is below the CMC value of SDS. The fluorescence spectra were collected between 640-700nm, with

excitation at 620nM. The calibration curve was made using lysate of untreated cells, similarly processed, with added know amounts of PTK3_2 and fluorescence measured.

Preliminary results indicate H9 cells treated with a 1.5 μM concentration of PTK3_2 protein took up 6 attomoles of PTK3_2 protein per cell after 180 minutes of treatment. Since H9 cells are a derivative of subcutaneous T-lymphocytes, cellular volume of Jurkat cells, a T-lymphocyte cell line, were used as a surrogate. Cellular volume of Jurkat cells from previously published data (*122*) was 0.7 picoliters. This volume was used to determine the concentration of the transducers within each cell, or about 9 μM of fluorescently labeled protein within the cells. This is very much an approximate value around which one can expect the intracellular concentration to be since for errors like number of cells, cell volumes are high.

The above value of 9 μM additionally is based on Jurkat cells, which are spherical and uniform in size. The H9 cells do not show similar uniformity in size or shape. As similar values are not available for H9, we can only extrapolate values based on Jurkat cells to H9. If one were to treat the cell as a semi-permeable membrane then one would expect the intracellular concentration to be equal to the extracellular concentration (1.5μM). This is not the case. Protein transduction is partially based on electrostatic interactions of the transducer protein with the cell surface followed by its uptake by different mechanisms. This electrostatic interaction of the transducer with the surface would increase the effective extracellular bound proteins thereby explaining the increased intracellular concentration. One would then expect that the effective intracellular concentration of highly positively charged to be much higher than other proteins.

Previously it has been shown that in HeLa cells there is a cargo dependent uptake of transduced proteins. The intracellular protein concentrations ranging from 20 attomoles /cell for BSA to 4.3 attomoles/cell for a FITC labeled secondary, polyclonal

goat, anti-mouse antibody (*123*). Since, our value is 9μM (as above), we can conclude that the protease transducer PTK3_2 a 27kDa protein has uptake characteristics between BSA a 66 kDa and a polyclonal antibody that is 150kDa in size, indicating size of molecule may not be the only criteria on which cellular uptake is determined.

TESTING IN HIV INFECTED H9 CELLS:

The goal of this project was to design, construct and test the protease transducers in HIV infected cells. Protease transducers were tested against H9 cells that were infected with HIV strain C. This HIV strain C is a subtype of the major class M which is increasingly found across the world.

To test the activity of the transducers, HIV-C infected H9 cells were used. After 4-5 days of infection, the cells were treated with an equimolar mix of the transducer proteins and incubated overnight. After overnight incubation, the cells were analyzed for viability by Trypan blue staining. The control for the carrier buffer was infected cells treated with buffer alone in equivalent volume as used for the transducers. Figure 4.13 shows the result of the experiment. It can be seen that cell viability reduces as a function of increasing protein concentration. However it can also be seen that equivalent volumes of buffer when added to the cells and compared to cells treated with the transducers show similar viability. This suggests the drop in viability is due to buffer used. The carrier buffer that was used in the experiment was 50 mM potassium phosphate, 150 mM NaCl, 1M proline and pH 8.0.

To rule out increased sensitivity of HIV infected cells to the buffer, we tested the same buffer against uninfected H9 cells under the same conditions as above. The uninfected cells show similar decrease in viability with increased volumes of this buffer used (Figure 4.15). We compared our buffer to PBS as a control. As is clear from the

result, PBS has no significant effect on cell viability. Therefore the drop in viability can be attributed directly to the carrier buffer.

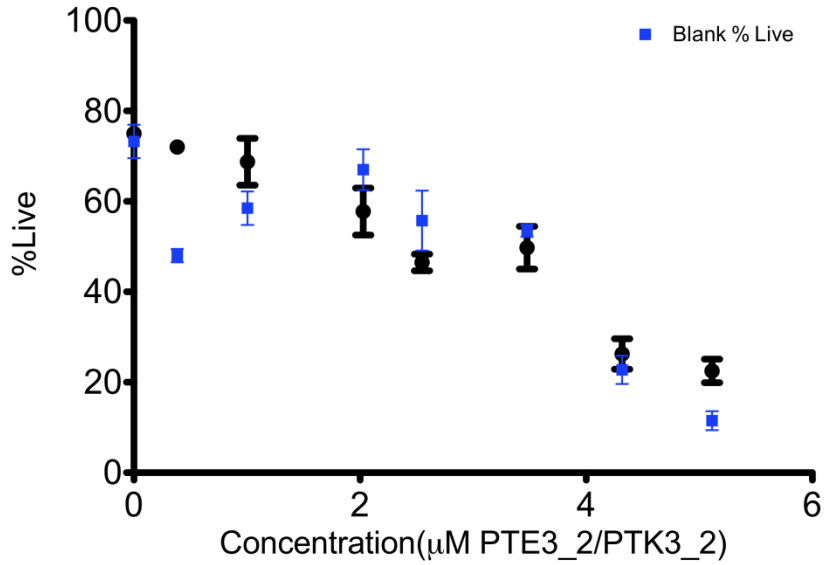

Figure 4.14: Testing the Protease transducers in HIV infected cells. HIV infected H9 cells were treated overnight with the protease transducers and analyzed by Trypan blue staining using a TC-10 counter. Taking three readings of each sample derives the SEM.

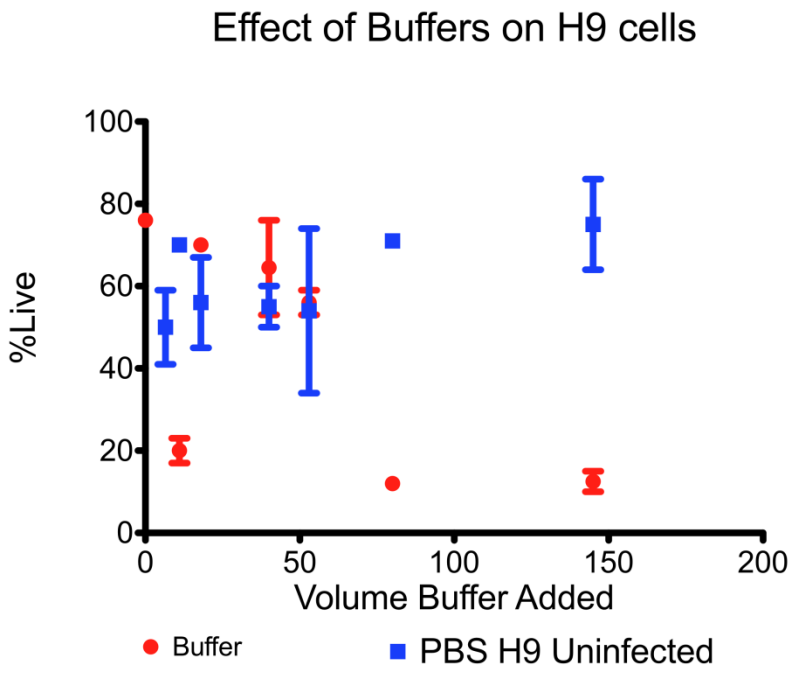

Figure 4.15: Testing the effect of buffersonH9 cells. H9 cells were treated overnight with the buffers and analyzed by Trypan blue staining using a TC-10 counter. Taking three readings of each sample derives the SEM. Buffer is 50 mM potassium phosphate, 150 mM NaCl, 1M Proline and pH 8.0.

CONCLUSION:

The main aim of this chapter was the construction and testing of the Protease activated transducer proteins PTE3_2 and PTK3_2. After designing the protease transducers, the main issue of solubility of the proteins that was previously experienced in all other constructs was overcome. The proteins are soluble in native buffer conditions; they are monomeric as seen by size exclusion chromatography and sedimentation velocity. The proteins are taken up by both Jurkat and H9 cells, with H9 cells being used for both uninfected and HIV infected studies. There is high correlation between concentration of protein used to treat the cell and its uptake, higher the concentration of the protein greater the uptake.

Serum, a complex medium that may interact with the transducers, was shown not to interfere with uptake. We have additionally shown there is a saturation of transduced protein observed in the cells by comparing incubation times and varying the concentrations of the proteins used.

As our designed protease transducers are activated by cleavage using HIV protease we tested them against HIV protease. The transducers are cleaved by the HIV protease to yield fragments corresponding to the expected cleavage products showing high degree of specificity, although there is incomplete cleavage seen in the 11Kd fragment. This indicates an area of design that can be improved. Additionally, when compared to the *gag-pol* poly protein, our protease transducers have a slower rate of cleavage. Improving the buffer conditions may improve rate of cleavage *in vitro*. Additionally, by making changes in the spacer regions surrounding the cleavage site one can improve the proteolytic rates. We also show that the protease transducer PTK3_2 has an intracellular concentration of 6 attomoles/cell, corresponding to an approximate concentration of 8uM/cell that is above the Kd for the active dimer formed on proteolytic cleavage. However this assumes complete availability of the transduced proteins PTK3_2 and PTE3_2 to HIV protease in the cytoplasm. If the protease transducers are predominantly in vesicles or sequestered away and not in the cytoplasm, they would not be available to form the active dimer even if efficiently cleaved by HIV protease. Determining this distribution of the transducers within cells would greatly improve upon the next iteration of design.

Another main issue currently under investigation is the ability of the transducers to induce apoptosis in HIV infected cells when compared to uninfected cells. By knowing if the cells are killed would help improve our later designs.

MATERIALS AND METHODS:

Construction of expression plasmids:

The genes for the two protease transducers PTE3_2 and PTK3_2 where ordered from DNA 2.0. The genes have been optimized for *E.coli* codon usage and are in a T7 expression system (pJExpress414). The expression plasmid has an Ampicillin resistance marker.

Expression and Purification and refolding of the protease transducers:

The plasmids for the transducers were transformed into BL21 (DE3) cells. The transformed cells plated onto a Carbenicillin supplement LB agar plate. Individual colony was transferred to 50ml of LB medium supplemented with 100ug/ml of Carbenicillin. The culture was grown overnight and transferred to 2L of 2YT medium. When the OD600 reached 0.6 the cells were induced with 1mM IPTG. The cells were grown overnight at room temperature. After overnight growth, the cells were spun down and the pellet resuspended in 300mM NaCl, 50mM Tris, 5mM BME, and pH 8.0. The cell suspension was sonicated and the suspension spun down at 14000 rpm in an SS-34 rotor. The pellet was the resuspended in 6M Guanidine Hydrochloride, 50mM Tris, 5mM BME, pH 8.0 by constant stirring for 5 hr and the suspension spun down to get rid of cell debris. The supernatant was loaded onto a Ni-NTA column pre-equilibrated with 6M guanidine hydrochloride, 50mM Tris, 5mM BME, 10mM imidazole and pH 8.0. The column was washed and the protein eluted with 6M guanidine hydrochloride, 50mM Tris, 5mM BME, pH 8.0 supplemented with 1M imidazole. The protein that eluted was diluted to 0.05-0.1mgs/ml by the addition of 300mM NaCl, 50mM potassium phosphate, 5 mM BME, pH 8.0. The diluted protein was dialyzed against 300mM NaCl, 50mM potassium phosphate, 5mM BME, pH 8.0 to get rid of any guanidine.

The dialyzed protein was concentrated using a Vivaspin 20 (MWCO 10K) and the concentrated protein was loaded onto a Superdex-75 column pre-equilibrated with 50mM potassium phosphate, 300mM NaCl, pH 8.0 and 5mM BME. The protein that elutes a monomer was collected and cut with TEV protease to get rid of the His tag. Tev in a ratio of 1:10 TEV to protein was added and the sample digested overnight at room temperature. The cut his tag was removed by running the protein over a clean Ni-NTA fast flow column equilibrated with 300mM NaCl, 50mM potassium phosphate, 5mM BME, pH 8.0.

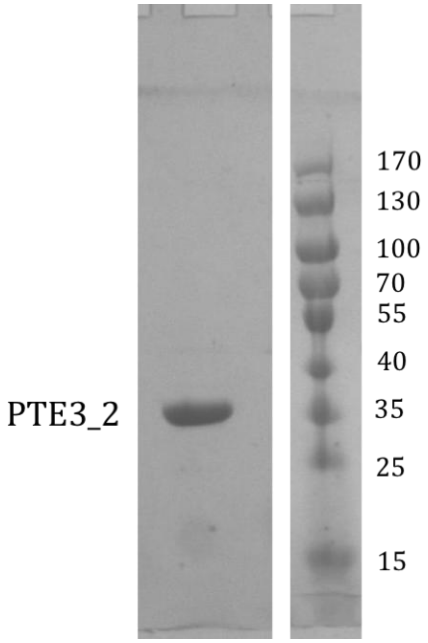

Figure 4.16: PTE3_2 purified from Superdex-75 column.

Labeling the proteins:

Fluorescent labeling of the proteins were done after refolding. The proteins after being purified on the Superdex 75 column were treated with 1mM DTT (fresh) and incubated at room temperature for 4-6 hrs. After incubation, the proteins were desalted using a Zeba 10ml desalting spin column (Pierce Biotech). The columns were equilibrated with a minimum of 25ml of 300mM NaCl, 50mM potassium phosphate,

5mM TCEP, 1mM EDTA, pH 6.9 (labeling buffer). Desalting was done following manufacturer protocol.

The desalted proteins at concentration of 0.5-1mg/ml were immediately mixed with 10 fold molar excess of the maleimide dye. The reaction was allowed to incubate overnight at room temperature in the dark. After overnight incubation the proteins treated with 50mM BME. The proteins were then desalted using a Zeba 10ml-desalting column into 300mM NaCl, 50mM potassium phosphate, and pH8.0.

$$[P] = \frac{A_{280} - (A_{643} * CF)}{\varepsilon}$$

$$D = \frac{A_{643}}{\varepsilon_{dye} * [P]}$$

Correction factor (CF) for Alexa Fluor 633 –Maleimide (Invitrogen) determined to be 0.28 in 50mM sodium phosphate, 300mM NaCl pH 8.0.

Cleavage by HIV protease:

The pure individual transducers were dialyzed against two different cleavage buffers

1) 50mM MES, (pH 6.0), 1mM EDTA, 0.9M NaCl, 1mM DTT, 10% Glycerol, 0.1% Triton X-100 (*124*) and into
2) 10mM Na. acetate, 1M NaCl, pH 5.0, 1mM DTT (*125*)

After overnight dialysis, the transducers were incubated with HIV Protease L63P (Sigma Aldrich, H1415), a more stable version of the wild type HIV Protease with reduced autocatalytic activity. 10 units of the protease were added to 0.1mgs/ml of the individual transducers and incubated at room temperature. Cleavage of the transducers was followed by collecting samples at different time points, which were quenched in SDS loading buffer. The samples were analyzed on an SDS gel. Due to problems associated with the further purification of the fragments from the Triton X-100 containing buffer, all further cleavage experiments were done in sodium acetate and 1M NaCl.

For cleavage at pH 5.0, 0.18mgs of PTE3_2 in 200uL of 10mM Na. acetate, 1M NaCl, pH 5.0, 1mM DTT was cut with 40units of HIV protease (~4ug). The reaction was done at room temperature and at various intervals; 15uL of sample were collected and quenched with 3uL of 6X SDS loading dye. 10uL of the quenched sample was loaded onto a Bis-Tris gradient gel and analyzed by measuring the density of the bands using ImageJ. The densities were plotted using Prism.

Quantitative Estimation of Uptake into Cells:

H9 cells ($2.18X10^5$) in 200uL of media were treated with a fixed concentration of PTK3_2 (1.56uM). The cells were incubated for either 30, 60, 120, or 180 minutes. After incubation, the cells were collected in a 1.5ml eppendorf tube and spun at 5300g for 2 minutes. The pellet was resuspended in 200uL 1X Trypsin-EDTA and incubated for 5 minutes at 37°C. The cells were spun at 5300g for 2minutes. The supernatant was discarded and the pellet washed with PBS. Cells were then spun down and the pellet was resuspended in 70uL of lysis buffer (5% SDS, PBS) and vortexed. The cells were incubated at room temperature for 10 minutes before analysis. 50uL of cell lysate was mixed with 1800uL of PBS and analyzed by fluorescence with excitation at 620 and emission from 640-700nm. Slit sizes of 1mm were used for excitation and emission. The emission spectrum from 640-670nm was integrated and compared to a standard curve to derive concentration of protein in cells. For volume of cell Jurkat cells dimension of 11uM diameter were used(*122*).

Flow Cytometry:

Jukrat cells TIB152 (ATCC) and H9-Cells HTB-176 (ATCC) were propagated in RPMI1640 medium with L-glutamine, 25mM HEPES (GIBCO) supplemented with 10% FBS, 1% Penicillin-Streptomycin antibiotic solution (GIBCO) at 37°C, 5% CO_2. Cells that were highly viable as determined by trypan blue staining were selected.

Jukrat cells TIB152 (ATCC) and H9 cells (ATCC) were grown in RPMI1640 medium. $2X10^5$ cells per well were treated with the increasing concentrations PTE3_2, PTK3_2 and the two mixed in a 1:1 molar ratio. The proteins PTE3_2 and PTK3_2 were labeled with Alexa Fluor 488 and Alexa Fluor 633 Maleimide respectively. The cells were treated for 1 hr at 37°C. After 1 hr the cells were spun down at 1000g for 5 minutes and the supernatant discarded. The cells were resuspended in 200uL of fresh RPMI 1640 medium supplemented with FBS. For mean intensity measurements, the cells were spun down, supernatant discarded and then treated with 1X Trypsin (0.25% Trypsin-EDTA, GIBCO) for 5 minutes at 37°C, followed by quenching with media supplemented with 10% fetal bovine serum. The cells were analyzed on a FACS Canto II with excitation using the 488 laser and 635 laser and emission observed using the FITC 530/30 band pass and Alexa Fluor 633 670/40 band pass filters.

To determine the effect of the proteins on inducing apoptosis, the cells were labeled with Annexin V (BD) and 7-AAD. The data was analyzed using FACS Diva or FlowJo.

Summary

The primary aim was the design and development of anti-HIV transducer proteins which are activated by HIV protease. We set out to integrate two varied technologies, protein engineering and protein transduction into cells to achieve this goal. This has not been attempted previously with *de novo* designed multidomain proteins, since all previous attempts were limited to either simple peptides or well-characterized proteins like BSA, GFP and small transcription factors. It is possible to make proteins that address most of the required design parameters defined in Chapter 2. Also, it is possible for these complex multi-domain proteins to be transduced into cells in a manner similar to that observed in single domain proteins/peptides.

One of the big problems concerning protein design is protein solubility. Arginine and Proline as additives were shown to great enhance the solubility of these proteins; a choice of either based on the final goal. Arginine, not being particularly suited for cell cultures when compared to Proline.

We currently observe that the active heterodimer (CTD-E3/K3-DED) shows the induction of apoptosis. We believe that it is possible to increase the ability of the active heterodimers to induce apoptosis by modifying some key elements of the design. Future design iterations can include modifying the linker lengths connecting the active helix to the DED domain. This change allows one to modulate procaspase-8 recruitment. We can increase the length of the linker from the current 14 residues to lengths that are longer. This increase in length may prevent any steric clashes with the active monomer and procaspase-8. Alternatively, reducing the length of the linker can effectively reduce the volume sampled by the bound procaspase-8, increasing its effective concentration for procaspase-8 trans-cleavage.

Based on our results with the BPC-E3/K3 active dimers, the presence of N- and C-terminal residues to the coiled coil do not significantly affect the affinity of the

heterodimers. This allows the substitution of other coiled coils from the literature in future designs.

The designed protease transducers are soluble, monomeric proteins. The cell populations efficiently and uniformly take up the transducers that are multi-domain proteins. Based on the length of incubation times and concentration of the protein being incubated, one can transduce all cells uniformly. After transduction, protease transducers have intracellular concentrations that are in the range reported for other large transduced proteins.

By testing the protease transducers with HIV protease, cleavage of the transducer substrate is observed. However, the efficiency of cleavage is less than that observed for *gag-pol* polyprotein. Future design efforts will be directed to improving the efficiency of proteolytic cleavage by changing the length of the two linkers connecting the WW domain to the blocking helix and the linker connecting the blocking helix to the active helix. The increase in linker length will enhance accessibility to the cleavage site by HIV protease. Further modeling with these changed lengths should yield better designs with improved cleavage efficiencies.

The cells take up the active dimers; the distribution within the cell using fluorescence imaging appears uniform. Only by doing confocal microscopy can this uniform distribution or possible sequestration within endosomal vesicles be confirmed, which would reduce the effective concentration. It may be possible to overcome limited cytosolic distribution if that is the case by redesigning the coiled coils that yield the active dimers. Increasing the length of the coiled coils from the current IAAL-E3/K3 to the VAAL-E4/K4 pair would increase their affinity significantly. This in turn can be used to improve active dimer formation from the low bioavailability of protease transducers.

The protease transducers do not induce apoptosis at lower concentration in uninfected Jurkat cells. At higher concentrations, there is evidence of apoptosis which

may be due to proteolytic cleavage by intracellular proteases. We have attempted to address this issue by identifying cellular proteases and mapping their cleavage sites onto the transducer sequence. The information on all human cellular proteases and their targets sites is limited and we may have to approach cellular cleavage of the transducers by alternative methods like western blotting followed by identification of cleavage products. This design can be a template to develop new transducers against other viral proteins like HCV protease, HIV Nef by applying the ideas developed in this dissertation.

Appendix

Hexa-His tagged Amino Acid Sequence:

P5501
HMGYGRKKRR QRRRGYPYDV PDYAGSTTVA QLEEKVKTLR AQNYELKCRV
QRLREQVAQL ASGSGSGSGS GSGSGSMDPF LVLLHSVSSS LSSSELTELK
YLSLGRVGKR KLERVQSGLD LFSMLLEQND LEPGHTELLR ELLASLRRHD
LLRRVDDFEL E

CTD-STOPDED
HMGYGRKKRR QRRRGYPYDV PDYAGSTTVA QLEEKVKTLR AQNYELKCRV
QRLREQVAQL ASGSGSGSGS GSGSGS

CTD-DED
HMYGRRARRR RRRGYPYDVP DYAGCGGSGS GSGSGSGSGS GSMDPFLVLL
HSVSSSLSSS ELTELKYLSL GRVGKRKLER VQSGLDLFSM LLEQNDLEPG
HTELLRELLA SLRRHDLLRR VDDFELE

CTD-TETRA
HMYGRRARRR RRRGYPYDVP DYAGCGGSTT VAQLEEKVKT LRAQNYELKS
RVQRLREQVA QLASGSGSGS GSGSGSGSMD PFLVLLHSVS SSLSSSELTE
LKYLSLGRVG KRKLERVQSG LDLFSMLLEQ NDLEPGHTEL LRELLASLRR
HDLLRRVDDF ELE

CTD-E3-DED
HMYGRRARRR RRRYPYDVPD YAGCGGEIAA LEKEIAALEK EIAALEKGSG
SGSGSGSGSG SMDPFLVLLH SVSSSLSSSE LTELKYLSLG RVGKRKLERV
QSGLDLFSML LEQNDLEPGH TELLRELLAS LRRHDLLRRV DDFELE

CTD-K3-DED
HMYGRRARRR RRRYPYDVPD YAGCGGKIAA LKEKIAALKE KIAALKEGSG
SGSGSGSGSG SMDPFLVLLH SVSSSLSSSE LTELKYLSLG RVGKRKLERV
QSGLDLFSML LEQNDLEPGH TELLRELLAS LRRHDLLRRV DDFELE

CTD-NF-E3-DED
GHMRRARRRR RRGETSLGSG CSEIAALEKE IAALEKEIAA LEKGTGLPSY
DEALHGSMDP FLVLLHSVSS SLSSSELTEL KYLSLGRVGK RKLERVQSGL
DLFSMLLEQN DLEPGHTELL RELLASLRRH DLLRRVDDFE LE

CTD-NF-K3-DED
GHMRRARRRR RRGETSLGSG CSKIAALKEK IAALKEKIAA LKEGTGLPSY
DEALHGSMDP FLVLLHSVSS SLSSSELTEL KYLSLGRVGK RKLERVQSGL
DLFSMLLEQN DLEPGHTELL RELLASLRRH DLLRRVDDFE LE

BPE3
HMLETSLGDY KDDDDKGSGC SEIAALEKEI AALEKEIAAL EKGTGLPSYD
EALHGSMDPF LVLLHSVSSS LSSSELTELK YLSLGRVGKR KLERVQSGLD
LFSMLLEQND LEPGHTELLR ELLASLRRHD LLRRVDDFEL E

BPK3
HMLETSLGDY KDDDDKGSGC SKIAALKEKI AALKEKIAAL KEGTGLPSYD
EALHGSMDPF LVLLHSVSSS LSSSELTELK YLSLGRVGKR KLERVQSGLD
LFSMLLEQND LEPGHTELLR ELLASLRRHD LLRRVDDFEL E

CTD-K3-DEDF
HMRRARRRRR RGETSLGSGC SKIAALKEKI AALKEKIAAL KEGTGLPSYD
EALHGSMDPF LVLLHSVSSS LSSSELTELK YLSLGRVGKR KLERVQSGLD
LFSMLLEQND LEPGHTELLR ELLASLRRHD LLRRVDDFEL EDYKDDDDK

CTD-MRFP
GHMRRARRRR RRMASSEDVI KEFMRFKVRM EGSVNGHEFE IEGEGEGRPY
EGTQTAKLKV TKGGPLPFAW DILSPQFQYG SKAYVKHPAD IPDYLKLSFP
EGFKWERVMN FEDGGVVTVT QDSSLQDGEF IYKVKLRGTN FPSDGPVMQK
KTMGWEASTE RMYPEDGALK GEIKMRLKLK DGGHYDAEVK TTYMAKKPVQ
LPGAYKTDIK LDITSHNEDY TIVEQYERAE GRHSTGA

E3-L1-DED
HMYGRRARRR RRRYPYDVPD YAGCGGEIAA LEKEIAALEK EIAALEKGGG
SGGGTGGGSG GMDPFLVLLH SVSSSLSSSE LTELKYLSLG RVGKRKLERV
QSGLDLFSML LEQNDLEPGH TELLRELLAS LRRHDLLRRV DDFELE

E3-L2-DED
HMYGRRARRR RRRYPYDVPD YAGCGGEIAA LEKEIAALEK EIAALEKGAS
GGGSTRGHYM DPFLVLLHSV SSSLSSSELT ELKYLSLGRV GKRKLERVQS
GLDLFSMLLE QNDLEPGHTE LLRELLASLR RHDLLRRVDD FELE

PTK3_2
MGHHHHHHSS GLFKRHNDYD IPTTENLYFQ GRRARRRRRR GPLGSGEEEP
LPPRWSMQVA PNGRTFFIDH ASRRTTWIDP RNGRASSGSG IFLETSLGSD
YGSGDKGSEI AALEKEIAAN EKEIAALEKS GSGSGIFLET SLGDYKDDDD
KGSGCSKIAA LKEKIAALKE KIAALKEGTG LPSYDEALHG SMDPFLVLLH
SVSSSLSSSE LTELKYLSLG RVGKRKLERV QSGLDLFSML LEQNDLEPGH
TELLRELLAS LRRHDLLRRV DDFELE

PTE3_2
MGHHHHHHSS GLFKRHNDYD IPTTENLYFQ GRRARRRRRR GPLGSGEEEP
LPPRWSMQVA PNGRTFFIDH ASRRTTWIDP RNGRASSGSG IFLETSLGSD
YGSGDKGSKI AALKEKIAAN KEKIAALKES GSGSGIFLET SLGDYKDDDD
KGSGCSEIAA LEKEIAALEK EIAALEKGTG LPSYDEALHG SMDPFLVLLH
SVSSSLSSSE LTELKYLSLG RVGKRKLERV QSGLDLFSML LEQNDLEPGH
TELLRELLAS LRRHDLLRRV DDFELE

PTK3-1
HMYGRRARRR RRRYPYDVPD YAGRRRVTVR KADAGGLGIS IKGGRENKMP
ILISKIFKGL AADQTEALFV GDAILSVNGE DLSSATHDEA VQALKKTGKE
VVLEVKYMKS GSGSAEYVRA LFDFNGNDEE DLPFKKGDIL RIRDKPEEQW
WNAEDSEGKR GMIPVPYVEK YGCKIAALKE KIAALKEKIA ALKEGSGSGM
DPFLVLLHSV SSSLSSSELT ELKYLSLGRV GKRKLERVQS GLDLFSMLLE
QNDLEPGHTE LLRELLASLR RHDLLRRVDD FELEGIRKIL FLDGPPPVPP
RRSGSGSGSG SGVKESLV PTE

PTE3-1
HMYGRRARRR RRRYPYDVPD YAGRRRVTVR KADAGGLGIS IKGGRENKMP
ILISKIFKGL AADQTEALFV GDAILSVNGE DLSSATHDEA VQALKKTGKE
VVLEVKYMKS GSGSAEYVRA LFDFNGNDEE DLPFKKGDIL RIRDKPEEQW
WNAEDSEGKR GMIPVPYVEK YGCEIAALEK EIAALEKEIA ALEKGSGSGM
DPFLVLLHSV SSSLSSSELT ELKYLSLGRV GKRKLERVQS GLDLFSMLLE
QNDLEPGHTE LLRELLASLR RHDLLRRVDD FELEGIRKIL FLDGPPPVPP
RRSGSGSGSG SGVKESLV

CTD-PROTEASE
MGHHHHHHSS GLFKRHNDYD IPTTENLYFQ GHMYGRRARR RRRRDYKDDD
DKCGPQITLW KRPLVTIKIG GQLKEALLDT GADDTVIEEM NLPGRWKPKM
IGGIGGFIKV RQYDQIIEIA GHKAIGTVLV GPTPVNIIGR NLLTQIGATL
NF

CTD-NEF
HMYGRRARRR RRRYPYDVPD YAGCEAQEEE EVGFPVRPQV PLRPMTYKAA
VDLSHFLKEK GGLEGLIHSQ RRQDILDLWI YHTQGYFPDW QNYTPGPGVR
YPLTFGWSYK LVPVEPDKVE EANKGENTSL LHPVSLHGMD DPEREVLEWR
FDSRLAFHHV ARELHPEYFK NMDPFLV

DNA sequences for proteins constructed.

>P5501
GGTACCTTATTCCAGTTCGAAGTCGTCTACACGGCGCAGCAGGTCGTGACGACGCAGGC
TTGCCAGCAGTTCACGCAGCAGTTCCGTGTGGCCTGGTTCCAGGTCGTTCTGTTCCAGC
AGCATAGAGAACAGATCCAGGCCGGACTGAACACGCTCCAGCTTACGTTTGCCCACACG
ACCCAGGGACAGATATTTCAGTTCCGTCAGTTCGGAAGAGGACAGAGAAGAAGAAACAG
AATGCAGCAGCACCAGGAACGGGTCCATGCTGCCGGAACCGGAGCCAGAGCCAGAACCA
GAGCCAGAGCCGCTTGCCAGCTGTGCTACCTGCTCACGCAGACGCTGAACGCGACATTT
CAGCTCATAGTTTTGTGCACGCAGGGTTTTGACTTTTTCTTCCAGCTGTGCAACAGTAG
TAGAGCCCGCATAGTCTGGTACATCGTATGGATAACCACGACGACGTTGACGACGTTTC
TTGCGACCGTAGCCCATATG

>CTD-E3-DED
GTCGCTGACATATGTATGGTCGTCGTGCTCGTCGTCGTCGTCGTCGTTATCCTTATGAT
GTTCCGGACTACGCTGGTTGCGGTGGTGAAATCGCAGCACTGGAAAAAGAGATTGCTGC
ACTGGAGAAAGAGATCGCTGCGCTGGAGAAGGGTTCTGGTTCCGGTTCCGGCTCCGGTA
GCGGCTCTGGTTCTATGGACCCTTTTCTGGTACTGCTGCACTCTGTGTCTTCTTCCCTG
TCTAGCTCCGAACTGACCGAGCTGAAATACCTGTCCCTGGGTCGTGTTGGCAAGCGTAA
ACTGGAGCGTGTACAAAGCGGCCTGGATCTGTTCTCTATGCTGCTGGAGCAGAACGACC
TGGAACCGGGCCACACCGAGCTGCTGCGTGAACTGCTGGCATCCCTGCGCCGTCACGAC
CTGCTGCGTCGTGTTGATGATTTTGAGCTGGAGTAACCATGGCGTCA

>CTD-K3-DED
TCGCCCTTGTCGCTGACATATGTATGGTCGTCGTGCTCGTCGTCGTCGTCGTCGTTATC
CTTATGATGTTCCGGACTACGCTGGTTGCGGTGGTAAAATCGCAGCACTGAAAGAGAAA
ATTGCTGCACTGAAAGAGAAAATCGCTGCGCTGAAGGAGGGTTCTGGTTCCGGTTCCGG
CTCCGGTAGCGGCTCTGGTTCTATGGACCCTTTTCTGGTACTGCTGCACTCTGTGTCTT
CTTCCCTGTCTAGCTCCGAACTGACCGAGCTGAAATACCTGTCCCTGGGTCGTGTTGGC
AAGCGTAAACTGGAGCGTGTACAAAGCGGCCTGGATCTGTTCTCTATGCTGCTGGAGCA
GAACGACCTGGAACCGGGCCACACCGAGCTGCTGCGTGAACTGCTGGCATCCCTGCGCC
GTCACGACCTGCTGCGTCGTGTTGATGATTTTGAGCTGGAGTAACCATGGCGTCAA

>CTD-K3-DEDF
CATATGCGTCGTGCGCGTCGTCGTCGCCGTCGCGGTGAAACCAGCCTGGGTAGCGGCTG
CAGCAAGATCGCTGCGCTGAAAGAGAAGATTGCCGCGCTGAAAGAAAAGATCGCGGCTC
TGAAAGAGGGTACCGGTCTGCCGAGCTATGATGAAGCCTTGCACGGTAGCATGGATCCG
TTTCTGGTTTTGCTGCATAGCGTTAGCTCGAGCCTGAGCTCTAGCGAGTTGACCGAGCT
GAAATACCTGAGCCTGGGCCGTGTCGGTAAACGCAAGCTGGAGCGTGTTCAGAGCGGCC
TGGATTTGTTTAGCATGCTGCTGGAACAAAACGACTTGGAACCGGGCCACACCGAGCTG
CTGCGTGAGCTGCTGGCATCCCTGCGTCGTCACGACCTGCTGCGCCGTGTGGACGACTT
CGAGCTGGAGGACTACAAGGACGACGATGATAAGTAACCATGCGTGTGGAAGCCGAATT
CCAGCACACTGGCGGCCGTTACTAGTGGATCCGAGCTCGGT

>CTD-E3-DEF
CATATGCGTCGTGCGCGTCGTCGTCGCCGTCGCGGTGAAACCAGCCTGGGTAGCGGCTG
CAGCGAGATCGCTGCGCTGGAGAAAGAGATTGCCGCGCTGGAAAAAGAAATCGCGGCTC
TGGAAAAAGGTACCGGTCTGCCGAGCTATGATGAAGCCTTGCACGGTAGCATGGATCCG
TTTCTGGTTTTGCTGCATAGCGTTAGCTCGAGCCTGAGCTCTAGCGAGTTGACCGAGCT
GAAATACCTGAGCCTGGGCCGTGTCGGTAAACGCAAGCTGGAGCGTGTTCAGAGCGGCC
TGGATTTGTTTAGCATGCTGCTGGAACAAAACGACTTGGAACCGGGCCACACCGAGCTG
CTGCGTGAGCTGCTGGCATCCCTGCGTCGTCACGACCTGCTGCGCCGTGTGGACGACTT
CGAGCTGGAGGACTACAAGGACGACGATGATAAGTAACCATGCGTGTGGAAGCCG

>CTD-E3-L1-DED
CATATGTATGGTCGTCGTGCTCGTCGTCGTCGTCGTCGTTATCCTTATGATGTTCCGGA
CTACGCTGGTTGCGGTGGTGAAATCGCAGCACTGGAAAAAGAGATTGCTGCACTGGAGA
AAGAGATCGCTGCGCTGGAGAAGGGTGGCGGATCTGGAGGCGGTACTGGAGGGGGATCA

GGAGGAATGGACCCTTTTCTGGTACTGCTGCACTCTGTGTCTTCTTCCCTGTCTAGCTC
CGAACTGACCGAGCTGAAATACCTGTCCCTGGGTCGTGTTGGCAAGCGTAAACTGGAGC
GTGTACAAAGCGGCCTGGATCTGTTCTCTATGCTGCTGGAGCAGAACGACCTGGAACCG
GGCCACACCGAGCTGCTGCGTGAACTGCTGGCATCCCTGCGCCGTCACGACCTGCTGCG
TCGTGTTGATGATTTTGAGCTGGAGTAACCATGG

>CTD-E3-L2-DED
CATATGTATGGTCGTCGTGCTCGTCGTCGTCGTCGTCGTTATCCTTATGATGTTCCGGA
CTACGCTGGTTGCGGTGGTGAAATCGCAGCACTGGAAAAAGAGATTGCTGCACTGGAGA
AAGAGATCGCTGCGCTGGAGAAGGGTGCTTCTGGAGGCGGTTCTACTAGAGGTCATTAT
ATGGACCCTTTTCTGGTACTGCTGCACTCTGTGTCTTCTTCCCTGTCTAGCTCCGAACT
GACCGAGCTGAAATACCTGTCCCTGGGTCGTGTTGGCAAGCGTAAACTGGAGCGTGTAC
AAAGCGGCCTGGATCTGTTCTCTATGCTGCTGGAGCAGAACGACCTGGAACCGGGCCAC
ACCGAGCTGCTGCGTGAACTGCTGGCATCCCTGCGCCGTCACGACCTGCTGCGTCGTGT
TGATGATTTTGAGCTGGAGTAACCATGGCGTCAAGCC

>CTD-NF-K3-DED
CATATGCGTCGTGCGCGTCGTCGTCGCCGTCGCGGTGAAACCAGCCTGGGTAGCGGCTG
CAGCAAGATCGCTGCGCTGAAAGAGAAGATTGCCGCGCTGAAAGAAAAGATCGCGGCTC
TGAAAGAGGGTACCGGTCTGCCGAGCTATGATGAAGCCTTGCACGGTAGCATGGATCCG
TTTCTGGTTTTGCTGCATAGCGTTAGCTCGAGCCTGAGCTCTAGCGAGTTGACCGAGCT
GAAATACCTGAGCCTGGGCCGTGTCGGTAAACGCAAGCTGGAGCGTGTTCAGAGCGGCC
TGGATTTGTTTAGCATGCTGCTGGAACAAAACGACTTGGAACCGGGCCACACCGAGCTG
CTGCGTGAGCTGCTGGCATCCCTGCGTCGTCACGACCTGCTGCGCCGTGTGGACGACTT
CGAGCTGGAGGACTACAAGGACGACGATGATAAGTAACCATGCGTGTGGAAGCCGAATT
CCAGCACACTGGCGGCCGTTACTAGTGGATCCGAGCTCGGT

>BPK3 (K3-DED-2-4)
CATATGCTGGAAACCAGCCTGGGCGACTACAAGGACGACGATGATAAGGGTAGCGGCTG
CAGCAAGATCGCTGCGCTGAAAGAGAAGATTGCCGCGCTGAAAGAAAAGATCGCGGCTC
TGAAAGAGGGTACCGGTCTGCCGAGCTATGATGAAGCCTTGCACGGTAGCATGGATCCG
TTTCTGGTTTTGCTGCATAGCGTTAGCTCGAGCCTGAGCTCTAGCGAGTTGACCGAGCT
GAAATACCTGAGCCTGGGCCGTGTCGGTAAACGCAAGCTGGAGCGTGTTCAGAGCGGCC
TGGATTTGTTTAGCATGCTGCTGGAACAAAACGACTTGGAACCGGGCCACACCGAGCTG
CTGCGTGAGCTGCTGGCATCCCTGCGTCGTCACGACCTGCTGCGCCGTGTGGACGACTT
CGAGCTGGAGTAACCATGGAAGCCGAATTCTGCAGATATCCATCACACTGGCGGCCGCT
CGAGCATG

>CTD-PROTEASE
CCATGGTTAAAAATTCAGGGTCGCACCGATCTGGGTCAGCAAATTACGACCGATGATGT
TCACAGGGGTTGGACCAACCAGGACCGTGCCAATCGCTTTGTGGCCCGCAATCTCAATG
ATTTGGTCGTATTGACGCACCTTGATGAAGCCGCCGATACCACCAATCATTTTCGGTTT
CCAACGACCCGGCAGGTTCATTTCCTCGATGACCGTATCGTCAGCGCCGGTATCCAACA
GGGCTTCCTTCAGCTGACCGCCAATCTTAATAGTAACCAGCGGACGTTTCCACAGCGTA
ATCTGCGGACCGCACTTATCGTCGTCATCTTTATAGTCGCGACGACGACGGCGACGTGC
GCGGCGACCGTACATATG

>mRFP
ATGGCCTCCTCCGAGGACGTCATCAAGGAGTTCATGCGCTTCAAGGTGCGCATGGAGGG
CTCCGTGAACGGCCACGAGTTCGAGATCGAGGGCGAGGGCGAGGGCCGCCCCTACGAGG
GCACCCAGACCGCCAAGCTGAAGGTGACCAAGGGCGGCCCCCTGCCCTTCGCCTGGGAC
ATCCTGTCCCCTCAGTTCCAGTACGGCTCCAAGGCCTACGTGAAGCACCCCGCCGACAT
CCCCGACTACTTGAAGCTGTCCTTCCCCGAGGGCTTCAAGTGGGAGCGCGTGATGAACT
TCGAGGACGGCGGCGTGGTGACCGTGACCCAGGACTCCTCCCTGCAGGACGGCGAGTTC
ATCTACAAGGTGAAGCTGCGCGGCACCAACTTCCCCTCCGACGGCCCCGTAATGCAGAA
GAAGACCATGGGCTGGGAGGCCTCCACCGAGCGGATGTACCCCGAGGACGGCGCCCTGA
AGGGCGAGATCAAGATGAGGCTGAAGCTGAAGGACGGCGGCCACTACGACGCCGAGGTC
AAGACCACCTACATGGCCAAGAAGCCCGTGCAGCTGCCCGGCGCCTACAAGACCGACAT
CAAGCTGGACATCACCTCCCACAACGAGGACTACACCATCGTGGAACAGTACGAGCGCG
CCGAGGGCCGCCACTCCACCGGCGCCTAATAACCATGGCACTCCACCGGCGCCTAA

>CTD-mRFP
CATATGCGCCGTGCGCGTCGTCGTCGCNGTCGCATGGCCTNCTCCGAGGACGTCATCAA
GGAGTTCATGCGCTTCAAGGTGCGCATGGAGGGNTCCGTGAACGNCCACGAGTTCGAGA
TCGAGGGCGAGGGCGAGGGCCGCCCNTACGAGGGCACCCAGACCGCCAAGCTGAAGGTG
ACCAAGGGCGGCCCCCTGCCCTTCGCCTGGGACATCCTGTCCCNTCAGTTCCAGTATGG
CTCCAAGGCNTACGTGAAGCACCCCGCCGACATCCCCGACTACTTGAAGCTGTCCTTCC
CCGAGGGCTTCAAGTGGGAGCGCGTGATGAACTTCGAGGACGGCGGCGTGGTGACCGTG
ACCCAGGACTCCTCCCTGCAGGACGGCGAGTTCATCTACAAGGTGAAGCTGCGCGGCAC
CAACTTCCCCTCCGACGGCCCCGTAATGCAGAAGAAGACCATGGGCTGGGAGGCCTCCA
CCGAGCGGATGTACCCCGAGGACGGCGCCCTGAAGGGCGAGATCAAGATGAGGCTGAAG
CTGAAGGACGGCGGCCACTACGACGCCGAGGTCAAGACCACCTACATGGCCAAGAAGCC
CGTGCAGCTGCCCGGCGCCTACAAGACCGACATCAAGCTGGACATCACCTCCCACAACG
AGGACTACACCATCGTGGAACAGTACGAGCGCGCCGAGGGCCGCCACTCCACCGGCGCC
TAATAACCATGGAAG

>CTD-NEF
CATATGTACGGTCGTCGCGCTCGTCGTCGTCGCCGTCGCTATCCTTATGATGTGCCGGA
CTATGCCGGTTGCGAAGCGCAGGAGGAGGAAGAAGTTGGCTTCCCGGTCCGTCCGCAGG
TCCCTCTGCGTCCGATGACCTACAAGGCGGCAGTTGATTTGTCTCACTTCCTGAAAGAA
AAAGGTGGCCTGGAGGGTCTGATTCACAGCCAACGCCGCCAAGATATTCTGGACTTGTG
GATCTATCACACGCAGGGTTACTTCCCGGATTGGCAAAACTATACTCCGGGTCCAGGTG
TTCGTTACCCACTGACGTTTGGCTGGAGCTACAAGCTGGTGCCGGTTGAGCCGGATAAG
GTTGAGGAGGCGAATAAGGGTGAAAACACCAGCCTGCTGCATCCGGTGTCCCTGCACGG
CATGGACGACCCGGAGCGCGAGGTCCTGGAATGGCGTTTTGACAGCCGTTTGGCGTTTC
ATCACGTGGCACGCGAGCTGCACCCGGAATACTTCAAAAACATGGATCCGTTTTTGGTG
TGATAACCATGGAAG

>PTK3

GAACATATGTATGGTCGTCGTGCTCGTCGCCGCCGTCGTCGTTATCCTTATGATGTTCC
GGACTACGCTGGTCGCCGTCGCGTGACCGTTCGTAAAGCTGACGCAGGCGGCCTGGGTA
TTTCCATCAAAGGTGGTCGCGAGAACAAGATGCCGATCCTGATCAGCAAGATTTTTAAG
GGCCTGGCCGCCGACCAAACGGAAGCTCTGTTTGTTGGTGACGCGATCTTGAGCGTGAA

CGGCGAGGACTTGAGCTCTGCAACTCACGACGAGGCGGTTCAGGCGCTGAAAAAGACGG
GTAAGGAGGTGGTGCTGGAGGTCAAATACATGAAAAGCGGTTCCGGTAGCGCGGAGTAC
GTTCGTGCCCTGTTTGACTTTAACGGTAATGATGAGGAAGATCTGCCGTTCAAGAAAGG
CGATATTTTGCGTATTCGTGACAAACCAGAGGAACAGTGGTGGAACGCAGAGGACAGCG
AAGGTAAACGTGGCATGATTCCGGTGCCGTATGTTGAGAAGTACGGCTGCAAAATCGCG
GCACTGAAGGAGAAAATTGCAGCACTGAAAGAGAAGATTGCAGCGCTGAAGGAGGGTAG
CGGTTCGGGCATGGACCCGTTTCTGGTTCTGCTGCACAGCGTCAGCAGCAGCCTGAGCA
GCAGCGAGCTGACCGAGCTGAAGTATCTGAGCCTGGGCCGCGTTGGCAAGCGCAAATTG
GAGCGCGTTCAGTCGGGCCTGGATCTGTTTTCCATGCTGCTGGAACAGAACGACCTGGA
ACCGGGTCACACCGAACTGCTGCGCGAATTGCTGGCGAGCCTGCGCCGCCACGACTTGC
TGCGTCGTGTTGACGATTTCGAACTGGAGGGTATCCGCAAGATTCTGTTCTTGGATGGC
CCGCCTCCGGTGCCACCTCGTCGTTCGGGTAGCGGCAGCGGTTCTGGCTCGGGCGTTAA
AGAGAGCTTGGTCTAACCATGG

>PTE3

GACGCCATGGTTAAACCAGGCTCTCTTTAACACCGCTGCCAGAACCGCTACCAGAGCCG
CTGCGACGCGGTGGGACCGGCGGCGGACCGTCCAGGAACAGGATTTTACGGATGCCTTC
CAGCTCAAAGTCGTCAACGCGACGCAGCAGGTCGTGACGGCGCAAGCTCGCCAGCAGCT
CGCGCAGCAGCTCCGTGTGACCCGGTTCCAAGTCATTCTGCTCCAGCAACATGGAGAAC
AGATCCAGGCCGCTTTGCACACGCTCCAGTTTGCGCTTACCCACGCGACCCAAGCTCAA
GTATTTCAGCTCGGTCAGTTCGCTGGAGGACAGGCTGCTGCTGACGCTATGCAGCAGCA
CCAGAAACGGGTCCATACCGCTACCGCTGCCCTTTTCCAGTGCCGCGATTTCTTTCTCC
AGTGCTGCGATTTCCTTCTCCAGCGCCGCAATTTCGCAACCGTACTTCTCGACATACGG
AACCGGAATCATACCGCGTTTGCCTTCGCTATCCTCTGCGTTCCACCACTGTTCTTCCG
GTTTATCACGGATGCGCAGAATGTCACCCTTCTTGAAAGGCAAGTCCTCCTCGTCATTG
CCGTTGAAGTCAAACAACGCACGGACGTATTCTGCGCTGCCGGAACCGCTCTTCATGTA
CTTGACTTCCAAAACCACTTCCTTACCGGTCTTTTTCAGGGCCTGGACCGCTTCGTCAT
GGGTTGCGCTGGACAGATCCTCACCGTTGACGCTCAGGATGGCATCACCCACAAACAGC
GCTTCGGTTTGGTCTGCAGCCAGGCCTTTAAAAATTTTCGAAATCAGAATCGGCATCTT
GTTTTCACGACCACCCTTGATGCTGATACCCAGGCCACCCGCATCTGCTTTACGAACAG
TCACACGGCGGCGGCCGGCATAGTCCGGGACATCATAAGGATAACGGCGGCGACGACGA
CGAGCACGACGACCATACATATG

Design of the First generation Protease and Nef transducers:

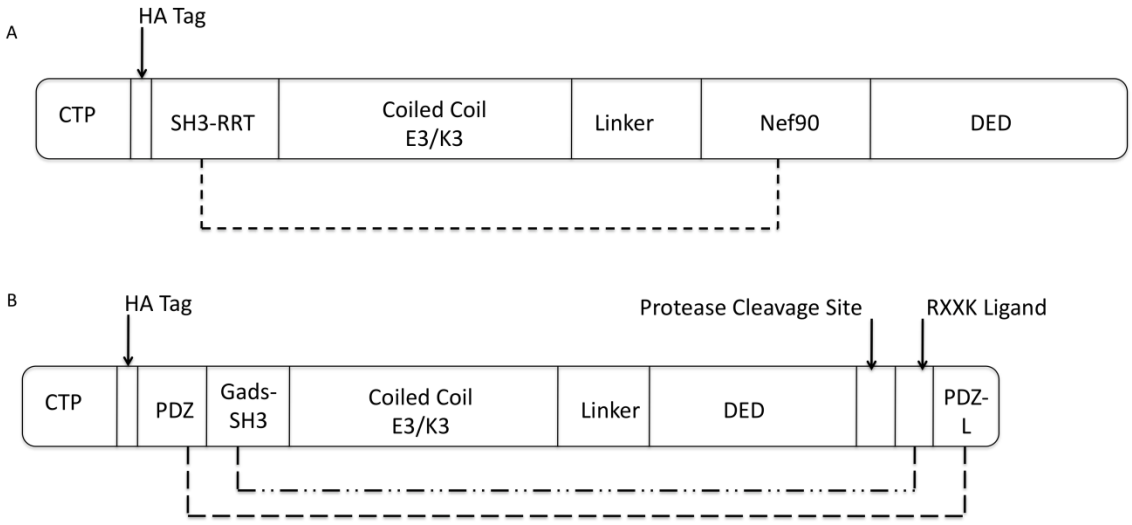

Figure A.1: Block representation of the first generation transducers that were constructed. A) The Nef Transducer N90TE3/K3. B) The Protease transducer PTE3/K3. The designs were based on maintaining closed inactive molecules through intramolecular interactions.

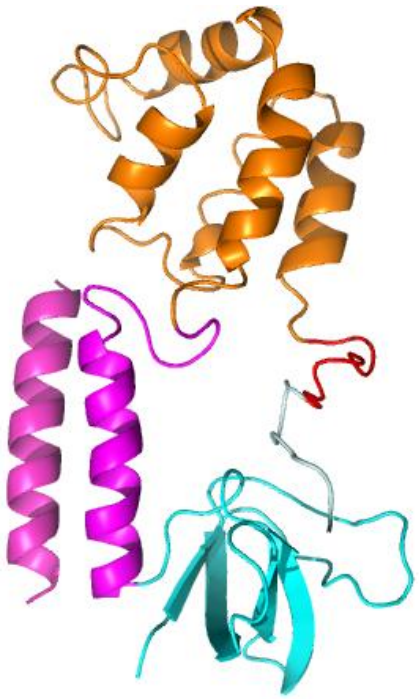

Figure A.2: Model of the first generation Protease transducer (PTK3). Model was built using X-Ray or NMR data deposited in the PDB. The model were constructed in XFit and analyzed for helix formation (magenta) when in the closed state. The design was abandoned due to the formation of the full helix and poor solubility of the proteins PTE3 and PTK3.

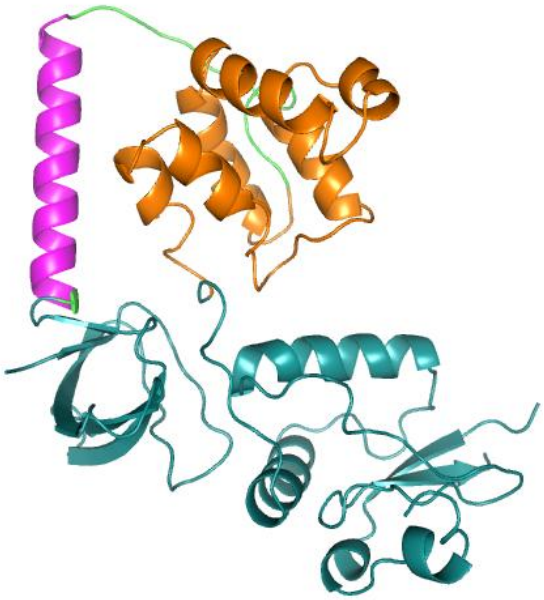

Figure A.3: Model of the first generation Nef transducer NTE3. The model clearly indicates the formation of a whole single helix (magenta) even in the closed state of the inactive protein; The DED domain is colored orange. The design was abandoned due to the formation of the full helix and poor solubility of the proteins N90TE3 and N90TK3.

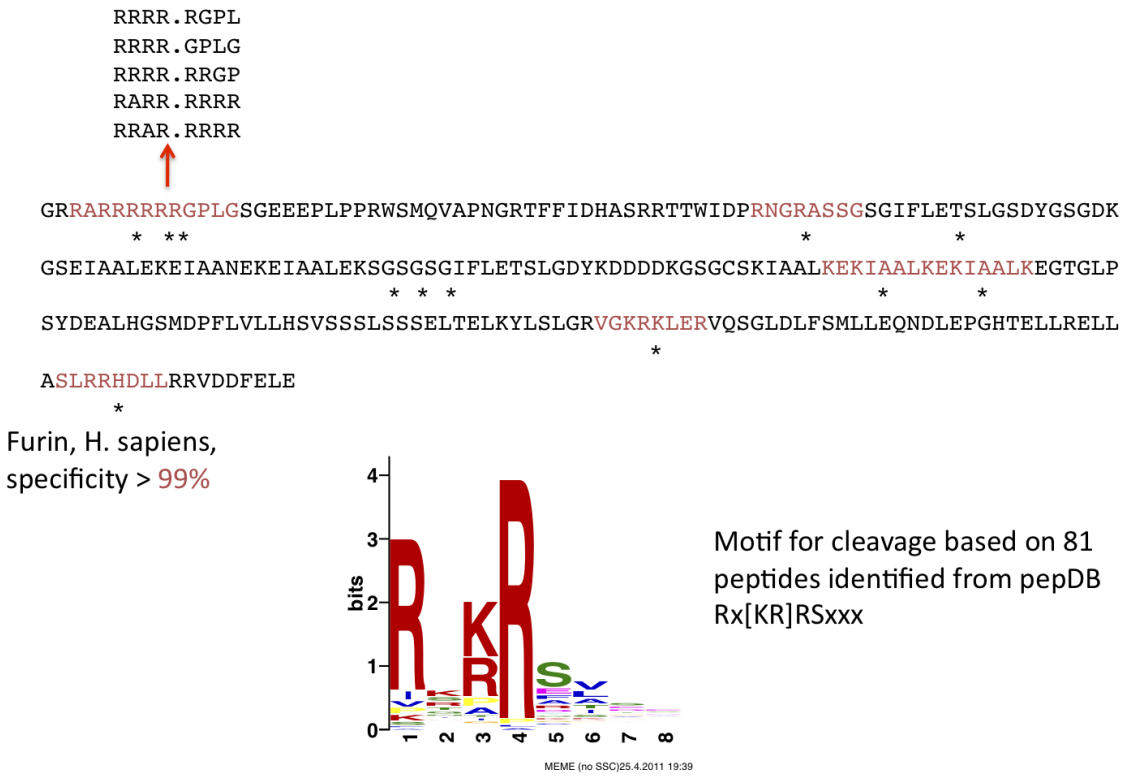

Figure A.4: Cleavage of PTK3_2 by Furin. The cleavage sites were predicted after analyzing unique peptide substrates followed by construction of the cleavage Motif.

References

1. Blankson, J. N., Persaud, D., and Siliciano, R. F. (2002) The challenge of viral reservoirs in HIV-1 infection, Annu Rev Med 53, 557-593.
2. Peterlin, B. M., and Trono, D. (2003) Hide, shield and strike back: how HIV-infected cells avoid immune eradication, Nat Rev Immunol 3, 97-107.
3. Geeraert, L., Kraus, G., and Pomerantz, R. J. (2008) Hide-and-seek: the challenge of viral persistence in HIV-1 infection, Annu Rev Med 59, 487-501.
4. Saksena, N. K., and Haddad, D. N. (2003) Viral reservoirs an impediment to HAART: new strategies to eliminate HIV-1, Curr Drug Targets Infect Disord 3, 179-206.
5. de Lorenzo, V., Serrano, L., and Valencia, A. (2006) Synthetic biology: challenges ahead, Bioinformatics 22, 127-128.
6. Pawson, T., and Linding, R. (2005) Synthetic modular systems--reverse engineering of signal transduction, FEBS Lett 579, 1808-1814.
7. Lim, W. A. (2002) The modular logic of signaling proteins: building allosteric switches from simple binding domains, Curr Opin Struct Biol 12, 61-68.
8. Dueber, J. E., Yeh, B. J., Chak, K., and Lim, W. A. (2003) Reprogramming control of an allosteric signaling switch through modular recombination, Science 301, 1904-1908.
9. Yeh, B. J., Rutigliano, R. J., Deb, A., Bar-Sagi, D., and Lim, W. A. (2007) Rewiring cellular morphology pathways with synthetic guanine nucleotide exchange factors, Nature 447, 596-600.
10. Howard, P., Chia, M., Del Rizzo, S., Liu, F., and Pawson, T. (2003) Redirecting tyrosine kinase signaling to an apoptotic caspase pathway through chimeric adaptor proteins, P Natl Acad Sci USA 100, 11267.
11. Hatzivassiliou, E. G., Tsichritzis, T., and Mosialos, G. (2005) Induction of apoptosis by rewiring the signal transduction of Epstein-Barr virus oncoprotein LMP1 toward caspase activation, J Virol 79, 5215-5219.
12. Wu, Y. I., Frey, D., Lungu, O. I., Jaehrig, A., Schlichting, I., Kuhlman, B., and Hahn, K. M. (2009) A genetically encoded photoactivatable Rac controls the motility of living cells, Nature 461, 104-108.
13. Gougeon, M. L. (2003) Apoptosis as an HIV strategy to escape immune attack, Nat Rev Immunol 3, 392-404.
14. Ross, T. M. (2001) Using death to one's advantage: HIV modulation of apoptosis, Leukemia 15, 332-341.
15. Finkel, T. H., Tudor-Williams, G., Banda, N. K., Cotton, M. F., Curiel, T., Monks, C., Baba, T. W., Ruprecht, R. M., and Kupfer, A. (1995) Apoptosis

occurs predominantly in bystander cells and not in productively infected cells of HIV- and SIV-infected lymph nodes, Nat Med 1, 129-134.

16. Greenway, A. L., Holloway, G., McPhee, D. A., Ellis, P., Cornall, A., and Lidman, M. (2003) HIV-1 Nef control of cell signalling molecules: multiple strategies to promote virus replication, J Biosci 28, 323-335.

17. Collins, K. L., Chen, B. K., Kalams, S. A., Walker, B. D., and Baltimore, D. (1998) HIV-1 Nef protein protects infected primary cells against killing by cytotoxic T lymphocytes, Nature 391, 397-401.

18. Geleziunas, R., Xu, W., Takeda, K., Ichijo, H., and Greene, W. C. (2001) HIV-1 Nef inhibits ASK1-dependent death signalling providing a potential mechanism for protecting the infected host cell, Nature 410, 834-838.

19. Yoon, K., Jeong, J. G., and Kim, S. (2001) Stable expression of human immunodeficiency virus type 1 Nef confers resistance against Fas-mediated apoptosis, AIDS Res Hum Retroviruses 17, 99-104.

20. Wolf, D., Witte, V., Laffert, B., Blume, K., Stromer, E., Trapp, S., d'Aloja, P., Schurmann, A., and Baur, A. S. (2001) HIV-1 Nef associated PAK and PI3-kinases stimulate Akt-independent Bad-phosphorylation to induce anti-apoptotic signals, Nat Med 7, 1217-1224.

21. Zhu, Y., Roshal, M., Li, F., Blackett, J., and Planelles, V. (2003) Upregulation of survivin by HIV-1 Vpr, Apoptosis 8, 71-79.

22. Conti, L., Matarrese, P., Varano, B., Gauzzi, M. C., Sato, A., Malorni, W., Belardelli, F., and Gessani, S. (2000) Dual role of the HIV-1 vpr protein in the modulation of the apoptotic response of T cells, J Immunol 165, 3293-3300.

23. Gibellini, D., Re, M. C., Ponti, C., Vitone, F., Bon, I., Fabbri, G., Grazia Di Iasio, M., and Zauli, G. (2005) HIV-1 Tat protein concomitantly down-regulates apical caspase-10 and up-regulates c-FLIP in lymphoid T cells: a potential molecular mechanism to escape TRAIL cytotoxicity, J Cell Physiol 203, 547-556.

24. Zauli, G., Gibellini, D., Caputo, A., Bassini, A., Negrini, M., Monne, M., Mazzoni, M., and Capitani, S. (1995) The human immunodeficiency virus type-1 Tat protein upregulates Bcl-2 gene expression in Jurkat T-cell lines and primary peripheral blood mononuclear cells, Blood 86, 3823-3834.

25. Tanaka, Y., Kameoka, M., Ota, K., Itaya, A., Ikuta, K., and Yoshihara, K. (1999) Establishment of persistent infection with HIV-1 abrogates the caspase-3-dependent apoptotic signaling pathway in U937 cells, Exp Cell Res 247, 514-524.

26. Moir, S., Chun, T. W., and Fauci, A. S. (2011) Pathogenic mechanisms of HIV disease, Annu Rev Pathol 6, 223-248.

27. Perelson, A. S., Essunger, P., Cao, Y., Vesanen, M., Hurley, A., Saksela, K., Markowitz, M., and Ho, D. D. (1997) Decay characteristics of HIV-1-infected compartments during combination therapy, Nature 387, 188-191.

28. Chun, T. W., Stuyver, L., Mizell, S. B., Ehler, L. A., Mican, J. A., Baseler, M., Lloyd, A. L., Nowak, M. A., and Fauci, A. S. (1997) Presence of an inducible

HIV-1 latent reservoir during highly active antiretroviral therapy, Proc Natl Acad Sci U S A 94, 13193-13197.

29. Finzi, D., Hermankova, M., Pierson, T., Carruth, L. M., Buck, C., Chaisson, R. E., Quinn, T. C., Chadwick, K., Margolick, J., Brookmeyer, R., Gallant, J., Markowitz, M., Ho, D. D., Richman, D. D., and Siliciano, R. F. (1997) Identification of a reservoir for HIV-1 in patients on highly active antiretroviral therapy, Science 278, 1295-1300.

30. Petitjean, G., Al Tabaa, Y., Tuaillon, E., Mettling, C., Baillat, V., Reynes, J., Segondy, M., and Vendrell, J. P. (2007) Unintegrated HIV-1 provides an inducible and functional reservoir in untreated and highly active antiretroviral therapy-treated patients, Retrovirology 4, 60.

31. Choudhary, S. K., and Margolis, D. M. (2011) Curing HIV: Pharmacologic approaches to target HIV-1 latency, Annu Rev Pharmacol Toxicol 51, 397-418.

32. Dahl, V., Josefsson, L., and Palmer, S. (2010) HIV reservoirs, latency, and reactivation: prospects for eradication, Antiviral Res 85, 286-294.

33. Siliciano, J. D., Kajdas, J., Finzi, D., Quinn, T. C., Chadwick, K., Margolick, J. B., Kovacs, C., Gange, S. J., and Siliciano, R. F. (2003) Long-term follow-up studies confirm the stability of the latent reservoir for HIV-1 in resting CD4+ T cells, Nat Med 9, 727-728.

34. Archin, N. M., Espeseth, A., Parker, D., Cheema, M., Hazuda, D., and Margolis, D. M. (2009) Expression of latent HIV induced by the potent HDAC inhibitor suberoylanilide hydroxamic acid, AIDS Res Hum Retroviruses 25, 207-212.

35. Williams, S. A., Chen, L. F., Kwon, H., Fenard, D., Bisgrove, D., Verdin, E., and Greene, W. C. (2004) Prostratin antagonizes HIV latency by activating NF-kappaB, J Biol Chem 279, 42008-42017.

36. Sahu, G. K., and Cloyd, M. W. (2011) Latent HIV in primary T lymphocytes is unresponsive to histone deacetylase inhibitors, Virol J 8, 400.

37. Yang, H. C., Shen, L., Siliciano, R. F., and Pomerantz, J. L. (2009) Isolation of a cellular factor that can reactivate latent HIV-1 without T cell activation, Proc Natl Acad Sci U S A 106, 6321-6326.

38. Pawson, T., and Nash, P. (2003) Assembly of cell regulatory systems through protein interaction domains, Science 300, 445-452.

39. Dueber, J. E., Mirsky, E. A., and Lim, W. A. (2007) Engineering synthetic signaling proteins with ultrasensitive input/output control, Nat Biotechnol 25, 660-662.

40. Bashor, C. J., Helman, N. C., Yan, S., and Lim, W. A. (2008) Using engineered scaffold interactions to reshape MAP kinase pathway signaling dynamics, Science 319, 1539-1543.

41. Sallee, N. A., Yeh, B. J., and Lim, W. A. (2007) Engineering modular protein interaction switches by sequence overlap, J Am Chem Soc 129, 4606-4611.

42. Shi, Y. (2004) Caspase activation, inhibition, and reactivation: a mechanistic view, Protein Science 13, 1979-1987.

43. Thorburn, A. (2004) Death receptor-induced cell killing, Cell Signal 16, 139-144.

44. Salvesen, G., and Dixit, V. (1999) Caspase activation: the induced-proximity model, P Natl Acad Sci USA 96, 10964.

45. Donepudi, M., Mac Sweeney, A., Briand, C., and Grutter, M. G. (2003) Insights into the regulatory mechanism for caspase-8 activation, Mol Cell 11, 543-549.

46. Chang, D., Xing, Z., Capacio, V., Peter, M., and Yang, X. (2003) Interdimer processing mechanism of procaspase-8 activation, The EMBO Journal 22, 4132-4142.

47. Chinnaiyan, A. M., O'Rourke, K., Tewari, M., and Dixit, V. M. (1995) FADD, a novel death domain-containing protein, interacts with the death domain of Fas and initiates apoptosis, Cell 81, 505-512.

48. Chinnaiyan, A. M., Tepper, C. G., Seldin, M. F., O'Rourke, K., Kischkel, F. C., Hellbardt, S., Krammer, P. H., Peter, M. E., and Dixit, V. M. (1996) FADD/MORT1 is a common mediator of CD95 (Fas/APO-1) and tumor necrosis factor receptor-induced apoptosis, J Biol Chem 271, 4961-4965.

49. Carrington, P. E., Sandu, C., Wei, Y., Hill, J. M., Morisawa, G., Huang, T., Gavathiotis, E., and Werner, M. H. (2006) The structure of FADD and its mode of interaction with procaspase-8, Mol Cell 22, 599-610.

50. Salvesen, G. S., and Dixit, V. M. (1999) Caspase activation: the induced-proximity model, Proc Natl Acad Sci U S A 96, 10964-10967.

51. Oberst, A., Pop, C., Tremblay, A. G., Blais, V., Denault, J. B., Salvesen, G. S., and Green, D. R. (2010) Inducible dimerization and inducible cleavage reveal a requirement for both processes in caspase-8 activation, J Biol Chem 285, 16632-16642.

52. Li, F. Y., Jeffrey, P. D., Yu, J. W., and Shi, Y. (2006) Crystal structure of a viral FLIP: insights into FLIP-mediated inhibition of death receptor signaling, J Biol Chem 281, 2960-2968.

53. Liu, J., and Rost, B. (2001) Comparing function and structure between entire proteomes, Protein Sci 10, 1970-1979.

54. Litowski, J. R., and Hodges, R. S. (2002) Designing heterodimeric two-stranded alpha-helical coiled-coils. Effects of hydrophobicity and alpha-helical propensity on protein folding, stability, and specificity, J Biol Chem 277, 37272-37279.

55. Hodges, R. S. (1996) Boehringer Mannheim award lecture 1995. La conference Boehringer Mannheim 1995. De novo design of alpha-helical proteins: basic research to medical applications, Biochem Cell Biol 74, 133-154.

56. Reinke, A. W., Grant, R. A., and Keating, A. E. (2010) A synthetic coiled-coil interactome provides heterospecific modules for molecular engineering, J Am Chem Soc 132, 6025-6031.

57. Diehl, M. R., Zhang, K., Lee, H. J., and Tirrell, D. A. (2006) Engineering cooperativity in biomotor-protein assemblies, Science 311, 1468-1471.

58. Eckert, D. M., Malashkevich, V. N., Hong, L. H., Carr, P. A., and Kim, P. S. (1999) Inhibiting HIV-1 entry: discovery of D-peptide inhibitors that target the gp41 coiled-coil pocket, Cell 99, 103-115.

59. Papapostolou, D., Smith, A. M., Atkins, E. D., Oliver, S. J., Ryadnov, M. G., Serpell, L. C., and Woolfson, D. N. (2007) Engineering nanoscale order into a designed protein fiber, Proc Natl Acad Sci U S A 104, 10853-10858.

60. Wolfe, S. A., Grant, R. A., and Pabo, C. O. (2003) Structure of a designed dimeric zinc finger protein bound to DNA, Biochemistry 42, 13401-13409.

61. Petka, W. A., Harden, J. L., McGrath, K. P., Wirtz, D., and Tirrell, D. A. (1998) Reversible hydrogels from self-assembling artificial proteins, Science 281, 389-392.

62. McAllister, K. A., Zou, H., Cochran, F. V., Bender, G. M., Senes, A., Fry, H. C., Nanda, V., Keenan, P. A., Lear, J. D., Saven, J. G., Therien, M. J., Blasie, J. K., and DeGrado, W. F. (2008) Using alpha-helical coiled-coils to design nanostructured metalloporphyrin arrays, J Am Chem Soc 130, 11921-11927.

63. Mapp, A. K., Ansari, A. Z., Ptashne, M., and Dervan, P. B. (2000) Activation of gene expression by small molecule transcription factors, Proc Natl Acad Sci U S A 97, 3930-3935.

64. Crick, F. H. C. (1953) Acta Crystallogr 6, 689-698.

65. Krylov, D., Mikhailenko, I., and Vinson, C. (1994) A thermodynamic scale for leucine zipper stability and dimerization specificity: e and g interhelical interactions, EMBO J 13, 2849-2861.

66. Lavigne, P., Kondejewski, L. H., Houston, M. E., Jr., Sonnichsen, F. D., Lix, B., Skyes, B. D., Hodges, R. S., and Kay, C. M. (1995) Preferential heterodimeric parallel coiled-coil formation by synthetic Max and c-Myc leucine zippers: a description of putative electrostatic interactions responsible for the specificity of heterodimerization, J Mol Biol 254, 505-520.

67. Burkhard, P., Stetefeld, J., and Strelkov, S. V. (2001) Coiled coils: a highly versatile protein folding motif, Trends Cell Biol 11, 82-88.

68. Zhou, N. E., Kay, C. M., and Hodges, R. S. (1994) The role of interhelical ionic interactions in controlling protein folding and stability. De novo designed synthetic two-stranded alpha-helical coiled-coils, J Mol Biol 237, 500-512.

69. Graddis, T. J., Myszka, D. G., and Chaiken, I. M. (1993) Controlled formation of model homo- and heterodimer coiled coil polypeptides, Biochemistry 32, 12664-12671.

70. Kohn, W. D., Monera, O. D., Kay, C. M., and Hodges, R. S. (1995) The effects of interhelical electrostatic repulsions between glutamic acid residues in controlling the dimerization and stability of two-stranded alpha-helical coiled-coils, J Biol Chem 270, 25495-25506.

71. Kohn, W. D., Kay, C. M., and Hodges, R. S. (1995) Protein destabilization by electrostatic repulsions in the two-stranded alpha-helical coiled-coil/leucine zipper, Protein Sci 4, 237-250.

72. Kohn, W. D., Kay, C. M., and Hodges, R. S. (1997) Positional dependence of the effects of negatively charged Glu side chains on the stability of two-stranded alpha-helical coiled-coils, J Pept Sci 3, 209-223.

73. Monera, O. D., Kay, C. M., and Hodges, R. S. (1994) Electrostatic interactions control the parallel and antiparallel orientation of alpha-helical chains in two-stranded alpha-helical coiled-coils, Biochemistry 33, 3862-3871.

74. Myszka, D. G., and Chaiken, I. M. (1994) Design and characterization of an intramolecular antiparallel coiled coil peptide, Biochemistry 33, 2363-2372.

75. O'Shea, E. K., Lumb, K. J., and Kim, P. S. (1993) Peptide 'Velcro': design of a heterodimeric coiled coil, Curr Biol 3, 658-667.

76. Hodges, R. S., Saund, A. K., Chong, P. C., St-Pierre, S. A., and Reid, R. E. (1981) Synthetic model for two-stranded alpha-helical coiled-coils. Design, synthesis, and characterization of an 86-residue analog of tropomyosin, J Biol Chem 256, 1214-1224.

77. Arndt, K. M., Pelletier, J. N., Muller, K. M., Alber, T., Michnick, S. W., and Pluckthun, A. (2000) A heterodimeric coiled-coil peptide pair selected in vivo from a designed library-versus-library ensemble, J Mol Biol 295, 627-639.

78. Fairman, R., Chao, H. G., Mueller, L., Lavoie, T. B., Shen, L., Novotny, J., and Matsueda, G. R. (1995) Characterization of a new four-chain coiled-coil: influence of chain length on stability, Protein Sci 4, 1457-1469.

79. Harbury, P. B., Zhang, T., Kim, P. S., and Alber, T. (1993) A switch between two-, three-, and four-stranded coiled coils in GCN4 leucine zipper mutants, Science 262, 1401-1407.

80. Moll, J. R., Ruvinov, S. B., Pastan, I., and Vinson, C. (2001) Designed heterodimerizing leucine zippers with a ranger of pIs and stabilities up to 10(-15) M, Protein Sci 10, 649-655.

81. Lindhout, D. A., Litowski, J. R., Mercier, P., Hodges, R. S., and Sykes, B. D. (2004) NMR solution structure of a highly stable de novo heterodimeric coiled-coil, Biopolymers 75, 367-375.

82. Lumb, K. J., and Kim, P. S. (1998) A buried polar interaction imparts structural uniqueness in a designed heterodimeric coiled coil, Biochemistry 37, 13042.

83. Lumb, K. J., and Kim, P. S. (1995) A buried polar interaction imparts structural uniqueness in a designed heterodimeric coiled coil, Biochemistry 34, 8642-8648.

84. Oakley, M. G., and Kim, P. S. (1998) A buried polar interaction can direct the relative orientation of helices in a coiled coil, Biochemistry 37, 12603-12610.

85. Ingham, R. J., Colwill, K., Howard, C., Dettwiler, S., Lim, C. S., Yu, J., Hersi, K., Raaijmakers, J., Gish, G., Mbamalu, G., Taylor, L., Yeung, B., Vassilovski, G.,

Amin, M., Chen, F., Matskova, L., Winberg, G., Ernberg, I., Linding, R., O'Donnell, P., Starostine, A., Keller, W., Metalnikov, P., Stark, C., and Pawson, T. (2005) WW domains provide a platform for the assembly of multiprotein networks, Mol Cell Biol 25, 7092-7106.

86. Kanelis, V., Bruce, M. C., Skrynnikov, N. R., Rotin, D., and Forman-Kay, J. D. (2006) Structural determinants for high-affinity binding in a Nedd4 WW3* domain-Comm PY motif complex, Structure 14, 543-553.

87. Navia, M. A., Fitzgerald, P. M., McKeever, B. M., Leu, C. T., Heimbach, J. C., Herber, W. K., Sigal, I. S., Darke, P. L., and Springer, J. P. (1989) Three-dimensional structure of aspartyl protease from human immunodeficiency virus HIV-1, Nature 337, 615-620.

88. Turner, B. G., and Summers, M. F. (1999) Structural biology of HIV, J Mol Biol 285, 1-32.

89. Kohl, N. E., Emini, E. A., Schleif, W. A., Davis, L. J., Heimbach, J. C., Dixon, R. A., Scolnick, E. M., and Sigal, I. S. (1988) Active human immunodeficiency virus protease is required for viral infectivity, Proc Natl Acad Sci U S A 85, 4686-4690.

90. Strack, P. R., Frey, M. W., Rizzo, C. J., Cordova, B., George, H. J., Meade, R., Ho, S. P., Corman, J., Tritch, R., and Korant, B. D. (1996) Apoptosis mediated by HIV protease is preceded by cleavage of Bcl-2, Proc Natl Acad Sci U S A 93, 9571-9576.

91. Nie, Z., Bren, G. D., Vlahakis, S. R., Schimnich, A. A., Brenchley, J. M., Trushin, S. A., Warren, S., Schnepple, D. J., Kovacs, C. M., Loutfy, M. R., Douek, D. C., and Badley, A. D. (2007) Human immunodeficiency virus type 1 protease cleaves procaspase 8 in vivo, J Virol 81, 6947-6956.

92. Dowdy, S. F., Schwarze, S. R., Ho, A., and Vocero-Akbani, A. (1999) In vivo protein transduction: Delivery of a biologically active protein into the mouse, Science 285, 1569-1572.

93. Beck, Z. Q., Hervio, L., Dawson, P. E., Elder, J. H., and Madison, E. L. (2000) Identification of efficiently cleaved substrates for HIV-1 protease using a phage display library and use in inhibitor development, Virology 274, 391-401.

94. Li, C. J., Friedman, D. J., Wang, C., Metelev, V., and Pardee, A. B. (1995) Induction of apoptosis in uninfected lymphocytes by HIV-1 Tat protein, Science 268, 429-431.

95. Schwarze, S. R., Ho, A., Vocero-Akbani, A., and Dowdy, S. F. (1999) In vivo protein transduction: delivery of a biologically active protein into the mouse, Science 285, 1569-1572.

96. Caron, N. J., Torrente, Y., Camirand, G., Bujold, M., Chapdelaine, P., Leriche, K., Bresolin, N., and Tremblay, J. P. (2001) Intracellular delivery of a Tat-eGFP fusion protein into muscle cells, Mol Ther 3, 310-318.

97. Kim, D., Kim, C. H., Moon, J. I., Chung, Y. G., Chang, M. Y., Han, B. S., Ko, S., Yang, E., Cha, K. Y., Lanza, R., and Kim, K. S. (2009) Generation of human

induced pluripotent stem cells by direct delivery of reprogramming proteins, Cell Stem Cell 4, 472-476.

98. Chen, J., Peterson, K. R., Iancu-Rubin, C., and Bieker, J. J. (2010) Design of embedded chimeric peptide nucleic acids that efficiently enter and accurately reactivate gene expression in vivo, Proc Natl Acad Sci U S A 107, 16846-16851.

99. Sandgren, S., Cheng, F., and Belting, M. (2002) Nuclear targeting of macromolecular polyanions by an HIV-Tat derived peptide. Role for cell-surface proteoglycans, J Biol Chem 277, 38877-38883.

100. Eguchi, A., Meade, B. R., Chang, Y. C., Fredrickson, C. T., Willert, K., Puri, N., and Dowdy, S. F. (2009) Efficient siRNA delivery into primary cells by a peptide transduction domain-dsRNA binding domain fusion protein, Nat Biotechnol 27, 567-571.

101. Pujals, S., and Giralt, E. (2008) Proline-rich, amphipathic cell-penetrating peptides, Adv Drug Deliv Rev 60, 473-484.

102. Wagstaff, K. M., and Jans, D. A. (2006) Protein transduction: cell penetrating peptides and their therapeutic applications, Curr Med Chem 13, 1371-1387.

103. Ter-Avetisyan, G., Tunnemann, G., Nowak, D., Nitschke, M., Herrmann, A., Drab, M., and Cardoso, M. C. (2009) Cell entry of arginine-rich peptides is independent of endocytosis, J Biol Chem 284, 3370-3378.

104. Mai, J. C., Shen, H., Watkins, S. C., Cheng, T., and Robbins, P. D. (2002) Efficiency of protein transduction is cell type-dependent and is enhanced by dextran sulfate, J Biol Chem 277, 30208-30218.

105. Kim, D., Jeon, C., Kim, J. H., Kim, M. S., Yoon, C. H., Choi, I. S., Kim, S. H., and Bae, Y. S. (2006) Cytoplasmic transduction peptide (CTP): new approach for the delivery of biomolecules into cytoplasm in vitro and in vivo, Exp Cell Res 312, 1277-1288.

106. McRee, D. E. (1999) XtalView/Xfit--A versatile program for manipulating atomic coordinates and electron density, J Struct Biol 125, 156-165.

107. Brunger, A. T., Adams, P. D., Clore, G. M., DeLano, W. L., Gros, P., Grosse-Kunstleve, R. W., Jiang, J. S., Kuszewski, J., Nilges, M., Pannu, N. S., Read, R. J., Rice, L. M., Simonson, T., and Warren, G. L. (1998) Crystallography & NMR system: A new software suite for macromolecular structure determination, Acta Crystallogr D Biol Crystallogr 54, 905-921.

108. Leaver-Fay, A., Tyka, M., Lewis, S. M., Lange, O. F., Thompson, J., Jacak, R., Kaufman, K., Renfrew, P. D., Smith, C. A., Sheffler, W., Davis, I. W., Cooper, S., Treuille, A., Mandell, D. J., Richter, F., Ban, Y. E., Fleishman, S. J., Corn, J. E., Kim, D. E., Lyskov, S., Berrondo, M., Mentzer, S., Popovic, Z., Havranek, J. J., Karanicolas, J., Das, R., Meiler, J., Kortemme, T., Gray, J. J., Kuhlman, B., Baker, D., and Bradley, P. (2011) ROSETTA3: an object-oriented software suite for the simulation and design of macromolecules, Methods Enzymol 487, 545-574.

109. Vocero-Akbani, A. M., Heyden, N. V., Lissy, N. A., Ratner, L., and Dowdy, S. F. (1999) Killing HIV-infected cells by transduction with an HIV protease-activated caspase-3 protein, Nat Med 5, 29-33.

110. Litowski, J. R., and Hodges, R. S. (2001) Designing heterodimeric two-stranded alpha-helical coiled-coils: the effect of chain length on protein folding, stability and specificity, J Pept Res 58, 477-492.

111. Aguilera, T. A., Olson, E. S., Timmers, M. M., Jiang, T., and Tsien, R. Y. (2009) Systemic in vivo distribution of activatable cell penetrating peptides is superior to that of cell penetrating peptides, Integr Biol (Camb) 1, 371-381.

112. Mittl, P. R., Deillon, C., Sargent, D., Liu, N., Klauser, S., Thomas, R. M., Gutte, B., and Grutter, M. G. (2000) The retro-GCN4 leucine zipper sequence forms a stable three-dimensional structure, Proc Natl Acad Sci U S A 97, 2562-2566.

113. Wilkinson, D. L., and Harrison, R. G. (1991) Predicting the solubility of recombinant proteins in Escherichia coli, Biotechnology (N Y) 9, 443-448.

114. Davis, G. D., Elisee, C., Newham, D. M., and Harrison, R. G. (1999) New fusion protein systems designed to give soluble expression in Escherichia coli, Biotechnol Bioeng 65, 382-388.

115. El-Andaloussi, S., Jarver, P., Johansson, H. J., and Langel, U. (2007) Cargo-dependent cytotoxicity and delivery efficacy of cell-penetrating peptides: a comparative study, Biochem J 407, 285-292.

116. Jones, S. W., Christison, R., Bundell, K., Voyce, C. J., Brockbank, S. M., Newham, P., and Lindsay, M. A. (2005) Characterisation of cell-penetrating peptide-mediated peptide delivery, Br J Pharmacol 145, 1093-1102.

117. Shaner, N. C., Campbell, R. E., Steinbach, P. A., Giepmans, B. N., Palmer, A. E., and Tsien, R. Y. (2004) Improved monomeric red, orange and yellow fluorescent proteins derived from Discosoma sp. red fluorescent protein, Nat Biotechnol 22, 1567-1572.

118. McNaughton, B. R., Cronican, J. J., Thompson, D. B., and Liu, D. R. (2009) Mammalian cell penetration, siRNA transfection, and DNA transfection by supercharged proteins, Proc Natl Acad Sci U S A 106, 6111-6116.

119. Lawrence, M. S., Phillips, K. J., and Liu, D. R. (2007) Supercharging proteins can impart unusual resilience, J Am Chem Soc 129, 10110-10112.

120. Todd, M. J., Semo, N., and Freire, E. (1998) The structural stability of the HIV-1 protease, J Mol Biol 283, 475-488.

121. Tritch, R. J., Cheng, Y. E., Yin, F. H., and Erickson-Viitanen, S. (1991) Mutagenesis of protease cleavage sites in the human immunodeficiency virus type 1 gag polyprotein, J Virol 65, 922-930.

122. Rosenbluth, M. J., Lam, W. A., and Fletcher, D. A. (2006) Force microscopy of nonadherent cells: a comparison of leukemia cell deformability, Biophys J 90, 2994-3003.

123. Mussbach, F., Franke, M., Zoch, A., Schaefer, B., and Reissmann, S. (2011) Transduction of peptides and proteins into live cells by cell penetrating peptides, J Cell Biochem 112, 3824-3833.

124. Short, G. F., 3rd, Laikhter, A. L., Lodder, M., Shayo, Y., Arslan, T., and Hecht, S. M. (2000) Probing the S1/S1' substrate binding pocket geometry of HIV-1 protease with modified aspartic acid analogues, Biochemistry 39, 8768-8781.

125. Velazquez-Campoy, A., Todd, M. J., Vega, S., and Freire, E. (2001) Catalytic efficiency and vitality of HIV-1 proteases from African viral subtypes, Proc Natl Acad Sci U S A 98, 6062-6067.